# A MINERALOGICAL AND GEOCHEMICAL STUDY OF SEVEN METEORITES FROM MALAWI, NAMIBIA AND LESOTHO

By

Annegret Lombard

**DISSERTATION**

Submitted in fulfilment of the requirements for the degree

**MASTER OF NATURAL SCIENCE**

in

**GEOLOGY**

in the

**FACULTY OF NATURAL AND AGRICULTURAL SCIENCES**

at the

**UNIVERSITY OF THE FREE STATE**

Supervisor: Prof M Tredoux (UFS)

Co-Supervisor: Prof AE Schoch (UFS)

November 2010

## TABLE OF CONTENTS

## DECLARATION

I declare that this thesis is my own work. It is being submitted for the degree of Master of Science in the Department of Geology, University of the Free State, Bloemfontein. This thesis has not been submitted for any degree or examination in any other University.

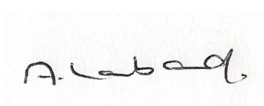

Annegret Lombard

19 December 2010

## ACKNOWLEDGEMENTS

The author would like to thank the following people for their valuable contributions and support:

- The personnel of the Department of Geology of the University of the Free State for their support and valuable advice as well as making the meteorites available for this study.
- Prof Alva Schoch for taking time to give valuable and insightful advice on scientific writing.
- Prof Willem van der Westhuizen, Dr Derik de Bruiyn, Dr Hermann Praekelt and Nico Scholtz for the help with the acquisition of the samples.
- My parents for their unwaivering support.
- All my friends and colleagues for their support.
- Last but not the least, my Heavenly Father that bless my life daily.

## ABSTRACT

Seven meteorites from Malawi, Namibia and Lesotho were studied using optical microscopy, scanning electron microscopy with energy dispersive X-ray spectrometry and electron microprobe analysis of mineral phases. Induced coupled plasma spectrometry and X-ray fluorescence techniques were used to obtain chemical information.

The Thuathe meteorite from Lesotho is a H4 ordinary chondrite according to major element chemistry and mineralogy. The shock features were classified as S2/3 and the weathering grade as W0. It contains Sb sulphides, which had not been previously reported in any chondritic meteorite. Berthierite and stibnite was observed under the SEM and confirmed by electron microprobe analyses. The chondrite normalised REE pattern is relatively flat with no significant LREE/HREE variation. Very slight enrichment of Ta and U compared to H-group chondrites are noted.

In this study the Machinga meteorite from Malawi is classified as an E6 ordinary chondrite according to major element chemistry and mineralogy, and the shock features were classified as S4, moderately shocked. Previously it had been classified as an L6 chondrite (Graham *et al,* 1984 and Koeberl *et al,* 1990). The rare earth element pattern is relatively flat with slight LREE/HREE variation from the norm. Slight enrichment of W, Pb and U is noted.

The Balaka meteorite from Malawi is a L6 ordinary chondrite that is weakly shocked (S2). These classifications were done with major element chemistry as well as the mineralogy of the meteorite. The rare earth element pattern is flat with nearly no variation between LREE and HREE. The normalised trace element diagram mirrors the trends of the trace element diagram of the L-group chondrites with respect to ordinary chondrites.

The Chisenga meteorite from Malawi is an IIIAB medium octahedrite according to chemistry and the bandwidth of kamacite (~1.5 mm) and taenite. Kamacite is the dominant Fe/Ni phase and Widmanstätten texture is prominent.

The unreported specimens from Asab in Namibia prove to be L6 ordinary chondrites according to major element chemistry and mineralogy. The shock features are classified as moderately shocked (S4) and the weathering grade is W2. The rare earth element spectrum for the sample 1 from Asab shows enrichment of LREE. Enrichment of Ba, Sr, Th and U is shown in this sample. Sample 2 from Asab shows slight La enrichment compared to L-group chondrites. Enrichment in Ba, Sb, Sr and U is shown in the chondrite normalised trace element diagram. Sample 3 from Asab displays a flat chondrite normalised REE pattern with nearly no variation between LREE and HREE. Chemical variation in these meteorite samples in the chondrite normalised trace element diagram shows enrichment of Ba, Sb and Sr. The general trends of the diagrams are similar indicating that the three unknown specimens are of the same fall.

**Keywords:** chondrite, mineralogy, geochemistry, classification, Thuathe, Machinga, Balaka, Chisenga, Asab

**OPSOMMING**

Sewe meteoriete van Malawi, Namibië en Lesotho is bestudeer met behulp van optiese mikroskopie, skandeer elektron mikroskopie met energiedispersie X-straal spektrometrie en elektrone mikrosonde vir mineral fase analises. Induktief gekoppelde plasma spektrometrie en X-straal fluoressensie tegnieke is gebruik om chemiese inligting in te win vir die geochemiese interpretasie van die meteoriete.

Die Thuathe meteoriet van Lesotho is 'n H4 gewone chondriet soos bepaal met hoofelement chemise samestelling en mineralogy. Die skok-eienskappe is as S2/3 geklassifiseer en the ververings grad as W0. Dit bevat Sb sulfiedes, wat nooit voorheen beskryf is in enige chondritiese meteoriete nie. Berthieriet en stibniet is met behulp van die SEM opgespoor en met behulp van die elektrone mikrosonde geanaliseer. Die chondriet genormaliseerde SAE patroon is relatief plat met geen merkbare variasie in LSAE en HSAE. Effense verryking van Ta en U in vergelyking met H-groep chondriete kom voor.

In hierdie studie is die Machinga meteoriet van Malawi geklassifiseer as 'n E6 gewone chondriet met matige skok (S4), na aanleiding van hoofelement chemise samestelling en minerlogie. Vorige outeurs het dit as 'n L6 chondriet geklassifiseer (Graham *et al,* 1984 en Koeberl *et al,* 1990). Die raar aard element patron is relatief plat met effense variasie van die LSAE/HSAE. Effense verryking van W, Pb en U is teenwoordig.

Die Balaka meteorite van Malwi is 'n L6 gewone chondriet met swak skok eienskappe (S2). Hierdie klassifikasies is met behulp van hoofelement chemiese samestelling asook mineralogie verkry. Die seldsame aard element patron is plat met feitlik geen variasie tussen die LSAE en HSAE. Die genormaliseerse spoorelement diagram vir die Balaka meteorite is 'n spieëlbeeld van die van L-groep chondriete.

Die Chisenga meteoriet van Malawi is 'n tipe IIIAB medium oktahedriet na aanleiding van chemise samestelling en die bandwydte van kamasiet (~1.5 mm) en taeniet. Kamasiet is die dominante Fe/Ni fase en Widmanstätten tekstuur is prominent.

Die drie onbekende voorbeelde vanaf Asab is L6 gewone chondriete na aanleiding van hoofelement chemise samestelling en mineralogie. Die skok-klassifikasie vir hierdie meteoriete is matig (S4) en die verwerings grad is W2. Die seldsame aard element patron vir monster 1 van Asab is verryk in LSAE. Ba, Sr, Th en U is verryk in hierdie monster. Monster 2 van Asab is effens verryk in La asook Ba, Sb, Sr en U. Die seldsame aard element patroon vir Monster 3 van Asab is plat met geen variasie tussen LSAE en HSAE. Ba, Sb en Sr is verryk in hierdie monster. Die algemene tendens van die diagramme is baie eenders wat aandui dat die monsters deel is van dieselfde gebeurtenis

**Sleutelwoorde:** chondriet, mineralogie, geochemie, klassifikasie, Thuathe, Machinga, Balaka, Chisenga, Asab

## LIST OF FIGURES

## LIST OF TABLES

# CHAPTER 1
# AN INTRODUCTION TO METEORITES

## 1.1 History

The first meteorite to be analysed by chemical methods fell at Lucé in France, on the 13th of September 1768. It was sent to the Institute de France by the Abbot Bachelay and there it was analysed by three chemists, Fourgeroux de Bonderoy, Cadet de Gassicourt and Antoine-Laurent de Lavoisier (Zanda and Rotaru, 2001). They did not consider it extraordinary, and concluded that it was pyrite-bearing sandstone that had been struck by lightning, and that it did not fall from the sky. The melted crust was interpreted as a thin layer of soil and grass that melted when lightning struck the rock. The examination of a second object, almost identical in composition, from Coutances in Normandy, did not alter these conclusions. It was concluded that lightning strikes pyrite-bearing material preferentially (Zanda and Rotaru, 2001).

A radically different view, that the rocks fell from the sky, came from the German physicist Ernst Florens Friedrich Chladni a year after a fall in 1794 in Sienna, Italy (Sears, 2004). Another fall took place on the 13th of December 1795 at Wold Cottage in England. A piece of the Wold Cottage fall came into the possession of Sir Joseph Banks, then president of the Royal Society. He recognised the similarities between this sample and a sample he had acquired from the fall in Sienna (Zanda and Rotaru, 2001). Reports of more falls in Portugal and India persuaded him to study the phenomenon. He gave the Sienna samples to the young chemist, Edward C Howard (Sears, 2004). Howard obtained the help of French mineralogist Jacques-Louis de Bournon, who separated each meteorite into its four main components: magnetic grains of metal, iron sulphides, "curious globes", and a fine-grained earthy matrix. Howard analysed each of the constituents separately and found striking similarities in the mineralogy, textures and chemical compositions of all the samples. His most important discovery was the significant quantities of nickel in all the iron meteorites. He concluded that the chemistry of the fallen bodies decisively set them apart from rocks of the Earth's crust (Zanda and Rotaru, 2001).

In 1802/3 these results were published in England and France. Leading scientists like Nicolas Louis Vauquelin, Laplace, Poisson and Biot were now also convinced that the stones fell from the sky, and that their origin had to be sought outside the Earth – probably in the volcanoes on the Moon (Zanda and Rotaru, 2001).

On 26 April 1803, at 1:00 pm, a shower of nearly 3 000 meteorites fell near the community of L'Aigle in Normandy. Analysed samples of the fall contained nickel and appeared to match other examined fallen bodies in some respects. Biot published a report in 1803 to put an end to the controversy and bring honour to Chladni for his vision. Decades would pass before the link between falls and fireballs would be established. Only more than a century and a half later, were meteorites recognised as impact debris from collisions of asteroids with one another and occasionally with other bodies in the solar system (Zanda and Rotaru, 2001).

Meteoroids are small extraterrestrial bodies, most of which probably originate in the asteroid belt between Mars and Jupiter, while others are linked to the Moon and Mars (Zanda and Rotaru, 2001). Their orbits sometimes become unstable and may fall gravitationally towards the Sun. As they pass the Earth's orbit they sometimes enter the Earth's atmosphere. If large enough, they will land on the Earth's surface and be called meteorites (Mason, 1962; Zanda and Rotaru, 2001). Meteorites can vary in size from dust-sized particles, to bodies up to several tons, such as the Gibeon meteorite swarm, or as a single meteorite such as the Hoba meteorite. Both of these meteorites are from Namibia (Glass, 1982; Lauretta and Kilgore, 2005). In summary, a meteorite starts as space debris, enters the Earth's atmosphere as a meteor and can burn up completely upon entering the Earth's atmosphere, or reach the surface more or less intact (Mason, 1962; Zanda and Rotaru, 2001).

Meteorites are usually named after a city or geographical feature, or after the post office nearest to where it fell or was found. The longitude and latitude of the fall site should also be given (Mason, 1962).

There are 75 million meteors visible to the naked eye daily, and 200 million kg of meteoritic material enter the atmosphere yearly, of which only one tenth of this mass reaches the surface of the earth (Zanda and Rotaru, 2001). The rest of the meteoritic material burns up in the atmosphere. Therefore for every 1000 $km^2$ only 100 g of meteoritic material reaches the surface of the earth per year (Zanda and Rotaru, 2001). Until the team of the Apollo II brought samples of moon rocks back to Earth for research, and recent rock analyses from Mars, meteorites were the only samples of extraterrestrial material available for scientific research. According to the Luna mission summaries and the NASA webpages various Nasa missions, as well as the Luna missions by the former USSR, have yielded more material for scientific study. Most meteorites are nearly a billion ($10^9$) years older than any rocks found on Earth, and some may be nearly unchanged since their formation 4600 million years ago (Bouvier *et al*, 2007; Amelin *et al*, 2005).

## 1.2 Composition of meteorites

In the study of meteorites, specimens are usually small and analyses must be done on small quantities to preserve some of the material for future studies. It is therefore better to use non-destructive methods of analysis, but classical wet chemistry techniques are the preferred method of meteorite analysis, and are destructive. Analytical techniques that may be used for meteorite analysis include wet chemical gravimetric analyses, X-ray fluorescence, neutron activation analysis, mass spectrometric techniques, radio-chemical neutron activation analysis, and electron microprobe techniques (Baedecker and Wasson, 1975; Bunch, Keil and Snetsinger, 1967; Dodd, 1981; Hutchison, 2004; Keil, 1968; Rubin and Keil, 1983; Van Niekerk and Keil, 2006).

The mineralogy of meteorites is rather simple compared to that of most terrestrial rocks. About 80 minerals have been identified in meteorites compared to the over 3000 found in terrestrial rocks from Earth (Glass 1982). Olivine, pyroxene and feldspar are the most common silicate minerals in chondritic meteorites (Wasson, 1974). Fayalite and forsterite constitute the olivine end members; feldspars generally consist of plagioclase although other feldspars have been reported, and pyroxene can be divided into three common types, monoclinic high-calcium pyroxene (augite to diopside), monoclinic low-calcium pigeonite, and orthorhombic low-calcium pyroxene (Wasson, 1974).

The average composition of meteoritic matter provides the best information on the relative abundances of non-volatile elements of the solar system. Cosmic abundances of elements are largely based on the interpretation of meteorite data. Chondrites in particular also serve as analogues for the bulk composition of the earth (Mason, 1962; Anders and Grevesse, 1989; Braerley and Jones, 1998; Krot *et al*, 2004). The most commonly held theory for the origin of the solar system states that it formed in a well-mixed part of an interstellar cloud. The sun formed when gravitational collapse of a portion of the cloud formed a disc of gas, and the dust formed the planets (Hutchison, 2004). Therefore a solar system formed with a chemical composition identical or closely similar to that of the sun (Hutchison, 2004). The disc may also be captured by a pre-existing sun. As the stars age the interstellar medium will be enriched in "heavy" elements and the galaxy composition thus changes with time (Hutchison, 2004). Radioactive nuclides give information regarding the origin, age and history of meteorites and the universe (Mason, 1962; Braerley and Jones, 1998; Krot *et al*, 2004), and the resulting chronology gives us insight into chondrite history: $U^{235}$, $U^{238}$, $Th^{232}$, $^{147}Sm$, $^{87}Sr$ and $^{40}K$ are long-lived radionuclides that together with their daughter isotopes are used in radiometric dating (Sears, 2004; Hutchison, 2004). Short-lived radionuclides such as $^{26}Al$, $^{53}Mn$, $^{107}Pu$ and $^{146}Sm$ were present when meteorites formed, but now only their daughter isotopes remain, which can be used to derive information about formation interval and amount of heat present during formation (Sears, 2004; Hutchison, 2004).

Cosmogenic nuclides are produced by nuclear reactions between particles from outside the meteorite (the solar wind) and the atoms comprising the meteorite (Sears, 2004; Hutchison, 2004). They shed light on the different phases of post-formation meteorite history, and seem to indicate that most meteorites come from relatively few parent bodies (Sears, 2004). The presence of cosmogenic nuclides is currently the best evidence for materials to be classified as extraterrestrial (Sears, 2004; Hutchison, 2004).

### 1.3 Classification

There are several ways to classify meteorites. Most simply they are divided into two groups determined by whether or not they were observed to fall, with those that were observed to fall being termed as "falls", and those that cannot be linked to a specific sighting, as "finds" (Mason, 1962; Krot *et al*, 2004).

Meteorites are also classified according to composition and structures as well as of their metallic Fe-Ni and silicate content (Dodd, 1981). These groups are the chondrites, achondrites, stony-iron meteorites and iron meteorites (Dodd, 1981).

The distinction between chondrites and other meteorites is fundamental. Chondrites are more numerous than any of the other meteorite classes among falls. Chondrites have a chemical composition that closely resembles that of a volatile-free sun (Anders and Grevesse, 1989). They are thus regarded as chemically primitive in contrast to other meteorites as well as the Earth and Moon rocks that are differentiated material. Differentiated material is distinctly non solar in composition and testifies to melting, crystallization and other chemical processes. Chondrites contain solar dust that has remained unaltered since its injection into the protosolar molecular cloud (Hutchison, 2004). In contrast to chondrites, differentiated meteorites, like Mars and Moon rocks, have experienced processes that obliterated the record of their early history. Chondrules are mm-sized near-spherical masses of silicates and more rarely metal or sulphide, that are present in most chondrites. Chondrites derive their name from chondrules. Textures in chondrites indicate that they have not been melted since formation by accretion of their different constituents (Hutchison, 2004). Subdivision of the major classes of chondrites are based on chemistry (Dodd, 1981 and Keil, 1969). For chondrites the Mg/Si, Al/Si and Fe/Si ratios are used to classify into H, L, LL, E and C chondrites (**Table 1.1 and 1.2**). Further classification in the groups (**Table 1.3**) includes using optical observation to determine the petrologic type (textural and mineralogical variation), weathering grade and shock grade (Dodd, 1981). Shock and weathering features can also be classified (Wasson, 1974; Stöffler *et al*, 1991).

**Table 1.1: Classification of chondrites after Dodd (1981) and Norton (1998).**

| Meteorite type | Abbreviation | Petrological type | Characteristics |
|---|---|---|---|
| ***Ordinary Chondrites (OC)*** | | | |
| | H | H 3-6 | High metal, high total iron |
| | L | L 3-6 | Metal, low total iron |
| | LL | LL 3-6 | Low metal, low total iron |
| ***Carbonaceous Chondrites (C)*** | | | |
| | CI (Ivuna) | CI (1) | Chondrule free, aqueously altered, hydrated phyllosilicates |
| | CM (Mighei) | CM 2 | Sparse small chondrules, aqueously altered, 50% hydrated silicates |
| | CR (Renazzo) | CR 2 | Primitive chondrules, metal, aqueously altered |
| | CO (Ornans) | CO 3 | Small chondrules, metals, calcium-aluminium inclusions |
| | CV (Vigarano) | CV 3 | Large chondrules, calcium-aluminium inclusions, slight aqueous alteration |
| | CK (Karoonda) | CK 3-6 | Large chondrules, dark silicates, calcium-aluminium inclusions |
| ***R-chondrite*** | | | |
| | R (Rumuruti) | R 3-6 | High iron<br>Brecciated clasts R 5-6<br>Matrix R 3-4 |
| ***E-chondrites*** | | | |
| | EH | EH 3-5 | High metal, high total iron, small chondrules, highly reduced |
| | EL | EL 3-6 | High iron, high total iron, larger chondrules. Highly reduced |

**Table 1.2: Classification of meteorites after Krot *et al* (2003).**

| | | | |
|---|---|---|---|
| **CHONDRITES** | Cabonaceous | *CI; CM; CO; CR; CB; CH; CV; CK* | |
| | Ordinary | *H; L; LL* | |
| | Enstatite | *EH; EL* | |
| | R | | |
| | K | | |
| **NON-CHONDRITES** | | *Irons* | *IAB; IC; IIAB; IIC; IID; IIE; IIIAB; IIICD; IIIE; IIIF; IVA; IVB* |

**Table 1.3: Petrologic classification of chondrites after Dodd (1981).**

| **Petrologic type** | | | | | |
|---|---|---|---|---|---|
| **Minerals** | **3** | **4** | **5** | **6** | **7** |
| **Olivine** | **Grossly inhomogeneous; igneous zoning common. CaO ≥0.1 wt%; locally chromian** | **Essentially homogeneous; Ca ≈ 0.06%** | **Homogeneous (PMD Fe ol≤1%): CaO ≈ 0.02 – 0.05 wt%** | | **Homogeneous** |
| **Pyroxenes** | **Chiefly twinned clino-enstatite, inhomogeneous; CaO ca. 0.2 – 0.5%** | **Bronzite & clino-bronzite; nearly homogeneous** | **Homogeneous bronzite. <1% CaO, increasing from type 5 – 6** | | **Calcic (≥1% CaO) + Ca-poor bronzite (≤0.5% CaO)** |
| | **Pigeonite, augite** | **Probable microcrystalline** | **Microcrystalline diopside** | **Diopside** | |
| **Plagioclase** | **Rare calcic; albitic glass in chondrules** | **Microcrystalline** | **Visible** | **Coarse $Ab_{82}Or_6$** | **Coarse (≥ 100 µm)** |
| **Ni-Fe** | **Inconsistent Fe-Ni profiles** | **Consistant diffusion profiles of Ni in kamacite and taenite, implying slow cooling through 500ºC** | | | |
| **Troilite** | **Ni-bearing** | **Essentially Ni free** | | | |
| **Chromite** | **Little inhomogeneous** | **Homogeneous, varying in composition with petrologic type** | | | |

Shock effects are determined by examining mineralogical and textural alteration in olivine and plagioclase, but since olivine is rare in enstatite chondrites, it is extended to orthopyroxene (Krot *et al*, 2004). Shock classification is used as an additional classification category for ordinary chondrites and carbonaceous chondrites. Rubin (2003) suggested the use of chromite and plagioclase as a shock indicator for ordinary chondrites. The generally accepted classification is based on the shock effects in olivine and plagioclase (Stöffler *et al*, 1991). The sample is studied microscopically to determine shock charateristics (Stöffler *et al*, 1991). In **Table 1.4** shock charateristics are summarised.

Weathering classification for meteorites in hand specimen is another commonly used criterion, as well as oxidation alteration visible in polished sections (Krot *et al*, 2004). Weathering classification can be observed in hand specimens or in polished thin sections (Krot *et al*, 2003), of which the latter is seldomly used. Weathering categories for hand specimens are a) minor rustiness, b) moderate rustiness, c) severe rustiness and d) evaporite minerals visible to the naked eye (Krot *et al*,2003). In **Table 1.5** weathering classification after Wlotzka *et al* (1993) for weathering in polished thin sections.

**Table 1.4: Shock classification after Stöffler *et al* (1991); Scott *et al* (1992) and Schmitt and Stöffler (1995).**

| **Shock stage** | **Effects from equilibration peak shock pressure** | |
|---|---|---|
| | **Olivine** | **Plagioclase** |
| Unshocked<br>S1 | Sharp optical extinction; irregular fractures | Sharp optical extinction; irregular fracture |
| Very weakly shocked<br>S2 | Undulatory extinction; irregular fractures | Undulatory extinction; irregular fractures |
| Weakly shocked<br>S3 | Planar fractures; undulatory extinction; irregular fractures | Undulatory extinction |
| Moderately shocked<br>S4 | Mosaicism (weak); planar fractures | Undulatory extinction; partially isotropic; planar deformation features |
| Strongly shocked<br>S5 | Mosaicism (strong); planar fractures; planar deformation features | Maskelynite |
| Very strongly shocked<br>S6 | Solid state recrystallisation or partial crystallisation; yellow-brown staining | Shock melted (normal glass) |
| Shock melted | Whole rock melting (impact melt rocks and melt breccias) | |

**Table 1.5: Terrestrial weathering classification after Wlotzka (1993).**

| Weathering stage | Description |
|---|---|
| W0 | No visible oxidation of metal or sulphides |
| W1 | Minor oxide veins and rims around metal and troilite |
| W2 | Moderate oxidation of ~20 – 60% of metal |
| W3 | Heavy oxidation of metal and troilite, 60 – 95% being replaced |
| W4 | Complete oxidation of metal and troilite, but no oxidation of silicates |
| W5 | Beginning alteration of mafic silicates, mainly along cracks |
| W6 | Massive replacement of silicates by clay minerals and oxides |

Structures such as Widmanstätten patterns in iron meteorites, and the type of chondrules in chondrites assist in the classification of meteorites (Dodd, 1981). The Widmanstätten pattern develops as the result of exsolution in the Fe-Ni solid solution series (Hutchison, 2004); the formation of the pattern is directly linked to cooling and composition of the solution (Wasson, 1974) as only γ-Ni, Fe is stable at temperatures above 800ºC and as this phase cools α-Ni,Fe exsolve to form plates parallel to the host (**Table 1.6**). According to Hutchison 2004, this texture is used to assign iron meteorites to three different major classes and trace element content again subdivides the irons into 12 groups.

**Table 1.6: Classification of iron meteorites after Dodd (1981) and Norton (1998).**

| Structural class | Texture | Band width (mm) | Chemical Class | Ni % |
|---|---|---|---|---|
| ***Hexahedrite*** (H) | Neumann Lines | >50 | IIA | 4.5 – 6.5 |
| ***Octahedrite*** (O) | Widmanstätten bands | | | |
| | Coarsest (Ogg) | 3.3 – 5 | IIB | 6.5 – 7.2 |
| | Coarse (Og) | 1.3 – 3.3 | IAB, IIIE | 6.5 – 7.2 |
| | Medium (Om) | 0.5 – 1.3 | IID, IIIAB | 7.4 – 10.3 |
| | Fine (Of) | 0.2 – 0.5 | IIIC, IVA | 7.8 – 12.7 |
| | Finest (Off) | <0.2 | IIID | 7.8 – 12.7 |
| | Plessitic (Opl) | <0.2 | IIC | Kamacite spindles |
| ***Ataxites*** (D) | Structureless | | IVB | >16 |

## 1.4 Context

The meteorites investigated in this study are: Thuathe meteorite (Lesotho), Machinga, Chisenga and Balaka meteorites (Malawi) and undescribed samples from Asab in Namibia.

The purpose of the investigation is to study the mineralogy and geochemistry of the meteorites to determine the classification, where necessary. The published results on the Thuathe, Machinga and Chisenga meteorites needs to be verified, and to confirm the unpublished data on the Balaka meteorite, as well as to classify the three unknown specimens from Namibia, by means of available mineralogical and geochemical data.

# CHAPTER 2
# MACROSCOPIC DESCRIPTION OF METEORITES STUDIED

## 2.1 The Thuathe meteorite (Lesotho)

### 2.1.1 Aquisition

The Thuathe bolide entered the atmosphere above Southern Africa on Sunday 21 July 2002 at approximately 15:45 SAST. A member of the department of Geology, UFS, observed the passage of the fireball, and the matter was immediately investigated (N. Scholtz, *pers. comm.*). Police stations, farmers, tour operators and local residents within the southern and eastern Free State were approached for eyewitness reports. Witnesses were asked to complete a “meteor reporting form”, which included date and time of sighting, tremors and sounds. If possible, latitude and longitude were provided, together with direction of sighting. Other information included light intensity and colour, velocity, duration of light and sound, and fragmentation (Lombard *et al*, 2003). The 10 most coherent responses are listed in **Table 2.1**. A sample of the meteorite was received by the Department of Geology UFS, about two months after the fall. The department immediately sent a team to Lesotho to acquire further samples from the fall site (**Figure 2.1**) for research. This was the first recorded meteorite to be recovered from Lesotho. Unfortunately most of the samples were chips of bigger pieces, broken off by locals to have more samples to sell; a few intact samples, showing undamaged fusion crusts were acquired, of which the biggest was 1,2 kg (Lombard *et al*, 2003).

### 2.1.2 Macroscopic description

The Thuathe fall constituted a meteorite shower. Appoximately 600 meteorite samples of various sizes have been recovered by various academic institutions as well as collectors, over a seven month period as recorded in a catalogue of the stones compiled by Ambrose, 2003. Some of the bigger meteorites made small impact craters as the one shown in **Figure 2.2** that is 30 cm in diameter.

**Table 2.1: Results from the meteor reporting forms of the Thuathe meteorite swarm that indicated the proximity of the fall site. N/a = were no information was given.**

| Nr# | Time SAST | Location of observer | Bearing from observer | Fireball duration | Fireball colour | Velocity | Sounds, shock waves or other comments |
|---|---|---|---|---|---|---|---|
| **1** | 15:50 | Umpukane – Farm on Clocolan/Marquard Road 027º50'12"S ; 027º30'25"E | 175º moving vertically downwards | 4 sec | White | Fast | No sound or shock waves heard or felt |
| **2** | 15:48 | Bloemfontein/Petrusburg Road 029º35'15"S ; 026º10'19"E | 098º moving vertically downwards | 5sec | White | Very fast | No sound or shock waves heard or felt |
| **3** | 15:50 | Alpha Estates Farm, Ladybrandt district on Lesotho border | n/a | n/a | n/a | n/a | Shock waves felt |
| **4** | 15:50 | Loch Logan, Bloemfontein 029º06'49"S ; 026º12'34"E | 100º | 2 sec | White with orange tail | Fast | No sound or shock waves heard or felt |
| **5** | Approx. 16:00 | Rouxville/Smithfield Road 030º15'48" ; 026º40'30"E | 022º | n/a | n/a | n/a | n/a |
| **6** | Approx. 16:00 | Botshabelo Mountain 029º15'10"S ; 026º45'30"E | 095º | 2sec | White | Fast | No sound or shock waves heard or felt |
| **8** | 15:50 | Pilot flying halfway between Ficksburg and Maseru | Moving vertically downward | n/a | Light orange | Fast | Flew through meteor smoke trail at 40 000 ft 029º10'00"S 027º45'00" |
| **9** | Approx. 16:00 | Farm Goedehoop, Ladybrandt district | n/a | n/a | n/a | n/a | Loud sound heard from the direction of Maseru |
| **10** | Approx. 16:00 | Farm Leeufontein, Theunissen district | 150º | 4 sec | White | Fast | No sound or shock waves heard or felt |

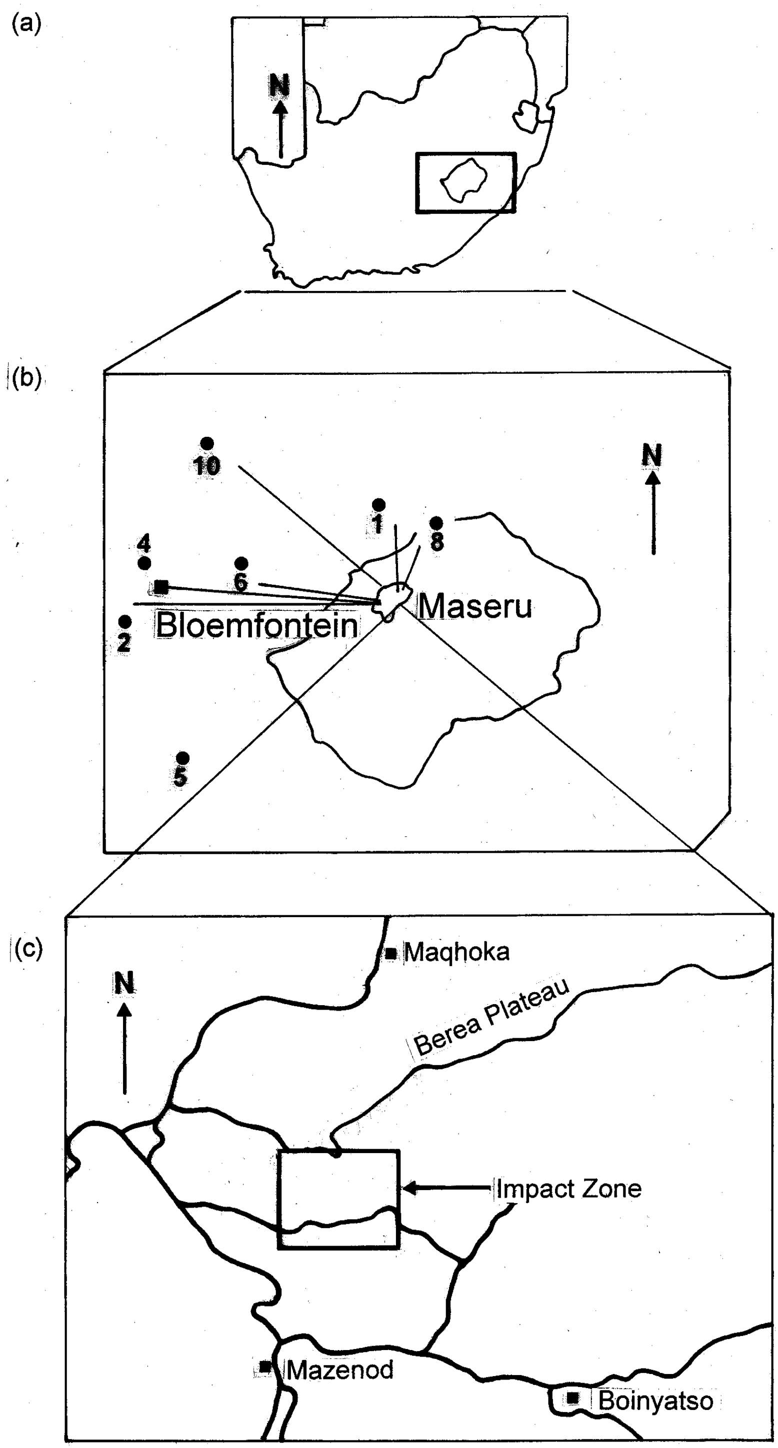


**Figure 2.1(a) Locality map; (b) Position of observations, numbers refer to Table 2.1; (c) The approximate 25-km$^2$ fall site.**


**Figure 2.2: Small crater of about 30 cm in diameter at the Thuathe meteorite fall site.**


**Figure 2.3(a): Photograph showing outside appearance of the Thuathe meteorites. Note the dark fusion crust and regmalypts (circled in yellow).**


**Figure 2.3(b): Photograph showing the lighter coloured interior of the Thuathe meteorite, containing chondrules (circled in yellow). Sulphides and metal phases constitute ~10% of the matrix.**

The specimens are all angular, dark grey in freshly cut surfaces with chondrules (~60 volume % of total silicates) (<1 mm) (**Figure 2.3b**). FeNi metal constitutes ~ 7 volume % of the surface, with ~ 93 volume % silicates. A dark brown fusion crust and regmaglypts are observed on the uncut surfaces (**Figure 2.3a**).

## 2.2 The Machinga meteorite (Malawi)

### 2.2.1 Aquisition

The Machinga meteorite fell near Mlelemba village in the southern Machinga province in Malawi on 22 January 1981, at 10h00 local time. The fall site is about 7,5 km SW of Machinga (**Figures 2.4 and 2.5**) at the co-ordinates 15º12'44"S, 35º14'32"E (Graham et.al., 1984). The nearest bigger town to the fall site is Zomba. The sample used for study was obtained by the Geological Survey of Malawi from the fall site and donated for this study.

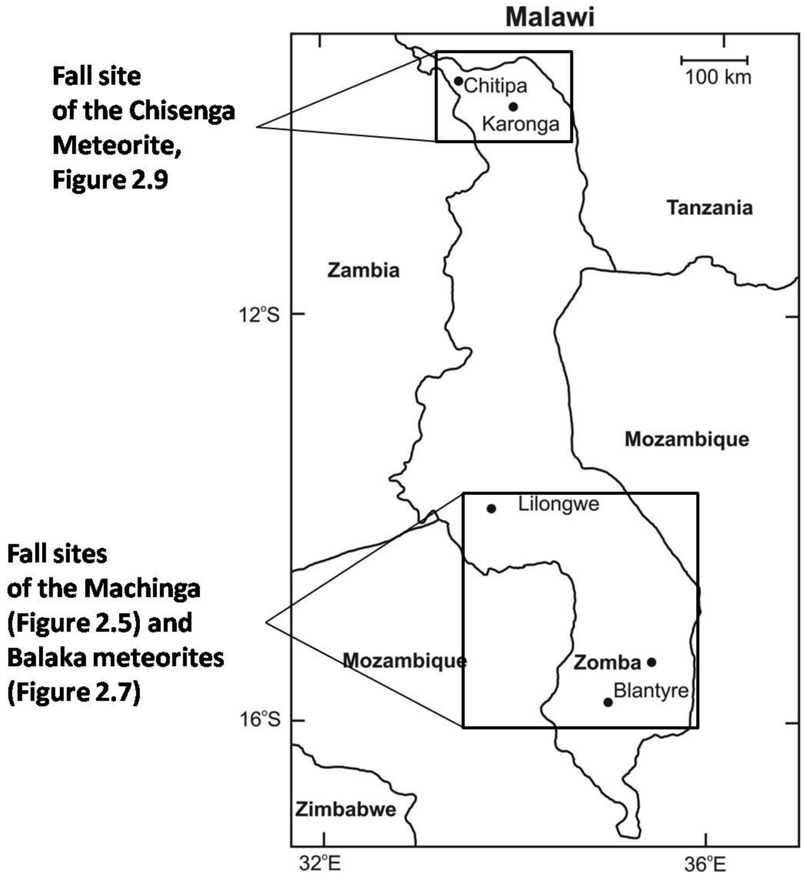


**Figure 2.4: A map of Malawi indicating the location of bigger villages and towns as references for fall sites.**

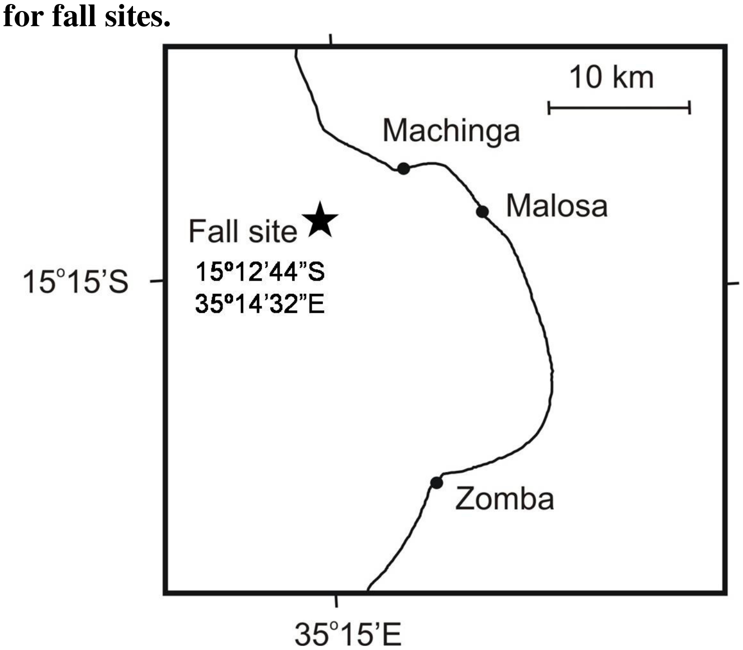


**Figure 2.5: Location of the fall site of the Machinga meteorite in the Machonga province of Malawi. Solid lines indicate roads.**

### 2.2.2 Macroscopic description

A single body weighing 93.2 kg was recovered and identified as a meteorite by the Geological Survey of Malawi. The meteorite is dark in colour and was nearly completely covered by a dark grey to black fusion crust, 1 mm thick and ~ 12% Fe-Ni mineral phases and sulphides are visible (**Figure 2.6**). Chondrules are visible in the hand specimen and up to 25 mm in size. There was flaking and small areas were broken off during the flight through the atmosphere and the impact (Graham et.al., 1984). The studied sample is dark in colour with visible metal phases ( ~ 12 volume %) and chondrules (~70 volume %). The piece does not include any fusion crust.

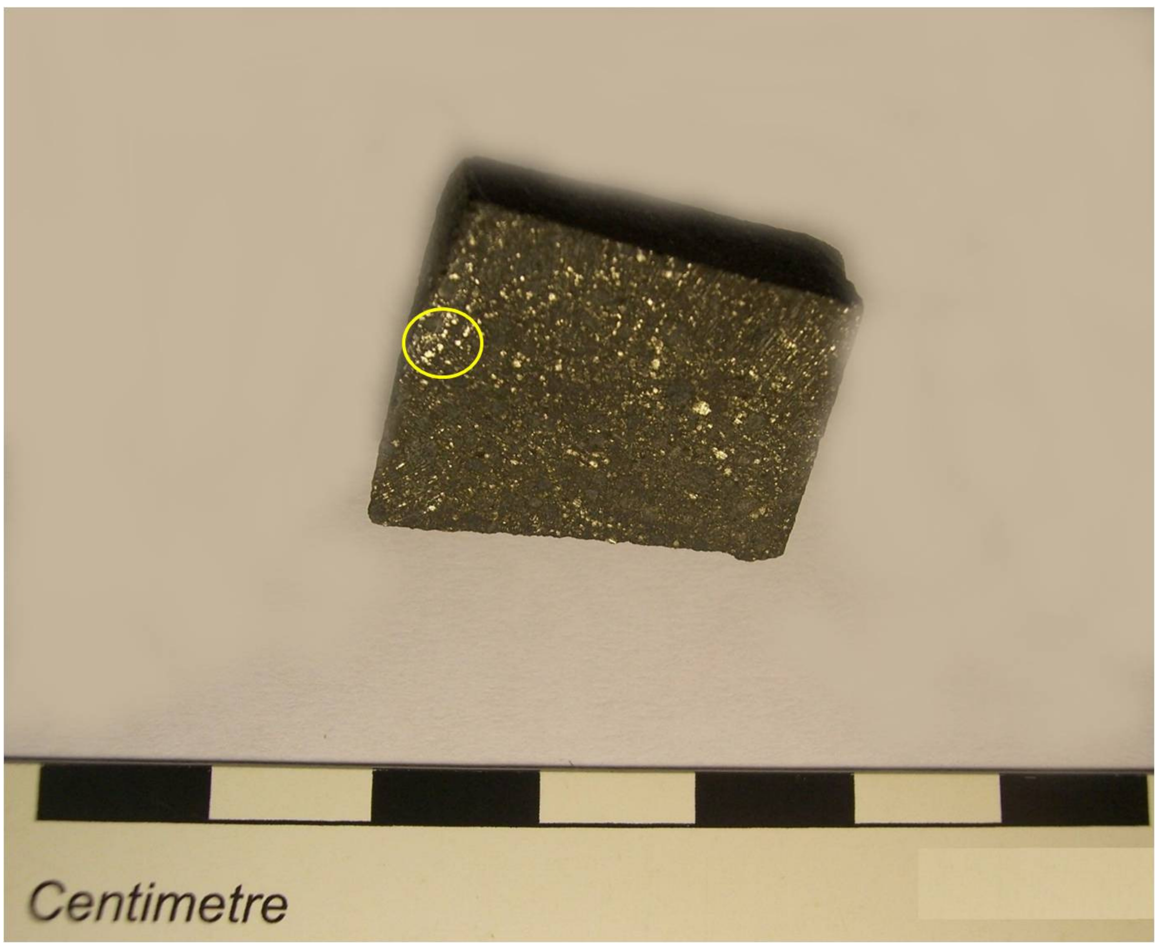


**Figure 2.6: The appearance of the Machinga meteorite, where Fe-Ni minerals and sulphides are visible, as illustrated in the circled area.**

## 2.3 The Balaka meteorite (Malawi)

### 2.3.1 Aquisition

The Balaka meteorite fell on 17 December 1985 (**Figure 2.7**) near the Balaka township (14º'58'18"S, 34º57'04"E) in Malawi. In **Figure 2.4** the proximity of the fall site to the town Zomba is illustrated. Samples for scientific research were collected by the Geological Survey of Malawi and donated for this study.

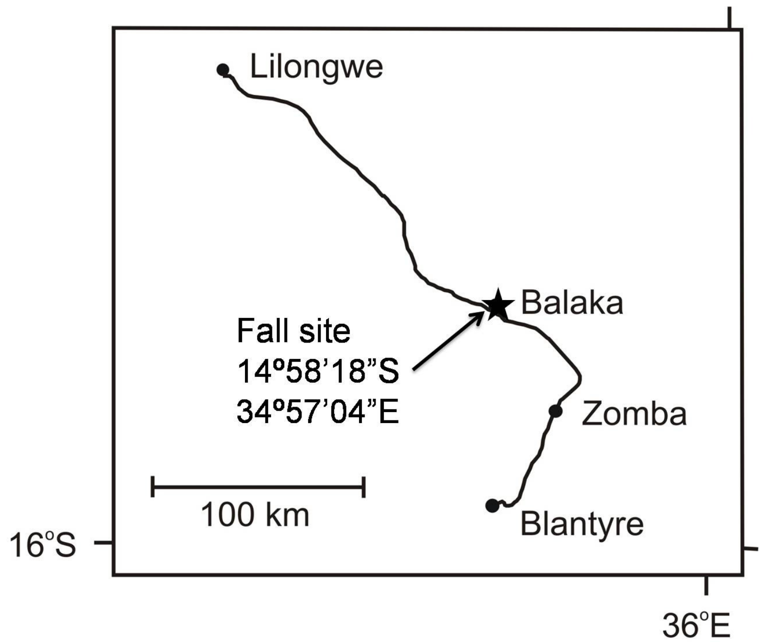


**Figure 2.7: The locality of the fall site of the Balaka meteorite in Malawi. Solid lines indicate roads.**

### 2.3.2 Macroscopic description

This meteorite is very light in colour and has visible iron staining (**Figure 2.8**). Less than 3% Fe-Ni mineral phases and sulphides are visible. Chondrules (~50 volume %), are also observed and up to 2 mm in size. No fusion crust or regmalypts are apparent in the studied sample. The weight of the Balaka meteorite was recorded as 2.26 kg at recovery.


**Figure 2.8: The iron stained (circled), lighter coloured outside appearance of the Balaka meteorite.**

## 2.4 The Chisenga meteorite (Malawi)

### 2.4.1 Aquisition

The Chisenga meteorite fell in the Chisenga area of the Chitipa District in Malawi (**Figure 2.4**) on the afternoon of 17 January 1988. The meteorite landed less than a kilometer from Chief Mulembe's Headquaters and about 50 km from Chitipa Bomba (10º03'34"S, 33º23'42"E) (**Figure 2.9**). The fall was eyewitnessed by a woman 12.5m from the fall site. The meteorite was extracted from a 30 cm deep crater by police and sent to the Geological Survey of Malawi for identification (Chapola, 1991). The Geological Survey in turn donated a representative sample of the meteorite to the University of the Free State for research.

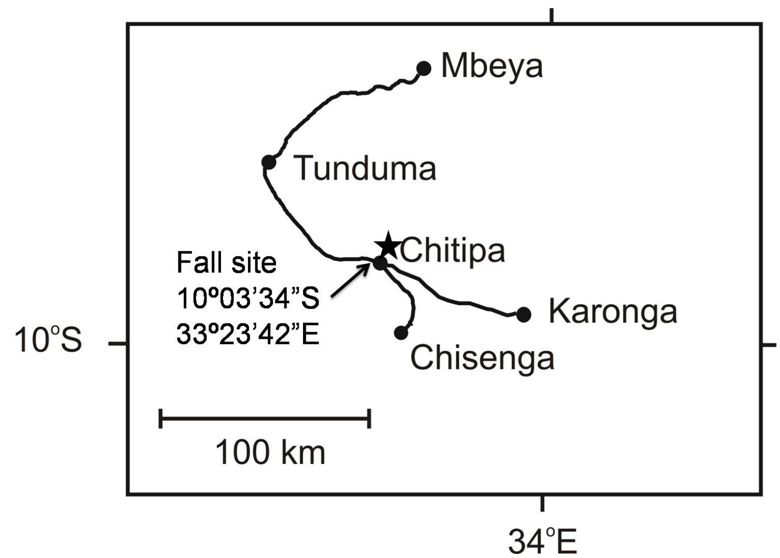


**Figure 2.9: The locality of the Chisenga meteorite fall in the north of Malawi, in the Chitipa district. Solid lines indicate roads.**

### 2.4.2 Macroscopic description

The meteorite is triangular in shape and weighs 3.92 kg (Chapola, 1991). It shows characteristic smooth thumb print-like depressions (regmaglypts) on its surface (**Figure 2.10(a)**). The fusion crust is black and only about 1 mm thick. The polished section (**Figure 2.10(b)**) shows Widmanstätten texture with lamellae of 1 – 2 mm in width.


**Figure 2.10(a): Regmaglypts (circled in yellow), visible on the outer surface of the Chisenga meteorite.**


**Figure 2.10(b): Widmanstätten texture in a polished sample of the Chisenga meteorite.**

## 2.5 The unreported meteorite specimens from Asab (Namibia)

### 2.5.1 Aquisition

Three meteorite specimens were donated to the Department of Geology of the University of the Free State by Ronnie MacKenzie, a private collector. The meteorites were obtained by Mackenzie from a farmer 11 km southeast of Asab in Namibia, in 2001 (**Figures 2.11 and 2.12**).

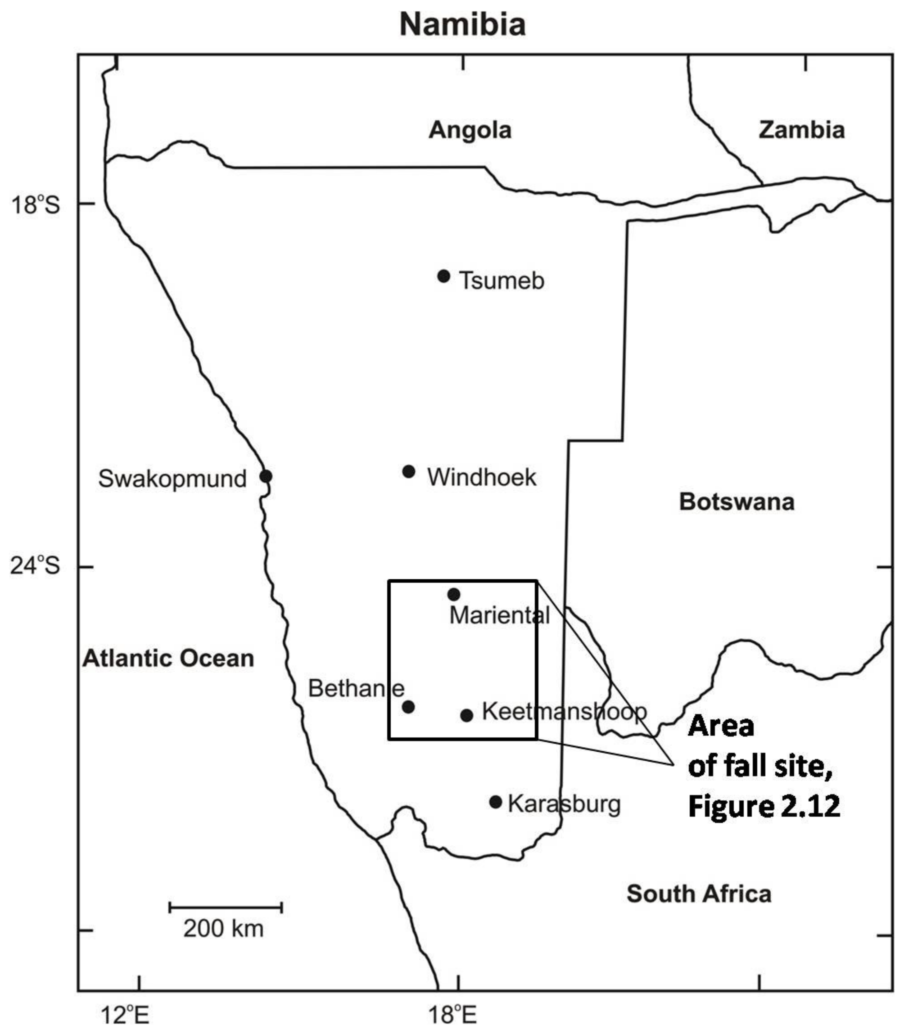


**Figure 2.11: A map of Namibia indicating larger towns in reference to the fall site of the unknown meteorite specimens from Asab. Asab is located near the town of Keetmanshoop**

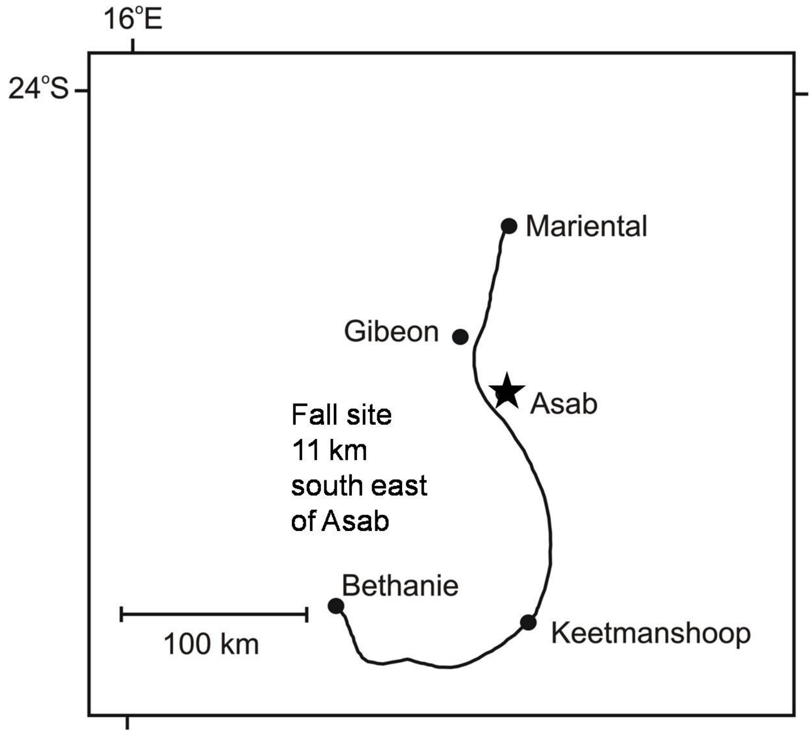


**Figure 2.12: The locality of the unknown meteorite specimens collected from Asab in Namibia. Solid lines indicate roads.**

### 2.5.2 Macroscopic description

The meteorite specimens are brown in colour with a dark brown fusion crust and regmalypts. Small areas were broken off during the flight through the atmosphere and the impact as illustrated in one of the samples in **Figure 2.13(a)**. Chondrules and iron staining are visible on the freshly cut surface of all three the meteorite specimens. Chondrules of up to 5 mm in size are noted in hand specimen (~ 75 volume %). This is illustrated in one of the specimens in **Figure 2.13(b)**. Less than 6% Fe-Ni mineral phases and sulphides are visible.


**Figure 2.13(a): The fusion crust and regmalypts (circled in yellow), on one of the unknown Namibian meteorites.**


**Figure 2.13(b): Chondrules (circled in yellow), as seen in a cut surface of one of the meteorites from Namibia.**

# CHAPTER 3
# ANALYTICAL TECHNIQUES

In the study of meteorites, specimens are usually small and analyses must be done on small quantities to preserve some of the material for future studies. It is therefore better to use non-destructive methods of analysis, but classical wet chemistry techniques are the preferred method of meteorite analysis, and are destructive.

## 3.1 Microscopy

Microscopic investigation was done with a Nikon Labophot pol microscope and an Olympus BX-51 polarizing microscope using the Altra 20 soft imaging system housed at the Department of Geology of the University of the Free State. Polished thin and thick sections were studied under incident and transmitted light, under plane polarised light and crossed polars. Thin and thick polished sections were prepared using paraffin as lubricant.

## 3.2 Electron Microprobe

The chemistry of individual mineral grains of the samples was determined by using electron microprobe techniques, which is based on the following principles: A narrow beam of electrons is focused on the polished surface of the sample to cover a 1 µm diameter spot. The electrons excite the atoms in the sample so that X-rays with characteristic wavelengths of the elements present will be emitted. These X-rays are detected by means of a proportional counter consisting of a gas-filled tube with Be-“windows” through which X-rays can enter. Incoming X-rays will ionize the gas atoms and produce free electrons that will move to the anode, while positive ions will move to the cathode, and an electronic pulse is produced by the X-ray photons that are absorbed. The size of the pulse reflects the number of ions produced, which is in turn proportional to photon energy. Pulses are counted to measure X-ray intensities and are expressed in counts per second. The the X-ray intensity at a given wavelength is proportional to the relative concentration of the element corresponding to that wavelength. By comparing the X-ray intensity with that in a standard sample of known composition, the concentration of the element in the sample is determined (Potts *et al*, 1995). The detection limit of the wavelength dispersive spectrometry depends on the element, and varies between 30 to 300 ppm.

In this study a Cameca Camebax electron microprobe was employed at the University of the Free State. A 2 µm beam diameter, 15 kV accelerating potential and a 30 mA beam current were employed. Mineral and pure metal standards were used in conjunction with PAP correction techniques (Pouchou and Picoir, 1984).

## 3.3 Whole rock and trace element analyses

### *3.3.1 Inductively coupled plasma spectrometry*

Major, trace element and specifically REE analyses on the Thuathe, Machinga, Balaka and Chisenga samples were performed by using inductively coupled plasma emission mass spectometry (ICP-MS) at the University of Kwazulu Natal, with an Elan 6100 ICP-MS. The samples were ground with an agate mortar and pestle. For each sample, 50 mg of powder was used. Each sample powder was individually digested in a microwave oven with a 60:40 high purity HF:$HNO_3$ solution. The sample mixture was then made up to 50 ml using 5% $HNO_3$-solution. The detection limits for this technique is dependent on the element analysed and varies between 0.01 – 10 ppm.

The Asab samples were ground with an agate mortar and pestle, pulverised in a Sieb Technik tungsten swing mill and micronized with a McCrone microniser. Major element analyses were obtained by means of Inductively Coupled Plasma Optical Emission Spectroscopy (ICP-OES) at Mintek. The samples were weighed and mixed with an alkaline flux, then fused and cooled. It was then leached in acidified water. The Varian Vista Radial Pro ICP-OES with a CCD detector with multi element standards were used. The detection limit depends on the elements analysed and varies between 0.05 – 0.11 weight %. ICP-MS analyses of REE elements were done at Mintek with a Shimadzu 8500 ICP-MS. Samples were subjected to multiple acid digestion procedures to dissolve the sample. The volume was made up with acidified water and tested against multi-element standards.

In both ICP-MS an ICP-OES the sample material is introduced into the spectrometer as an aerosol using an argon carrier gas. Aerosol particles are generated by nebulizing a sample solution. When carried through the hot plasma (up to 8000 °C), the sample material is dissociated, atomized and ionized within milliseconds. The ions enter the mass spectrometer via the so-called plasma interface, after which they become mass- and energy-filtered and the intensities of individual masses (elements) determined.

### *3.3.2 X-ray Fluorescence Spectrometry*

X-ray fluorescence (XRF) spectrometry is used to determine both major and trace element compositions of a sample. XRF spectrometry is based on the excitation of secondary X-rays within a sample by primary X-rays (Rollinson, 1993). The primary X-ray ionizes the component atoms which involve the ejection of 1 or more electrons from within the atom. The atom is then unstable, and electrons in higher orbitals will "fall" into the lower orbitals, and in doing so, release energy in the form of X-rays, which are unique to, i.e. characteristic of the specific element (Jenkins, 1988). The three specimens from Asab were analysed using a Spectro X-lab 2000 XRF with energy dispersive Si(Li) detector and Pd end-window X-ray tube. A semi-quantitative X-ray scan was performed at suppliers' standards. Three calibrations are used on this instrument, namely fundamental parameters for major element analysis, Compton empirical method for trace elements and the matrix mass attenuation coefficient for matrix analysis.

## 3.4 Scanning electron microscopy

A scanning electron microscope (SEM) can produce various types of signals. Secondary electron images and backscattered electron images are produced when the electron beam is scanned over the surface of the sample.

Secondary electron images are used for three dimensional surfaces which enable topography of the sample to be observed. Backscattered electron images offers more valuable information as it produces a greyscale image that is analogeous to the composition of the scanned sample as it varies with the atomic number of the elements present in the studied compound (Potts *et al*, 1995). X-ray images, or elemental maps are produced when the X-ray spectrometer is set up to record a specific element and the beam scanned across the surface (Potts *et al*, 1995).

For the analyses used in this study, the FEI Quanta 200 ESEM FEG with an Oxford Inca EDS system, at the University of the North West, Potchefstroom Campus was employed. A 15 kV to 20 kV accelerating potential was used at low vacuum and low pressure. Sections were observed in backscattered electron mode and element mapping and point analysis of carbon-coated polished sections of the meteorites were acquired using energy dispersive spectrometry.

Additional images and element map of the Chisenga meteorite was performed at Mintek making use of a Zeiss Evo MA15 SEM with Bruker EDS system. A 25 kV acceleration potential was used at high vacuum. Images were observed in back scattered electron mode. Element mapping using energy dispersive spectrometry was acquired on the carbon coated polished sections.

# CHAPTER 4
# MINERALOGY AND PETROGRAPHY

The mineralogical assemblages of meteorites serve to distinguish them from terrestrial rocks (Mueller and Saxena, 1977). The mineralogy of meteorites is fairly simple compared to that of terrestrial rocks. According to Wasson (1974) there are 24 common meteorite minerals.

Of these minerals olivine, pyroxene and plagioclase feldspar are the most common silicate minerals found in meteorites (**Table 4.1**). In recent years this list has been edited by various authors as the knowledge surrounding meteorite mineralogy has grown exponentially (Rubin, 1997). Rubin (1997) and Hutchison (2004) discuss the mineralogy of the different meteorite groups in detail and states that the number of minerals identified in meteorites has grown to ~275 which constitutes ~7% of the total number of well-characterised terrestrial minerals.

Homogeneity of the composition of olivine, pyroxene and plagioclase in ordinary chondrites can be use as an indicator of metamorphic grade (Wasson, 1974). With an increase in temperature, minerals will become more homogeneous, i.e. less chemical variation in composition would be apparent.

**Table 4.1: Average mineral compositions (M) and standard deviations (SD) for the electron microprobe analyses of olivine, pyroxene and plagioclase for the studied chondrites.**

| | | Thuathe M | SD | Machinga M | SD | Balaka M | SD | Asab M | SD |
|---|---|---|---|---|---|---|---|---|---|
| Olivine | Fo | 87 | 1.1 | 96 | 1.1 | 78 | 0.5 | 77 | 0.7 |
| | Fa | 13 | 1.1 | 4 | 1.1 | 22 | 0.5 | 22 | 0.7 |
| Pyroxene | En | 85 | 4.2 | 97 | 1.7 | 79 | 0.7 | 76 | 1.0 |
| | Fs | 13 | 2.5 | 2 | 1.7 | 19 | 0.7 | 23 | 1.4 |
| | Ws | 2 | 4.1 | 1 | 0.1 | 2 | 0.1 | 2 | 0.8 |
| Plagioclase | Ab | 78 | 7.0 | 86 | 1.5 | 83 | 4.2 | 89 | 1.7 |
| | An | 20 | 7.5 | 9 | 1.5 | 11 | 3.7 | 7 | 0.9 |
| | Or | 2 | 1.0 | 5 | 1.9 | 6 | 0.9 | 4 | 1.1 |

Chondrules are typically submillimeter-sized spherules observed in all chondrites except CI chondrites (Rubin, 2000 and Zanda, 2004). Chondrules have undergone melting and even in CI chondrites olivine and pyroxene chondrule relicts are found (Rubin, 2000; Sears, 2004 and Zanda, 2004). According to Rubin (2000), chondrites constitute ~80% of meteorites collected on Earth and that chondrules compose 15 – 75 volume % of chondrites. Chondrules avoided major aqueous and metamorphic alteration and it is commonly assumed that a significant fraction of the solids in the innermost part of a solar nebula are composed of chondrules (Rubin, 2000). Chondrules are very diverse in their properties and most are deficient in metal and sulphide in comparison to the host rock (Sears, 2004). Silicate-rich chondrules may exhibit rims that may be rich in metal and sulphides (Sears, 2004). Chondrules are studied by numerous researchers as they may produce answers to planet formation (Rubin, 2000; Sears, 2004 and Zanda, 2004). Sears (2004) discusses various classification schemes for chondrules that have been developed to understand chondrule formation. These schemes started as only textural classification schemes and are developing into composition-based schemes.

## 4.1 The Thuathe meteorite

Microscopically several metal, sulphide, oxide and silicate mineral phases were distinguished: kamacite, troilite, chalcopyrite, chromite, plagioclase, olivine and pyroxene. The matrix is very fine and contains plagioclase, pyroxene and olivine The metals and sulphides occur distributed throughout the matrix. Energy dispersive analyses (SEM) as well as wavelength dispersive analyses (electron microprobe) were used to differentiate between the different chemical phases and calculations (structural formulae) were performed. Kamacite occurs as the metal phase and chromite ($FeCr_2O_4$) is the oxide phase (**Table 4.2 and Appendix A**). The dominant sulphide phase is troilite (FeS) with subordinate chalcopyrite ($CuFeS_2$). The silicate minerals are albitic plagioclase ($Ab_{78}$) and forsteritic olivine ($Fo_{87}$) (**Tables 4.1, 4.2 and Appendix A**). Pyroxene proves to be both enstatitic and pigeonitic (**Table 4.1 and Figure 4.1**). Olivine, pyroxene and plagioclase show marked variation in chemical composition (**Table 4.1**). This indicates metamorphism of a lower degree grade. The mineralogy presented by Reimold *et al* (2004) and Ambrose *et* al (2003) who studied other samples of the same meteorite, is confirmed by this study. In the

Thuathe meteorite pyroxene chondrules dominate (~65 volume % of observed chondrules) (**Figures 4.2, 4.4 – 4.6**), but chondrules composed of olivine were also observed (**Figure 4.3**). A rare plagioclase chondrule containing sulphide droplet is illustrated in **Figure 4.7.** Chondrules are present but deficient in metal and sulphides compared to the host rock.

**Table 4.2: Mineral abundance in the Thuathe meteorite.**

| Mineral group | Mineral | Abundance |
|---|---|---|
| Silicates | Plagioclase | Major |
| | Olivine | Major |
| | Pyroxene | Intermediate |
| Oxides | Chromite | Accessory |
| Sulphides | Troilite | Minor |
| | Chalcopyrite | Accessory |
| | Berthierite | Accessory |
| | Stibnite | Accessory |
| Metal phases | Kamacite | Accessory |

**>50 wt% = dominant; 25 – 50 wt% = major; 15 – 25 wt% = intermediate; 5 – 15 wt% = minor; <5 wt% = accessory*

Antimony sulphides (berthierite and stibnite) were also observed in the meteorite (**Table 4.3 and Figure 4.8**) by means of an energy dispersive X-ray spectrometer with a 1µm beam. An element map confirms the presence of antimony in the grains of antimony sulphides (**Figure 4.9**). The results were verified by means of microprobe analyses (**Appendix A**) (De Bruiyn *et al* 2004). The occurrence is unusual as antimony sulphides are low temperature minerals and has never previously been reported as meteorite minerals (Pers. comm. A Rubin, 2003). The element antimony, has however been reported in mainly iron meteorites, where they are associated with schreibersite (Willis, 1981). Antimony as an element, has also been determined by means of neutron activation in various chondrites, achondrites, siderites and iron meteorites (Tanner and Ehmann, 1966; Tanner and Ehmann, 1967; Hamaguchi *et al*, 1966).

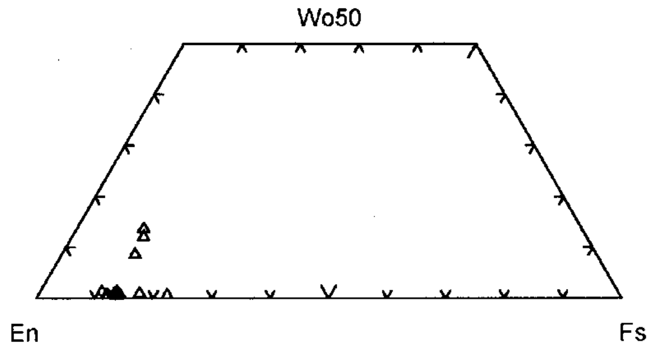


**Figure 4.1: Compositional distribution of pyroxene from the Thuathe meteorite as depicted on the pyroxene trapezium. (En = enstatite $MgSiO_3$; Fs = ferrosilite $FeSiO_3$; Wo = Wollastonite $CaSiO_3$).**

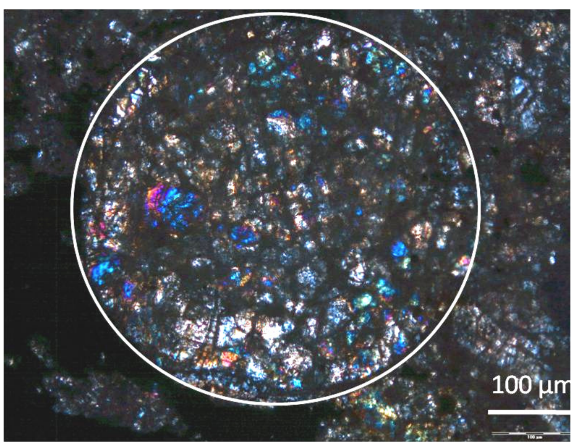


**Figure 4.2: Microphotograph of a poikilititic pyroxene clast chondrule in the Thuathe meteorite as observed under crossed polars in thin section.**

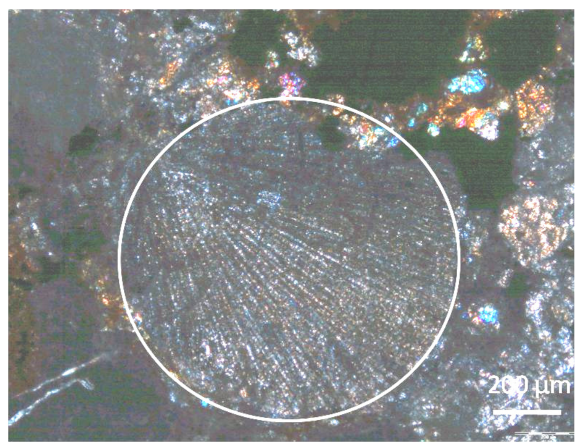


**Figure 4.3: Radial pyroxene chondrule as observed in the Thuathe meteorite under crossed polars in a thin section.**

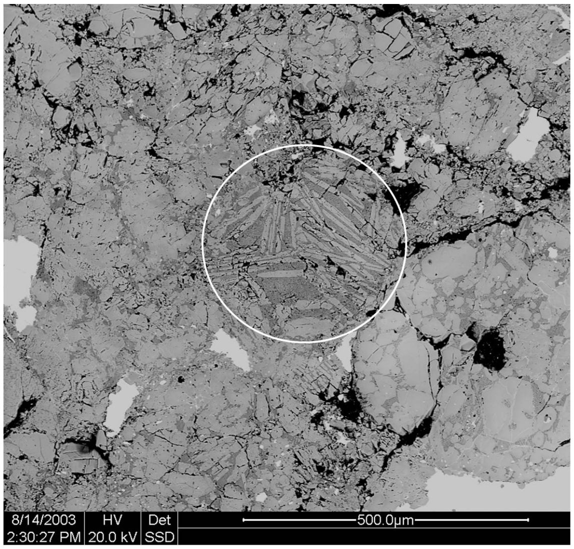

Figure 4.4: A Backscattered electron image of a radial barred pyroxene chondrule in the Thuathe.

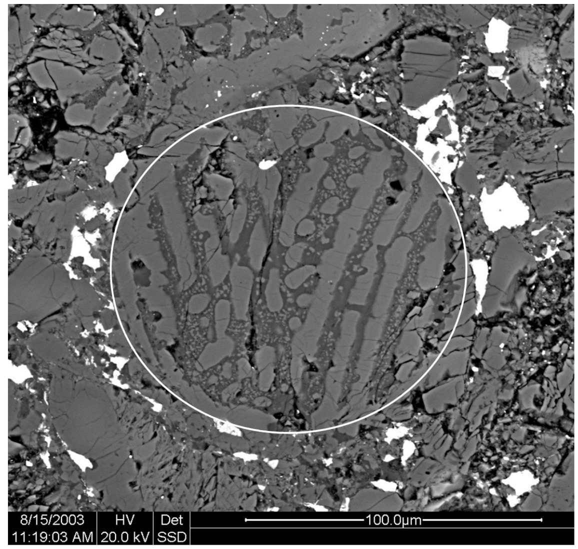

Figure 4.5: A Backscattered electron image of a barred pyroxene chondrule in the Thuathe meteorite, exhibiting a metallic rim consisting of troilite.

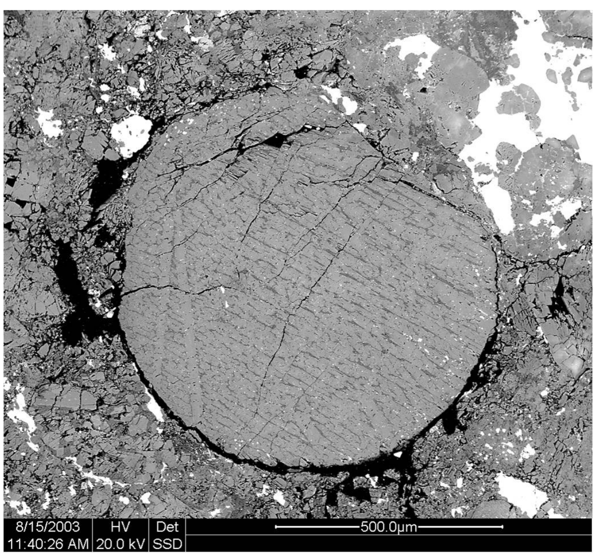

Figure 4.6: A Radiating chondrule of pyroxene as observed in the Thuathe meteorite in a backscattered electron image.

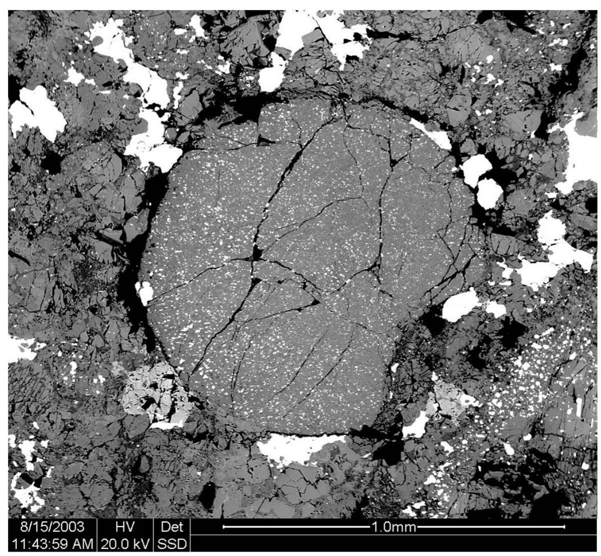

Figure 4.7: A rare plagioclase-rich chondrule containing sulphide droplets in a backscattered electron image of the Thuathe meteorite.

**Table 4.3: Mineral composition of the Sb-bearing mineral phases in the Thuathe meteorite.**

| | Berthierite | Stibnite |
|---|---|---|
| Sb | 57.01 | 69.76 |
| Fe | 12.96 | 1.16 |
| S | 29.9 | 29.05 |
| Ni | 0.13 | 0.05 |
| Total | 100.01 | 100.01 |
| **Structural Formulae** | | |
| Sb | 2 | 1.91 |
| Fe | 0.99 | 0.07 |
| S | 3.99 | 3.02 |
| Ni | 0.01 | 0 |

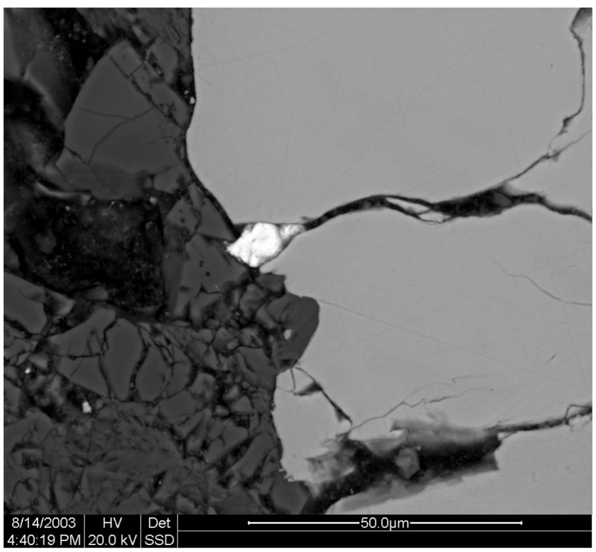


**Figure 4.8: Backscattered electron image illustrating a highly reflective antimony sulphide grain in the Thuathe meteorite.**

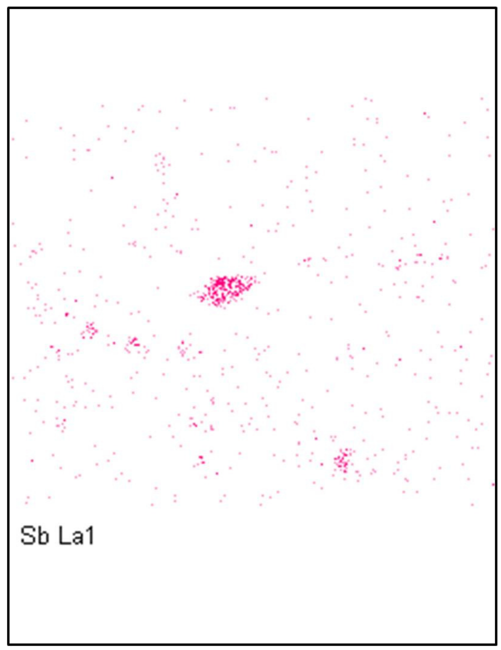


**Figure 4.9: An element map of the backscattered electron image illustrating the concentration of antimony in the antimony sulphide grain. Scale = same as Figure 4.4.**

Meteorite thermometry tends to fall into two categories (Wasson, 1974):

a) The recording of maximum temperature reached by the material in its present petrographic structure
b) The recording of equilibrium temperature, which is usually taken to be the lowest temperature at which co-existing minerals are able to maintain equilibrium.

Most systems utilised for terrestrial systems do not behave ideally. The best mineral thermometer for meteorites to date seems to be the orthopyroxene – augite system (Van Schmus and Koffman, 1967). Two different mineral pairs may be employed namely plagioclase – pyroxene and pyroxene - olivine (Onuma *et al*, 1972). The pyroxene – olivine system yields temperatures that are on average 100ºK higher than that of the plagioclase – pyroxene system (Onuma *et al*, 1972).

In the absence of an assemblage of well-defined and experimentally calibrated mineral assemblages, like in terrestrial rocks, mineral compositions are customarily employed to infer metamorphic temperatures experienced by ordinary chondrites. The systems orthopyroxene/clinopyroxene, orthopyroxene/olivine and clinopyroxene/olivine were utilized. Temperatures were determined by making use of the Mincalc Disk Operating System (DOS)-based computer program. The temperatures obtained were:

Orthopyroxene / clinopyroxene = 1129.6 ºC

Olivine / orthopyroxene = 1640 ºC

Olivine / clinopyroxene = 1213.1 ºC

The temperature estimates are very tentative as there is no infallible system that takes all the factors that play a role in the calculation of the formation temperatures of ordinary chondrites into account. Higher temperatures as seen in this study can be linked to chondrule formation in ordinary chondrites (Cervantes-de la Cruz *et al,* 2010). Kessel *et al* (2007) studied the thermal histories of equilibrated ordinary chondrites (H, L, LL) using the olivine/spinel system. Lower temperatures are attributed to thermal prograde metamorphic inside the chondrite parent body and temperatures for H4-6 chondrites vary between 733 and 754ºC, and peak metamorphic temperatures all exceed ~730ºC (Kessel *et al,* 2007 and Cervantes-de la Cruz *et al,* 2010).

### 4.2 The Machinga meteorite

The Machinga meteorite was examined microscopically and various different mineral phases were identified: pyroxene, olivine, plagioclase, troilite, magnetite, kamacite-taenite, calcite and gypsum (**Table 4.4)**. The chemical variation in the composition of olivine, pyroxene and plagioclase is relatively low, indicating higher degree grade metamorphism (**Table 4.1**). Olivine particles were noted under the microscope as part of the matrix as well as in chondrules (**Figures 4.10 - 4.12**). Olivine chondrules (~55 volume % of observed chondrules), and pyroxene condrules (~45 volume % of observed chondrules) occur in the Machinga meteorite. The matrix is very fine crystalline and iron staining is evident. Some chondrules show a metallic rim (**Figures 4.13 – 4.14**). Energy dispersive analysis as well as microprobe analysis confirmed the presence of rare calcite and gypsum as well as the silicate minerals, forsteritic olivine ($Fo_{96}$), albitic plagioclase ($Ab_{86}$) and enstatitic orthopyroxene (**Table 4.1 and Appendix B**). Magnetite is the oxide and troilite the sulphide phases. Analyses are presented in **Appendix B**. Kamacite-taenite is observed in **Figure 4.15.** Calcite is noted as a rare mineral in chondrules by Hutchison (2004), while gypsum is noted as occurring in the matrix of chondrites. Carbonates and sulphates are the products of aqueous alteration and typically occur in carbonaceous chondrites. Magnetite can be found as a rare phase in chondrules and as a minor phase in the chondrite matrix (Ramdohr, 1973 and Hutchison, 2004).

This meteorite was also previously studied (Koeberl *et al*, 1990) and the major mineral constituents reported were olivine, orthopyroxene and plagioclase, as confirmed by the current study. Accessory phases of metal, troilite, chromite and native copper were observed in this previous study. The native copper is associated with limonite and found in zones of aqueous alteration. Rare accessory phases of apatite and pentlandite were observed (Koeberl *et al*, 1990). This ambiguity in the mineralogy between the two studies emphasizes the inhomogeneous composition of different areas in the same meteorite.

**Table 4.4: Mineral abundance in the Machinga meteorite.**

| Mineral group | Mineral | Abundance |
|---|---|---|
| Silicates | Plagioclase | Major |
| | Olivine | Intermediate |
| | Pyroxene | Major |
| Oxides | Magnetite | Accessory |
| Sulphides | Troilite | Minor |
| Sulphates | Gypsum | Accessory |
| Carbonates | Calcite | Accessory |
| Metal phases | Kamacite - taenite | Accessory |

**>50 wt% = dominant; 25 – 50 wt% = major; 15 – 25 wt% = intermediate; 5 – 15 wt% = minor; <5 wt% = accessory*

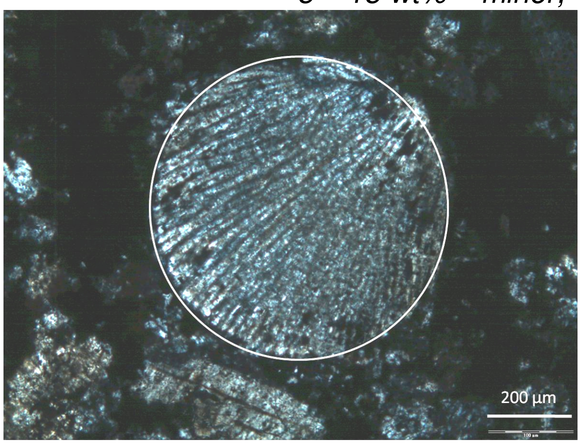


**Figure 4.10: Microphotograph of radial pyroxene chondrule in the Machinga meteorite as observed under crossed polars in thin section.**

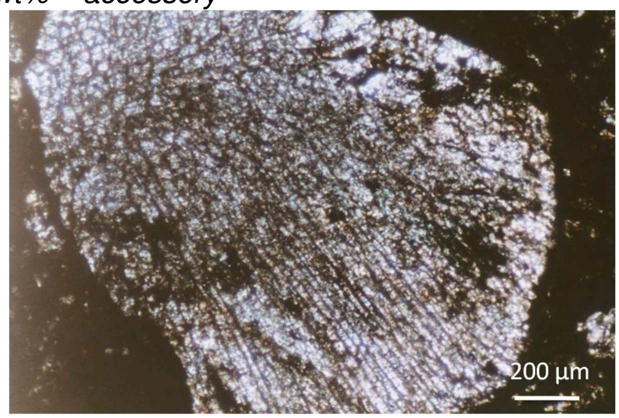


**Figure 4.11: Remnant of a radial pyroxene chondrule observed in the Machinga meteorite under crossed polars in thin section.**

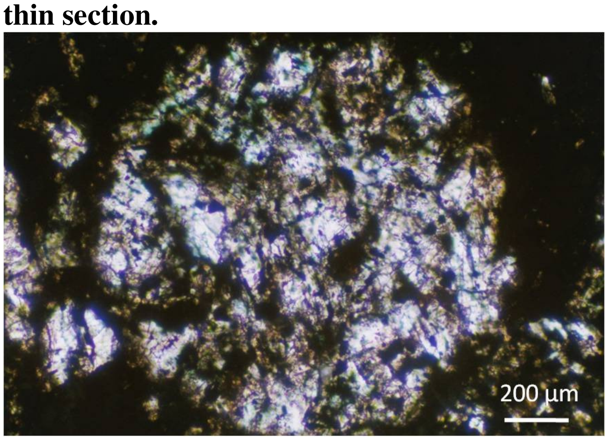


**Figure 4.12: Microphotograph of a porphyritc pyroxene chondrule in the Machinga meteorite as observed under crossed polars in thin section.**

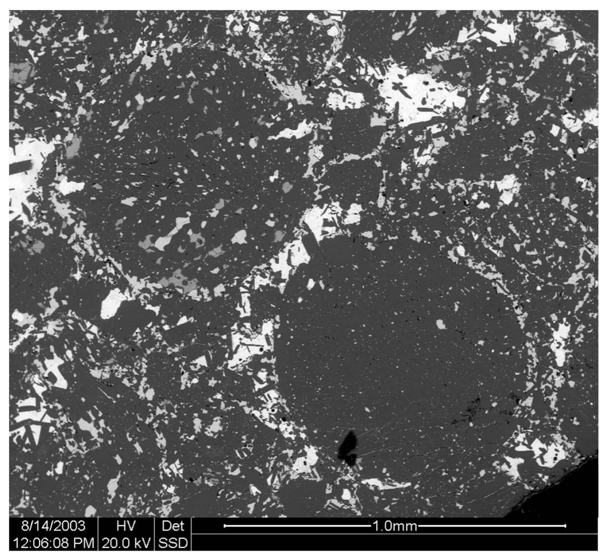


**Figure 4.13: A silicate chondrule exhibiting a metallic rim as observed in the Machinga meteorite in a backscattered electron image.**

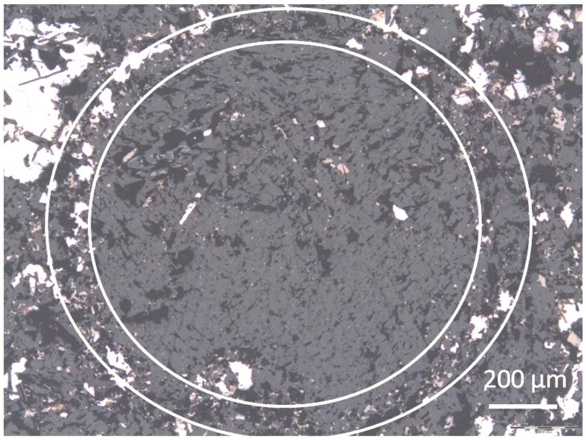


Figure 4.14: A silicate chondrule exhibiting a metallic rim as observed in the Machinga meteorite under plane polarised light in reflected light.

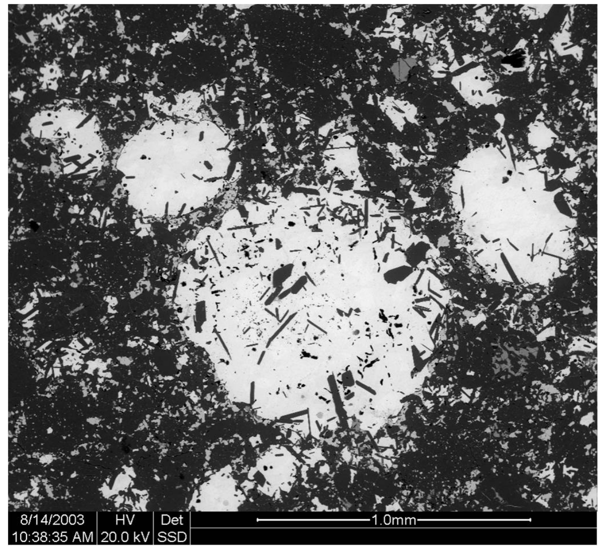


Figure 4.15: Backscattered electron image of kamacite-taenite droplets in the Machinga meteorite.

### 4.3 The Balaka meteorite

The Balaka meteorite has a very fine matrix and prominent alteration and iron staining and therefore mineral identification is very difficult. Energy dispersive analyses and microprobe analyses helped identify the mineral phases present in the meteorite. The mineralogy of the Balaka meteorite is simple and the silicates are represented by olivine ($Fo_{78}$) (**Figures 4.16- 4.17**), plagioclase ($Ab_{83}$) and enstatitic pyroxene (**Table 4.1 and Appendix C**). High degree grade metamorphism is indicated by the very low chemical variation in olivine and pyroxene. Plagioclase is slightly more variable. This can be ascribed to the fact that moer plagioclase is formed with an increase in metamorphic grade. The plagioclase formed will also be coarser and therefore have more variable composition. Chromite and Ti-magnetite represents the spinel minerals and troilite the sulphides (**Figure 4.18**) (**Table 4.5 and Appendix C**). The Fe-Ni minerals kamacite and taenite are also found in this meteorite. Chromite is a minor mineral in chondrules but is rarely found in the chondrite matrix. Magnetite, by contrast, is rarely found in chondrules but minor amounts may occur in the matrix of the chondrite (Hutchison, 2004). Olivine chondrules are dominant in this meteorite (~98 volume % of observed chondrules).

**Table 4.5: Mineral abundance in the Balaka meteorite.**

| Mineral group | Mineral | Abundance |
|---|---|---|
| Silicates | Plagioclase | Major |
| | Olivine | Major |
| | Pyroxene | Intermediate |
| Oxides | Chromite | Accessory |
| | Ti-magnetite | Accessory |
| Sulphides | Troilite | Accessory |
| Metal phases | Kamacite-taenite | Accessory |

**>50 wt% = dominant; 25 – 50 wt% = major; 15 – 25 wt% = intermediate; 5 – 15 wt% = minor; <5 wt% = accessory*

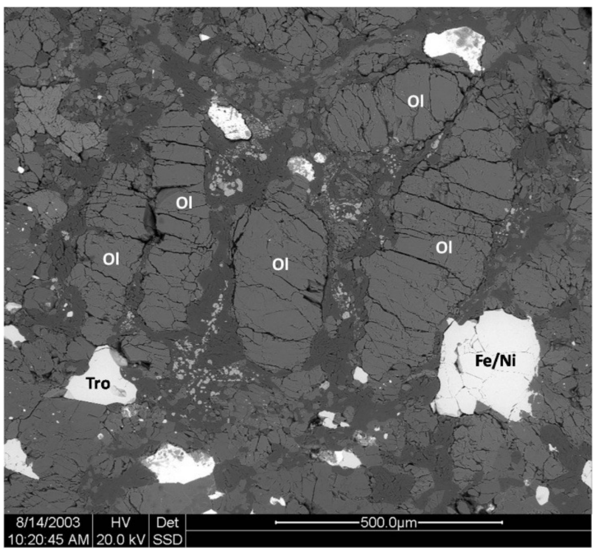


**Figure 4.16: A backscattered electron image of remnant olivine grains in the Balaka meteorite. (Fe/Ni = kamacite-taenite; Ol = olivine; Tro = troilite).**

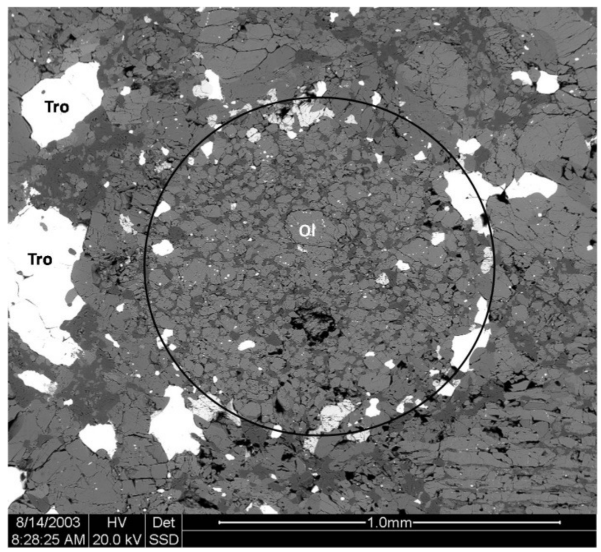


**Figure 4.17: A backscattered electron image of a porphyritic olivine chondrule with a metallic rim in the Balaka meteorite. (Ol = olivine; Tro = troilite).**

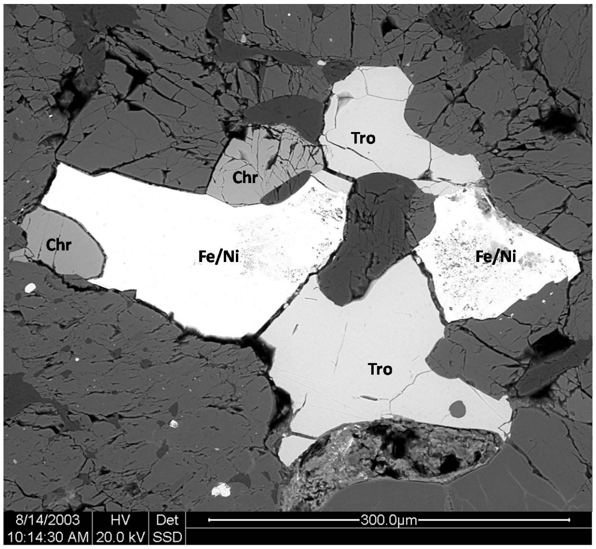

**Figure 4.18: A backscattered electron image of troilite, kamacite-taenite and chromite in the Balaka meteorite. (Chr = chromite; Fe/Ni = kamacite-taenite; Tro = troilite).**

### 4.4 The Chisenga meteorite

The Chisenga meteorite is and iron meteorite and therefore the Fe-Ni system and cooling rates must be taken into account to explain any textural features observed. In specifically iron meteorites the Fe-Ni minerals namely kamacite (αFe-Ni with ~5.5% Ni) and taenite (ɣFe-Ni with 27 – 65% Ni) gives rise to a texture naturally only formed in meteorites (Wedepohl, 1971). The Widmanstätten or octahedral pattern or texture consists of sets of lamellae oriented with respect to each other and is typical to octahedrites. This can be explained in terms of the Fe-Ni phase diagram. The width of the kamacite in octahedrites is controlled by three factors: the Ni concentration of the meteorite, the cooling rate and the nucleation temperature (Wasson, 1974). The cooling rate for the Chisenga meteorite was calculated with the equation:

$$\log CR = -2.040 \log BW - 8.940 \log [\mathrm{Ni}] + 8.700$$

Where $CR$ is the cooling rate in ºC/Myr; $BW$ is the bandwidth in units of mm and Ni concentration in given in weight%.

The calculated cooling rate for the Chisenga meteorite is 2.638 ºC/Myr.

Intergrowths of kamacite (~2 mm) and taenite (~0.1 mm) were observed in the Chisenga meteorite (**Figure 4.19**). Iron meteorites are known to consist mainly of iron-nickel alloys of kamacite (4 – 7.5% Ni) and taenite (15 – 50% Ni) as intergrowths (Chapola, 1991). In the Chisenga meteorite kamacite contains ~ 7 weight % Ni and taenite contains ~8 weight % Ni. **Figure 4.20** represents a section that was analysed by electron microprobe scanning over one of these lamellae and the weight % iron and nickel were plotted against the distance. It clearly shows the close relationship between these two elements as is common in iron meteorites. Troilite as well as Fe-Ni analyses and schreibersite analysis were obtained by means of energy dispersive analysis (**Table 4.6 and Appendix D**).

**Table 4.6: Mineral abundance in the Chisenga meteorite.**

| **Mineral group** | **Mineral** | **Abundance** |
|---|---|---|
| Sulphides | Troilite | Minor |
| | Schreibersite | Accessory |
| Metal phases | Kamacite-taenite | Dominant |

**>50 wt% = dominant; 25 – 50 wt% = major; 15 – 25 wt% = intermediate; 5 – 15 wt% = minor; <5 wt% = accessory*

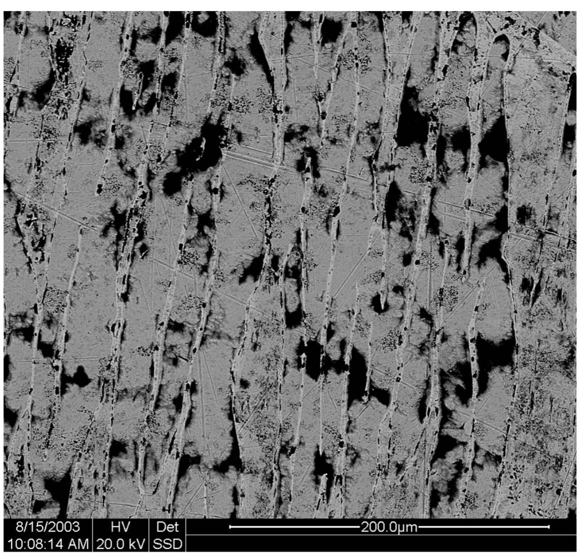


**Figure 4.19: A Backscattered electron image of very fine kamacite and taenite intergrowth also observed in the Chisenga iron meteorite.**

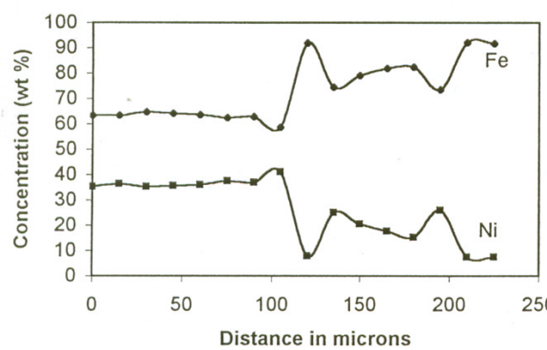


**Figure 4.20: Plot of distance against Ni and Fe across one of the lamellae such as those in Figure 4.19, in the Chisenga meteorite, that illustrates the relationship between these two elements.**

### 4.5 The unreported meteorite specimens from Asab

The three Namibian meteorite specimens were examined microscopically. All three samples showed large mineral grains with prominent iron staining associated with the sulphide and metal phases. Chondrules consisting of olivine (~45 volume % of observed chondrules) and pyroxene (55 volume % of observed chondrules) were noted (**Figures 4.21 – 4.23**). Energy dispersive analyses were confirmed by microprobe analyses (**Appendix E**). Olivine ($fo_{77}$), plagioclase ($ab_{89}$) and orthopyroxene ($fs_{76}$) as well as clinopyroxene ($fs_{65}$) were confirmed as the silicate phases by means of electron microprobe (**Tables 4.1, 4.7 and Appendix E**). High degree metamorphism is indicated by the very low chemical variation in the compositions of olivine, pyroxene and plagioclase. The sulphide troillite is and kamacite were observed with SEM (**Figure 4.24**). **Figures 4.26 – 4.30** illustrate the shock experienced by the Asab meteorites. Shock veins transect chondrules and the alteration of Fe-bearing phases to Fe-oxides is observed. The similar mineralogy and appearance of these samples confirms that the three samples are part of one event.

**Table 4.7: Mineral abundance in the Asab meteorites.**

| Mineral group | Mineral | Abundance |
|---|---|---|
| Silicates | Plagioclase | Major |
| | Olivine | Intermediate |
| | Pyroxene | Intermediate |
| Sulphides | Troilite | Accessory |
| Metal phases | Kamacite | Accessory |

**>50 wt% = dominant; 25 – 50 wt% = major; 15 – 25 wt% = intermediate; 5 – 15 wt% = minor; <5 wt% = accessory*

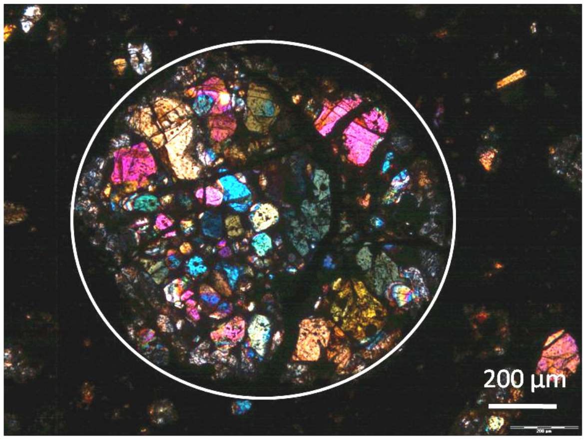


**Figure 4.21: Microphotograph of a poikilititic olivine chondrule as observed under crossed polars in thin section.**

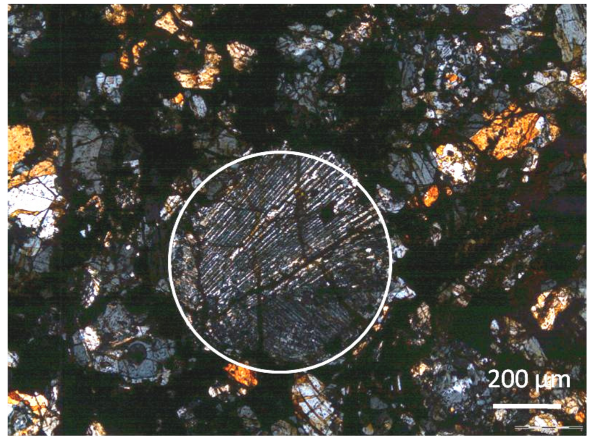


**Figure 4.22: Radial pyroxene chondrule as observed under crossed polars in a thin section.**

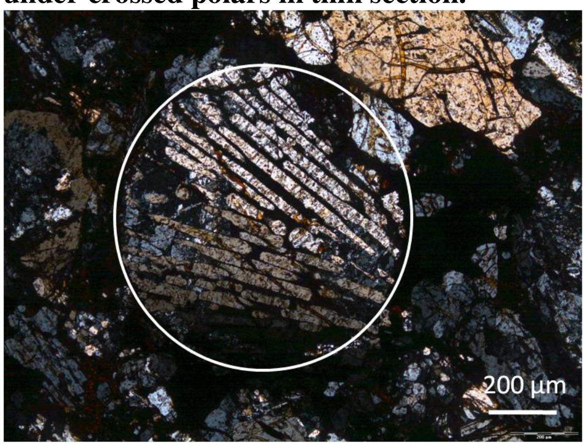


**Figure 4.23: Microphotograph of a radial pyroxene chondrule as observed under crossed polars in thin section.**

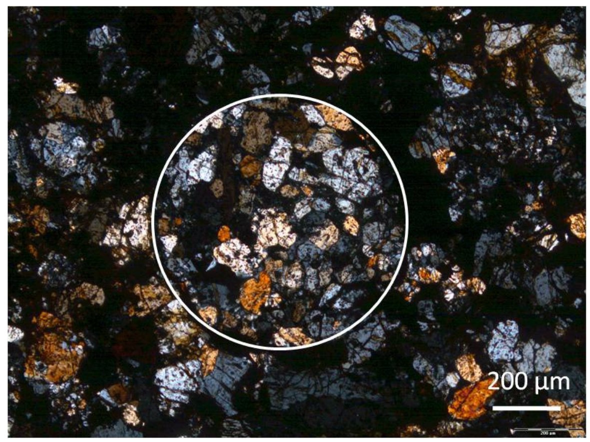


**Figure 4.24: Microphotograph of a poikilititic pyroxene chondrule as observed under crossed polars in thin section.**

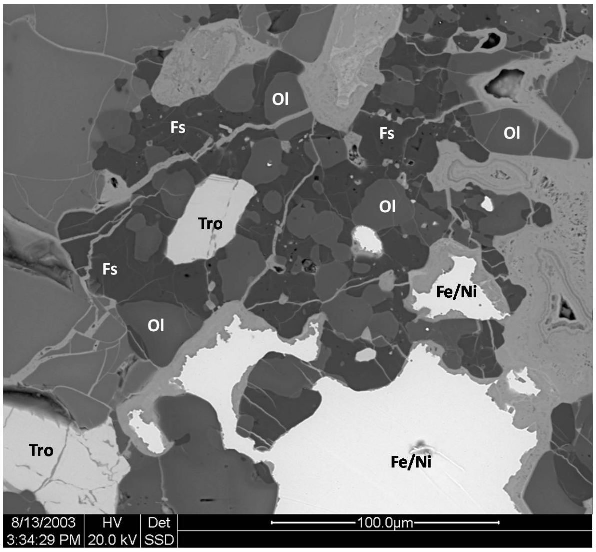


**Figure 4.25: Backscattered electron image of the mineral phases in the meteorite number 1 from Asab. (Fe/Ni = kamacite-taenite; Fs = feldspar; Ol = olivine; Tro = troilite).**

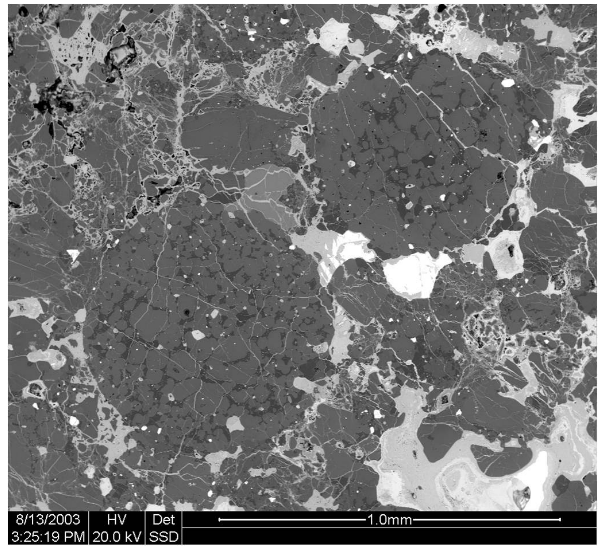


**Figure 4.26: Backscattered electron image of olivine chondrules in meteorite number 1 from Asab. Kamacite-taenite (white), and troilite (light grey) are observe together with Fe-oxides.**

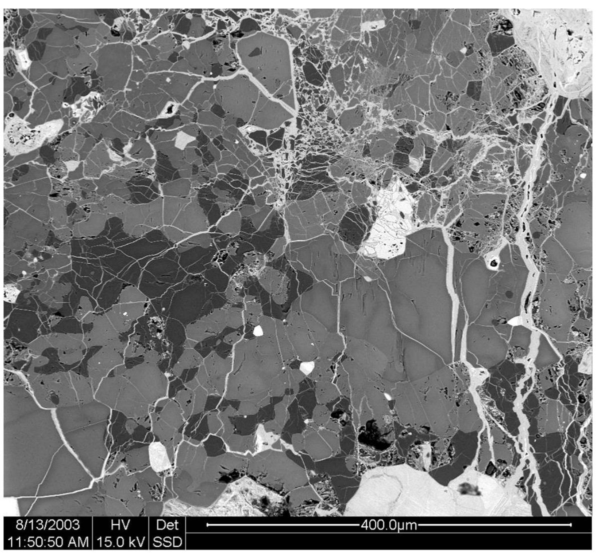


**Figure 4.27: Backscattered electron image of the sulphide and oxide filled shock veins in meteorite sample number 2 from Asab.**

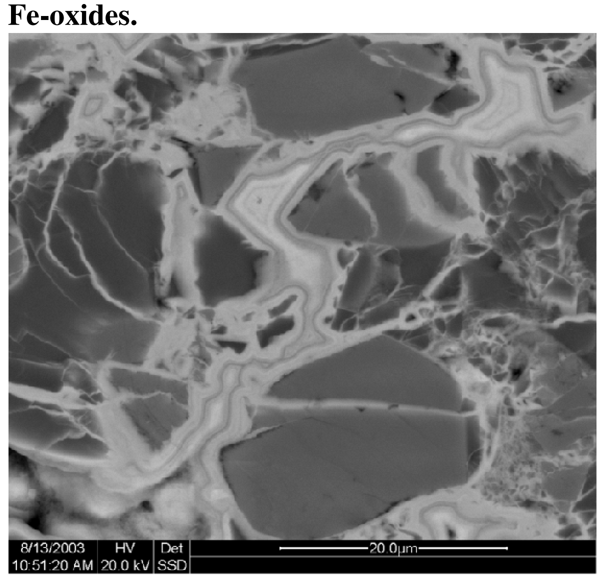


**Figure 4.28: Backscattered electron image of the Fe-oxide mineral phases filling shock veins in the 2nd meteorite sample from Asab.**

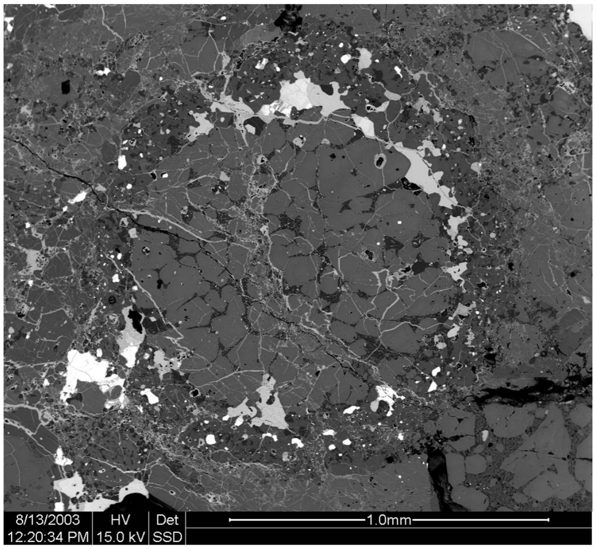


**Figure 4.29: Backscattered electron image of the 3rd meteorite sample from Asab.**

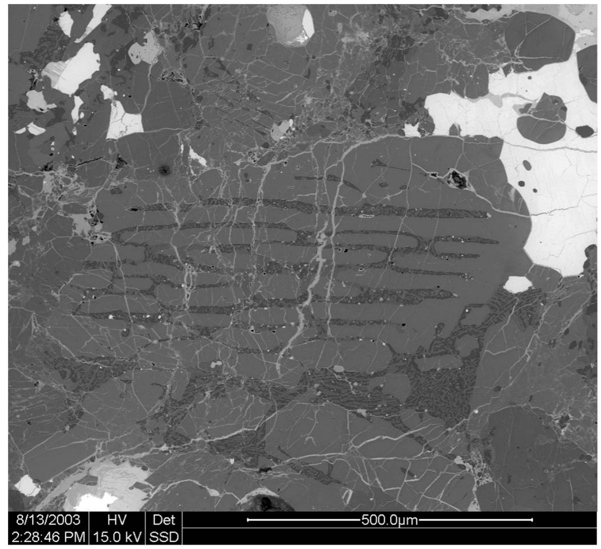


**Figure 4.30: Backscattered electron image of remnant pyroxene transacted by Ge-oxide filled shock veins in sample 3 from Asab.**

In this study the general mineralogy of the studied meteorites was determined, but mineralogy of meteorites can be used for various additional in-depth studies of meteorites that were not part of the scope of this study:

- Pressure-indicating mineral systems:
  According to Wasson (1974) a suitable mineral must form below a certain minimum pressure and must be capable of a metastable existence during the period between pressure release on breakup of the parent body and the investigation of the meteorite. The best known mineral that exhibits these properties in terrestrial and meteoritic samples is diamond. At pressures of below 14kb, diamonds to not exist stably, but transforms to stable graphite at a rate so slow that the diamond can exist on the Earth's surface during geologic time. The other system that can be consulted in the absence of diamonds are the silica polymorph system, but interpretations can be ambiguous (Wasson, 1974). Compositional data from co-existing minerals which share one or more components can also be used as a means of investigating formational pressure. The boundary between the taenite field and the two phase kamacite-taenite field is a good example as the Fe-Ni phase diagram is pressure sensitive. High pressure adds stability to close packed taenite phase relative to the kamacite phase (Ringwood and Kaufman, 1962).

- The Fe-FeO-MgO-$SiO_2$-$O_2$ system and Prior's rule

  The elements Fe, Mg, Si and O comprise nearly 90% of most chondrites. Meteorites contain metallic Fe and therefore the thermodynamic system Fe-FeO-MgO-$SiO_2$-$O_2$ has applicability (Wasson, 1974). Prior stated in 1916 that "the less the amount of Ni-Fe in chondritic stones, the richer it is in Ni, and the richer in Fe are the magnesium silicates". This is known as Prior's rule. The rule is quantitatively correct for intergroup chondrite comparisons. Ni, Fe, Mg Si and S abundances are the same in all meteorite groups. Ni would be highly concentrated in metal if it is present, Mg would concentrate in ferromagnesian silicates and the portion of Fe that is not bound to S would be distributed between the metal and the ferromagnesian silicates. The Fe concentration would vary between the metal and ferromagnesian silicates depending on the degree of oxidation of the chondrite. Prior speculated that the rule indicated that all meteorites formed from a single system, but this was disproved with modern day accurate analytical data (Wasson, 1974).

The details of the chemical composition of the minerals observed will be treated in the next chapter.

# CHAPTER 5
# ANALYTICAL RESULTS

In this study the the major and trace elements (**Table 5.1**) as well as REE composition (**Table 5.2**) of the Thuathe, Machinga, Balaka, and Chisenga meteorites were obtained by means of ICP-MS analysis (University of Kwazulu Natal, Chapter 3) and the unreported specimens from Asab in Namibia were chemically analysed by means of XRF as well as ICP-MS techniques (Mintek, Chapter 3) . The trace element compositions obtained for the general chondrite groups by Wasson and Kallemyn (1988) is given in **Table 6.1**. These data can be used as a reference for the studied samples. When compared to the reference chemical data, the studied meteorites tend to correlate with known chondrite groups.

## 5.1 Major element analyses

**Table 5.1: Major element analyses for the studied meteorites (wt%) as analysed by of ICP-MS (Thuathe, Machinga, Balaka and Chisenga) and XRF (ureported specimens froim Asab).**

| wt % | Thuathe | Thuathe (duplicate) | Machinga | Balaka | Chisenga | Asab 1 | Asab 2 | Asab 3 |
|---|---|---|---|---|---|---|---|---|
| $SiO_2$ | 34.29 | 34.88 | 34.58 | 38.90 | 3.09 | 36.10 | 36.91 | 39.93 |
| $Al_2O_3$ | 1.90 | 1.97 | 1.81 | 2.11 | 0.00 | 2.16 | 2.14 | 2.18 |
| $Fe_2O_3$ | na | na | 3.58 | 2.85 | 9.41 | 3.79 | 3.22 | 2.97 |
| FeO | 33.46 | 32.66 | 28.97 | 23.09 | 76.14 | 30.66 | 26.11 | 24.05 |
| Fe | na | na | na | na | 66.50 | na | na | Na] |
| MnO | 0.29 | 0.30 | 0.24 | 0.34 | 0.19 | 0.30 | 0.33 | 0.34 |
| MgO | 21.91 | 22.38 | 19.45 | 24.82 | *bdl* | 18.61 | 22.74 | 24.58 |
| CaO | 1.53 | 1.61 | 1.28 | 1.89 | *bdl* | 1.58 | 1.68 | 1.63 |
| $Na_2O$ | 0.82 | 0.66 | 0.68 | 1.01 | *bdl* | 0.73 | 0.85 | 1.04 |
| $K_2O$ | 0.09 | 0.09 | 0.09 | 0.11 | 0.02 | 0.22 | 0.25 | 0.22 |
| $TiO_2$ | 0.09 | 0.10 | 0.08 | 0.10 | *bdl* | 0.09 | 0.09 | 0.09 |
| $P_2O_5$ | 0.24 | 0.25 | 0.41 | 0.26 | 0.39 | 0.33 | 0.32 | 0.24 |
| $Cr_2O_3$ | 0.48 | 0.50 | 0.38 | 0.48 | 0.01 | 0.55 | 0.59 | 0.56 |
| NiO | 1.94 | 1.77 | 1.93 | 1.32 | 8.87 | 1.78 | 1.29 | 1.46 |
| S | 2.80 | 2.90 | 6.72 | 2.88 | 1.43 | Na | na | na |
| Total | 99.84 | 100.07 | 100.20 | 100.16 | 99.54 | 96.90 | 96.52 | 99.29 |

**below detection limit = bdl; not analysed = na*

## 5.2 Trace element analyses

**Table 5.2: Trace element analyses for the studied meteorites (ppb) analysed by means of ICP-MS.**

| ppb | Thuathe | Thuathe (Duplicate) | Machinga | Balaka | Chisenga | Asab 1 | Asab 2 | Asab 3 |
|---|---|---|---|---|---|---|---|---|
| Sc | 9220 | 8820 | 4520 | 9750 | 90 | 7390 | 8120 | 8820 |
| V | 45990 | 44360 | 50580 | 37860 | 1010 | 52080 | 57990 | 63690 |
| Co | 814080 | 989600 | 823880 | 291290 | 4467150 | 723400 | 542140 | 449960 |
| Cu | 89870 | 83810 | 131020 | 59270 | 92520 | 86490 | 86850 | 95480 |
| Zn | 60880 | 59330 | 89880 | 37400 | 145310 | 54680 | 22720 | 44970 |
| As | 1660 | 2620 | 2570 | 810 | 8520 | 1640 | 1230 | 640 |
| Rb | 2570 | 2490 | 2830 | 3310 | bdl | 2140 | 2840 | 2290 |
| Sr | 11510 | 11030 | 10050 | 13780 | 30 | 20180 | 24170 | 19720 |
| Y | 2020 | 1950 | 1760 | 2850 | 30 | 2990 | 2310 | 2250 |
| Zr | 5750 | 5420 | 4490 | 6880 | 10 | 6100 | 4110 | 5700 |
| Nb | 470 | 450 | 370 | 520 | 10 | 520 | 470 | 480 |
| Sb | na | na | na | na | na | 250 | 290 | 320 |
| Ba | 4130 | 3820 | 4150 | 4440 | 240 | 179870 | 177040 | 166120 |
| La | 310 | 330 | 340 | 380 | 120 | 1230 | 880 | 310 |
| Ce | 810 | 780 | 800 | 1100 | 20 | 3160 | 1050 | 810 |
| Pr | 120 | 110 | 110 | 160 | bdl | 330 | 130 | 130 |
| Nd | 560 | 550 | 560 | 810 | bdl | 1400 | 650 | 650 |
| Sm | 180 | 170 | 170 | 260 | bdl | 410 | 250 | 200 |
| Eu | 70 | 70 | 60 | 80 | bdl | 130 | 100 | 80 |
| Gd | 240 | 240 | 210 | 320 | bdl | 470 | 270 | 260 |
| Tb | 50 | 40 | 40 | 60 | bdl | 70 | 50 | 50 |
| Dy | 310 | 300 | 280 | 440 | bdl | 480 | 340 | 350 |
| Ho | 70 | 70 | 60 | 90 | bdl | 100 | 80 | 80 |
| Er | 200 | 190 | 180 | 280 | bdl | 290 | 220 | 220 |
| Tm | 30 | 30 | 30 | 50 | bdl | 40 | 40 | 30 |
| Yb | 210 | 200 | 180 | 290 | bdl | 280 | 230 | 240 |
| Lu | 30 | 30 | 30 | 40 | 0 | 40 | 40 | 40 |
| Hf | 150 | 150 | 100 | 180 | 0 | 170 | 160 | 170 |
| Ta | 40 | 50 | 30 | 30 | 3 | 30 | 20 | 20 |
| W | 210 | 240 | 260 | 170 | 629 | 220 | 130 | 70 |
| Pb | 450 | 390 | 3480 | 520 | 435 | Na | na | na |
| Th | 50 | 50 | 40 | 50 | 0 | 120 | 30 | 30 |
| U | 20 | 20 | 20 | 20 | 0 | 80 | 30 | 10 |

**below detection limit = bdl; not analysed = na*

According to the averaged values for elements in chondrites as published by Wasson and Kallemeyn (1988), the Thuathe meteorite shows chemical correlation with H-group chondrites, while the Machinga meteorite shows characteristics of E-group chondrites in especially the trace elements. However, the values are generally slightly lower than the values determined by Wasson and Kallemyn (1988). The Balaka meteorite mostly correlates with the reference values for L-group chondrites, but in general are slightly higher. The unknown meteorite samples from Asab shows correlation with the L-group eference samples, but in general, the values are slightly higher.

# CHAPTER 6
# GEOCHEMISTRY

In general the assumption was made that the composition of chondrites represents the average composition of the non-volatile part of solar matter (Mason, 1971; Krot *et* al, 2004), but abundance variations of elements between different chondrite classes and subclasses vary (Mason, 1966; Mason, 1971). Later work supports this hypothesis for most of the more abundant lithophile elements, but also confirmed marked differences for some of the minor and trace elements between the different classes of chondrites (Mason, 1971). Carbonaceous chondrites are the least differentiated and most homogeneous of meteorites and therefore are seen as the closest approximation to solar abundance (Krot *et al*, 2004).

Major and trace elements are fractionated between the different chondrite classes (Mason, 1971) and normalised rare earth element (REE) patterns are used to determine fractionation and partial melting in terrestrial rocks (Rollinson, 1993). Spidergrams can then also be used to show enrichment and depletion of REE in chondrites.

In this study the the major and trace elements as well as REE composition of the Thuathe, Machinga, Balaka, and Chisenga meteorites were obtained by means of ICP-MS analysis (University of Kwazulu Natal, Chapter 2) and the unreported specimens from Asab in Namibia were chemically analysed by means of XRF as well as ICP-MS techniques (Mintek, Chapter 2) . These data (Chapter 5) and the data for the ordinary chondrite groups in **Table 6.1** were used to plot chondrite normalised figures to compare the trends between not only the different plots but also the studied samples.

**Table 6.1: Trace element analyses for the ordinary chondrite groups (ppb), after Wasson and Kallemeyn (1988).**

| ppb | H-group | L-group | E-group |
|---|---|---|---|
| Sc | 7900 | 8600 | 5700 |
| V | 74000 | 77000 | 54000 |
| Co | 810000 | 590000 | 840000 |
| Cu | 82000 | 90000 | 185000 |
| Zn | 47000 | 50000 | 250000 |
| As | 2050 | 1550 | 3450 |
| Rb | 2900 | 3100 | 2600 |
| Sr | 10000 | 11100 | 7200 |
| Y | 2200 | 2100 | 1300 |
| Zr | 6300 | 5900 | 4900 |
| Nb | 360 | 390 | 250 |
| Sb | 70 | 68 | 196 |
| Ba | 4200 | 3700 | 2600 |
| La | 295 | 310 | 235 |
| Ce | 830 | 900 | 660 |
| Pr | 123 | 132 | 94 |
| Nd | 628 | 682 | 460 |
| Sm | 185 | 195 | 140 |
| Eu | 73 | 78 | 54 |
| Gd | 299 | 310 | 214 |
| Tb | 53 | 57 | 35 |
| Dy | 343 | 366 | 240 |
| Ho | 73 | 81 | 50 |
| Er | 226 | 248 | 166 |
| Tm | 39 | 39 | 25 |
| Yb | 205 | 220 | 160 |
| Lu | 31 | 33 | 24 |
| Hf | 180 | 170 | 140 |
| Ta | 22 | 23 | 15 |
| W | 160 | 110 | 140 |
| Pb | 240 | 370 | 1100 |
| Th | 42 | 43 | 30 |
| U | 12 | 13 | 9 |

**below detection limit = bdl; not analysed = na*

### 6.1 The Thuathe meteorite

The chondrite normalised spidergram (after Anders and Grevasse, 1989), of H-group chondrites as given by Wasson and Kallemyn (1988) serves as a reference for the Thuathe meteorite (**Figure 6.1**). The chondrite normalised REE pattern is relatively flat with no significant LREE/HREE variation. Compared to the chondrite normalised REE diagram for H-group chondrites (Wasson and Kallemeyn, 1988), a similar trend is shown. In the chondrite normalised trace element diagram (**Figure 6.2**), very slight enrichment of Ta and U compared to H-group chondrites are noted. These elements can be slightly enriched in H-group chondrites (Von Michaelis, 1964 and Mason, 1966). The depletions noted in Zn andPb is mirrored by the reference values by Wasson and Kallemeyn (1988) and is characteristic for H-group chondrites.

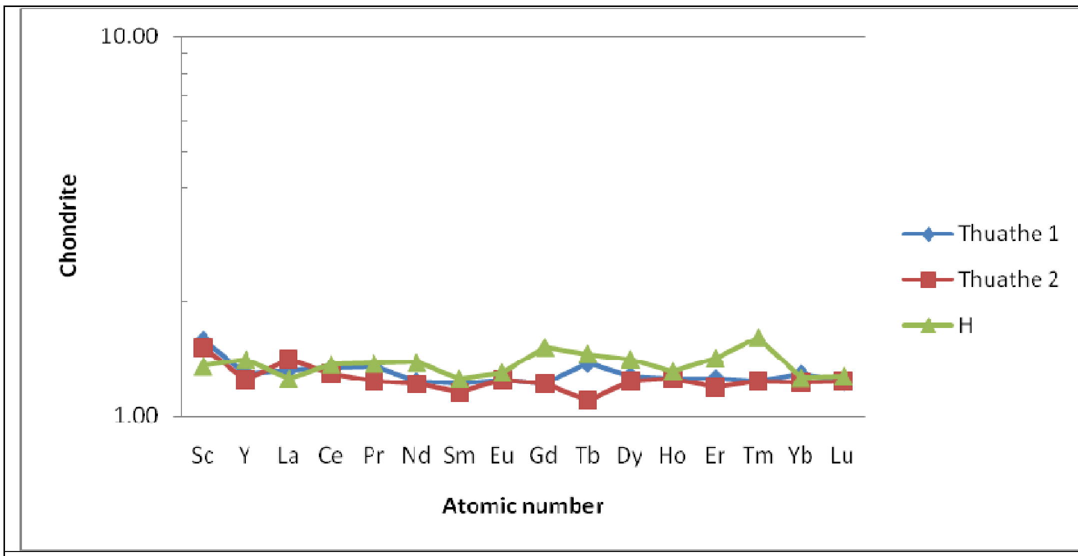


**Figure 6.1: Chondrite-normalised chemical variation of the REE's in the Thuathe meteorite as well as general H-group chondrites (Wasson and Kallemyn, 1988), plotted on a spidergram (normalised after Anders and Grevasse, 1989) to determine its relative enrichment/depletion with respect to chondrite.**

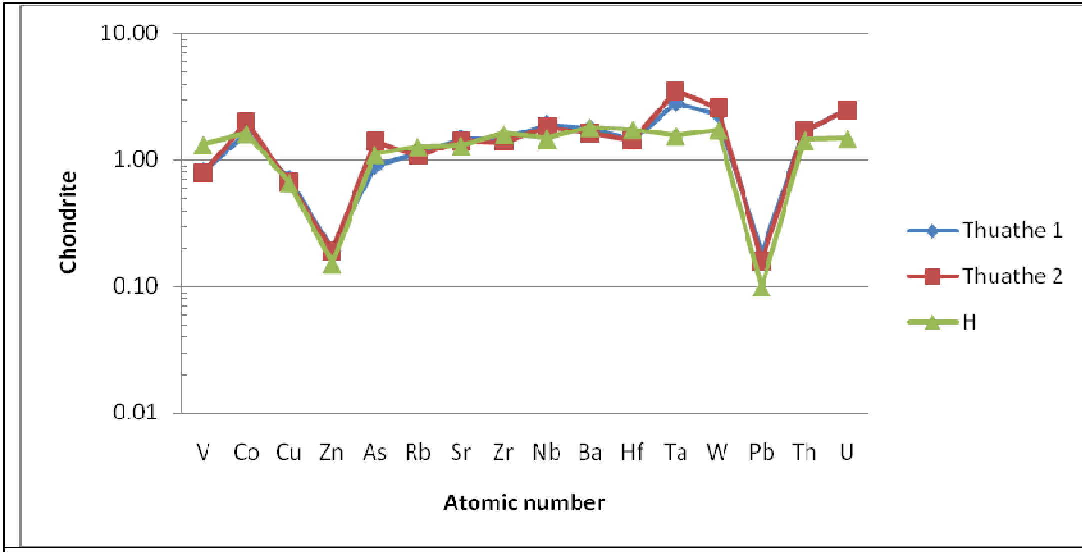


**Figure 6.2: Chondrite-normalised chemical variation of trace elements in the Thuathe meteorite as well as general H-group chondrites (Wasson and Kallemyn, 1988), plotted on a spidergram (normalised after Anders and Grevasse, 1989) to determine its relative enrichment/depletion with respect to chondrite.**

## 6.2 The Machinga meteorite

The chondrite normalised spidergram (after Anders and Grevasse, 1989), of E-group and L-group chondrites as given by Wasson and Kallemyn (1988) serves as a reference for the Machinga meteorite. The rare earth element pattern is relatively flat with slight LREE/HREE variation from the norm as described by Masuda *et al* (1973). The Machinga meteorite shows more similarities with the E-group chondrites than with the L-group chondrites (**Figure 6.3**). The trace element chondrite normalised diagram (**Figure 6.4**), shows similarities mostly with the E-group chondrites (**Table 5.2**). The trends cannot be conclusively matched with either the E-group or L-group chondrites. Slight enrichment of W, Pb and U is noted. Slight enrichment of W, Pb and U is noted which is the norm for E-group chondrites (Von Michaelis, 1964 and Mason, 1966). Marked depletions of Zn and Pb are observed in the reference values for L- and E-group chondrites. A marked depletion of Zn, corresponding to L-group chondrites, is observed in the Machinga meteorite.

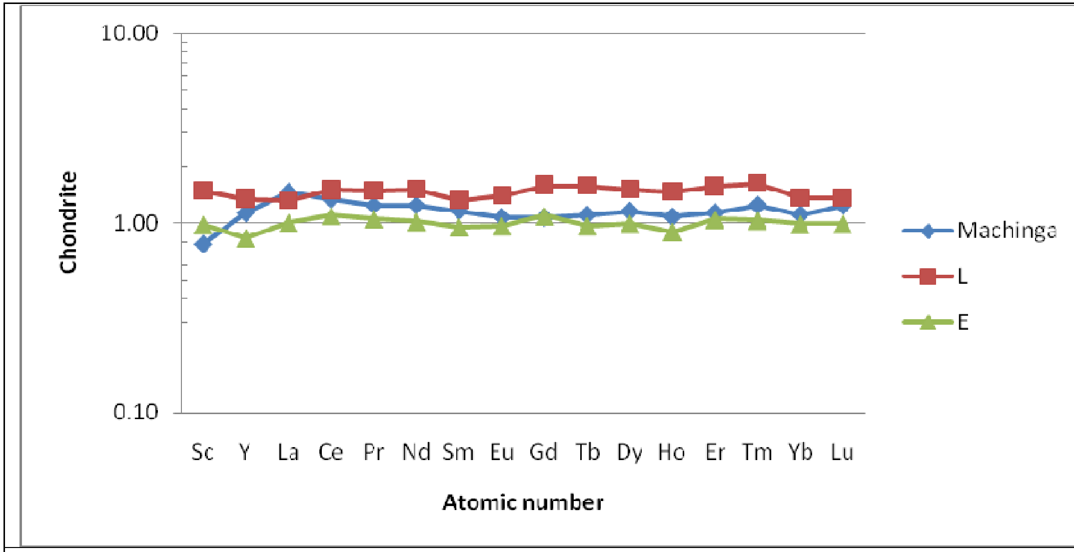


**Figure 6.3: Chondrite-normalised chemical variation of the REE's in the Machinga meteorite as well as general L-group and E-group chondrites (Wasson and Kallemyn, 1988), plotted on a spidergram (normalised after Anders and Grevasse, 1989) to determine its relative enrichment/depletion with respect to chondrite.**

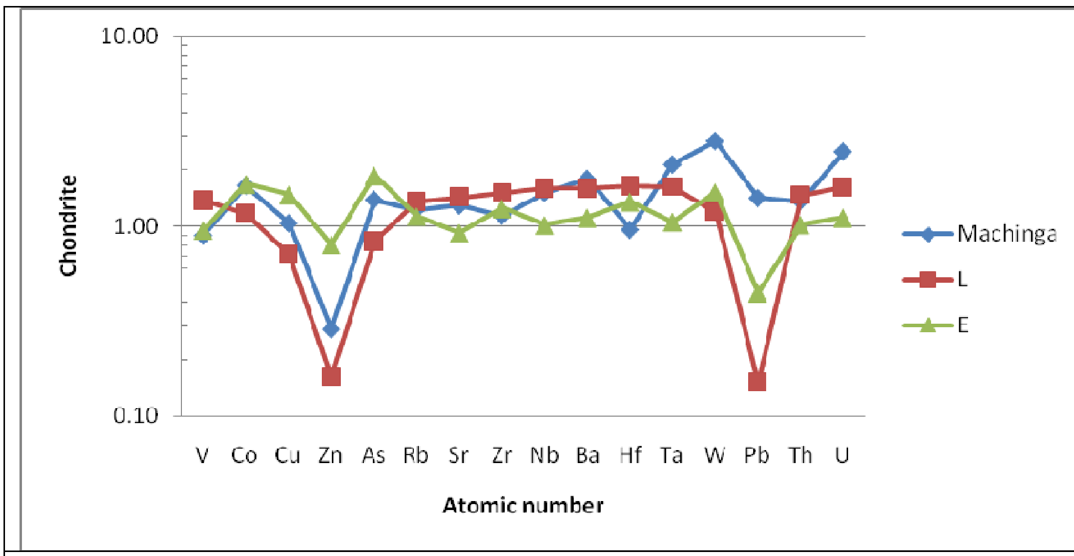


**Figure 6.4: Chondrite-normalised chemical variation of trace elements in the Machinga meteorite as well as general L-group and E-group chondrites (Wasson and Kallemyn, 1988), plotted on a spidergram (normalised after Anders and Grevasse, 1989) to determine its relative enrichment/depletion with respect to chondrite.**

## 6.3 The Balaka meteorite

The negative correlation between iron and nickel is obtained from analyses of kamacite and taenite. According to both the t- and F tests the correlation is statistically significant as the values obtained (regression Ni = 100.3953 – 1.0094 Fe; t = 285.13; F = 42168.18) are distinctly greater than values cited for statistical significance ($t_{0.01,10}$ = 3.169 and $F_{0.01,1:10}$ = 10.04) (Downie and Heath, 1970). The chondrite normalised spidergram (after Anders and Grevasse, 1989), of L-group chondrites as given by Wasson and Kallemyn (1988) serves as a reference for the Balaka meteorite. The rare earth element pattern is flat with nearly no variation between LREE and HREE (**Figure 6.5**). The normalised trace element diagram mirrors the trends of the trace element diagram of the L-group chondrites (**Figure 6.6**) with respect to ordinary chondrites (**Table 5.2**).

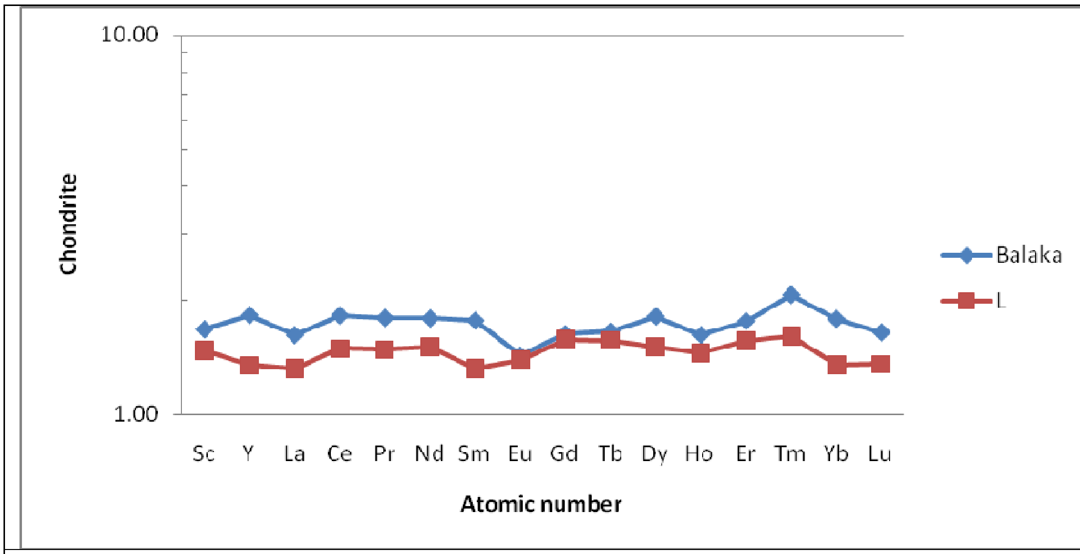


**Figure 6.5: Chondrite-normalised chemical variation of the REE's in the Balaka meteorite as well as general L-group chondrites (Wasson and Kallemyn, 1988), plotted on a spidergram (normalised after Anders and Grevasse, 1989) to determine its relative enrichment/depletion with respect to chondrite.**

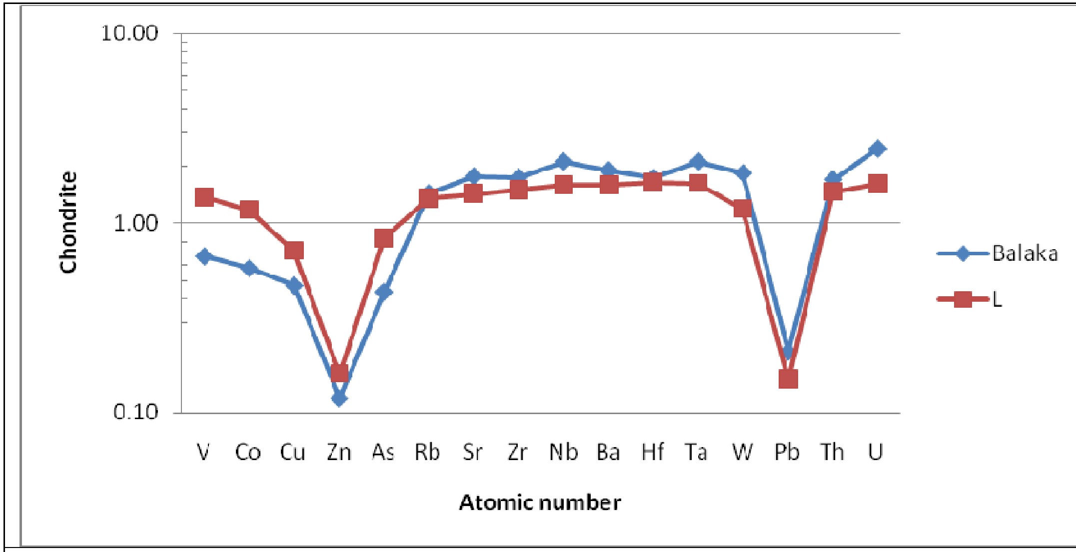


**Figure 6.6: Chondrite-normalised chemical variation of trace elements in the Balaka meteorite as well as general L-group chondrites (Wasson and Kallemyn, 1988), plotted on a spidergram (normalised after Anders and Grevasse, 1989) to determine its relative enrichment/depletion with respect to chondrite.**

### 6.4 The Chisenga meteorite

There is a negative correlation between iron and nickel. According to both the t- and F tests the correlation is statistically significant as the test values obtained (regression Ni = 100.0751754 – 1.007476956 Fe; t = 208.2473; F = 30549.8) are greater than those cited as minima for statistical significance ($t_{0.1,38}$ = 2.704 and $F_{0.1,1:38}$ = 7.35) (Downie and Heath, 1970). The chemistry of this Ni-rich meteorite (**Table 5.1 and Table 5.2**) is similar to the composition of metallic Fe-Ni in main-group pallasites (Goldstein, 2009).

### 6.5 The unreported meteorite specimens from Asab

The chondrite normalised spidergram (after Anders and Grevasse, 1989), of L-group chondrites as given by Wasson and Kallemyn (1988) serves as a reference for the unknown meteorite specimens from Asab. The Asab 1 unreported sample is the smallest of the three samples and shows the most chemical alteration of the three samples. The rare earth element spectrum for the sample 1 from Asab shows enrichment of LREE (**Figure 6.8**). This may be attributed to the highly weathered nature of this meteorite. Chemical alteration due to weathering in hot arid environments typically yields LREE enrichment (Crozaz *et.al.*, 2003). Enrichment of Ba, Sr, Th and U is shown in this sample. This is typical of chemical weathering in a hot arid environment (Crozaz *et.al.*, 2003 and Saunier *et.al.*, 2010).

Sample 2 from Asab shows slight La enrichment (**Figure 6.9**) compared to L-group chondrites. This can be ascribed to the enrichment of LREE typically seen in chemically altered chondrites in hot arid environments (Crozaz *et.al.*, 2003). Enrichment in Ba, Sb, Sr and U is shown in the chondrite normalised trace element diagram (**Figure 6.10**). This enrichment is typical in chemically weathered chondrites in a hot arid environment (Crozaz *et.al.*, 2003 and Saunier *et.al.*, 2010).

Sample 3 from Asab is the biggest of the three Asab samples. It displays a flat chondrite normalised REE pattern with nearly no variation between LREE and HREE (**Figure 6.11**). Chemical variation in these meteorite samples (**Table 5.2**) in the chondrite normalised trace element diagram shows enrichment of Ba, Sb and Sr, typical of chemical weathering in hot arid conditions (Crozaz *et.al.*, 2003 and Saunier *et.al.*, 2010).

The general trends of the diagrams of the three specimens from Asab are similar indicating that the three unknown specimens are of the same fall.

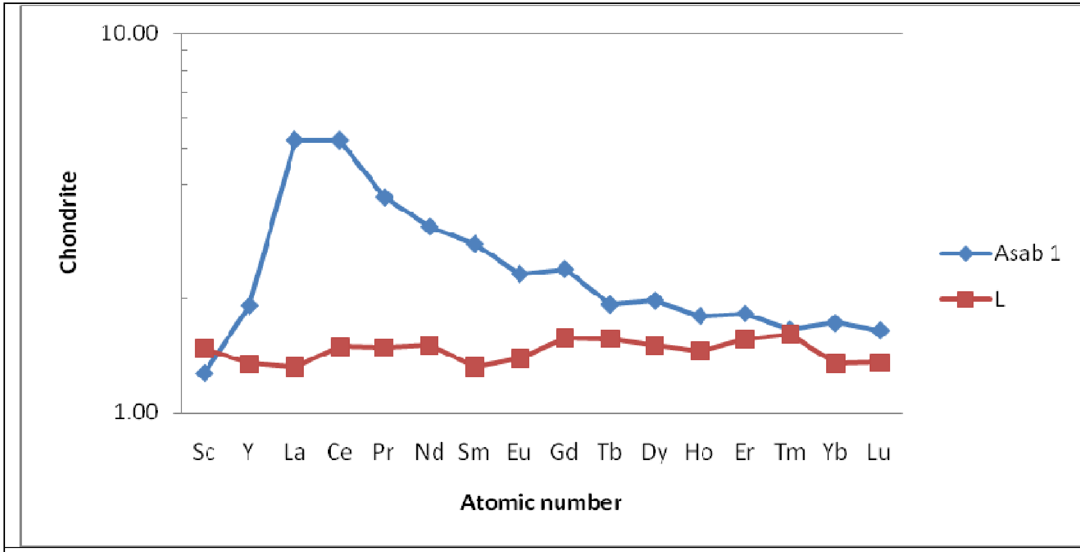


**Figure 6.7: Chondrite-normalised chemical variation of the REE's in the unreported meteorite sample Asab 1 as well as general L-group chondrites (Wasson and Kallemyn, 1988), plotted on a spidergram (normalised after Anders and Grevasse, 1989) to determine its relative enrichment/depletion with respect to chondrite.**

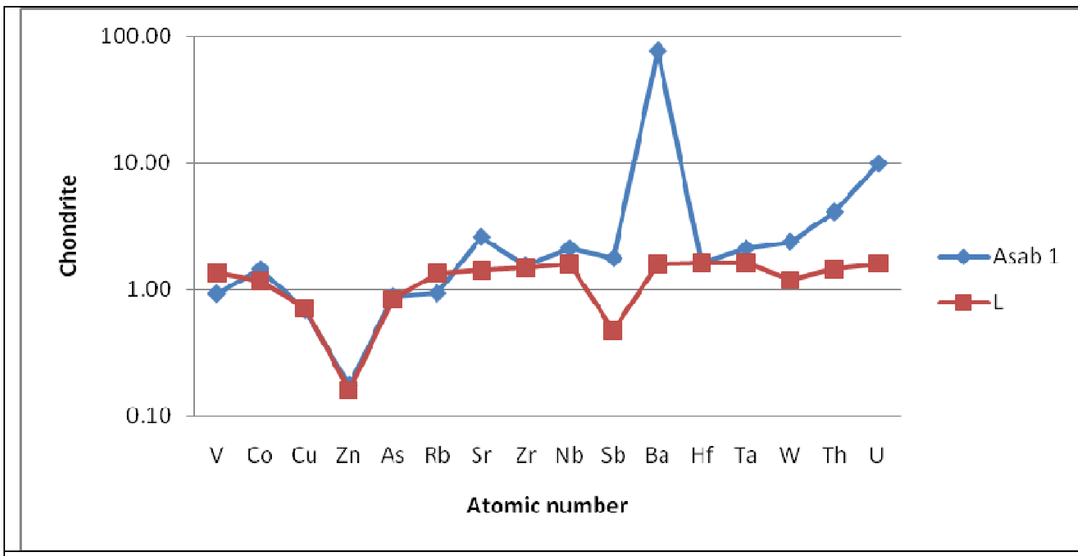


**Figure 6.8: Chondrite-normalised chemical variation of trace elements in the unreported meteorite sample Asab 1 as well as general L-group chondrites (Wasson and Kallemyn, 1988), plotted on a spidergram (normalised after Anders and Grevasse, 1989) to determine its relative enrichment/depletion with respect to chondrite.**

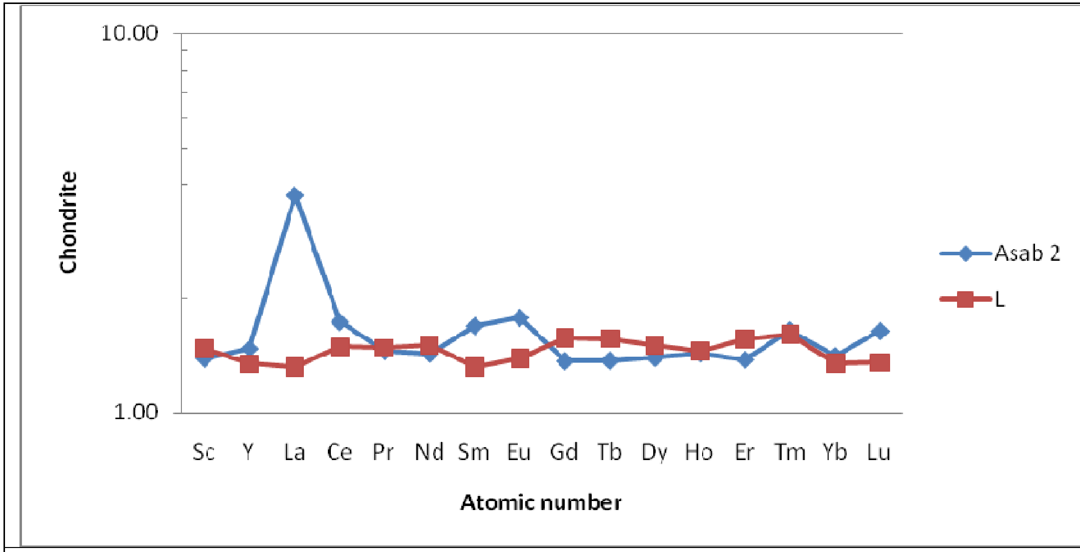


**Figure 6.9: Chondrite-normalised chemical variation of the REE's in the unreported meteorite sample Asab 2 as well as general L-group chondrites (Wasson and Kallemyn, 1988), plotted on a spidergram (normalised after Anders and Grevasse, 1989) to determine its relative enrichment/depletion with respect to chondrite.**

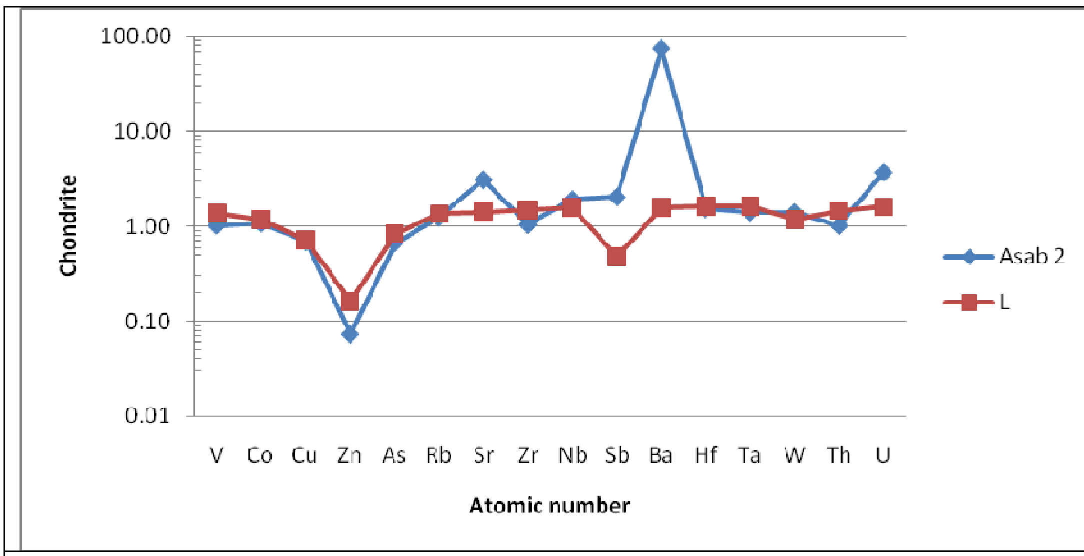


**Figure 6.10: Chondrite-normalised chemical variation of trace elements in the unreported meteorite sample Asab 2 as well as general L-group chondrites (Wasson and Kallemyn, 1988), plotted on a spidergram (normalised after Anders and Grevasse, 1989) to determine its relative enrichment/depletion with respect to chondrite.**

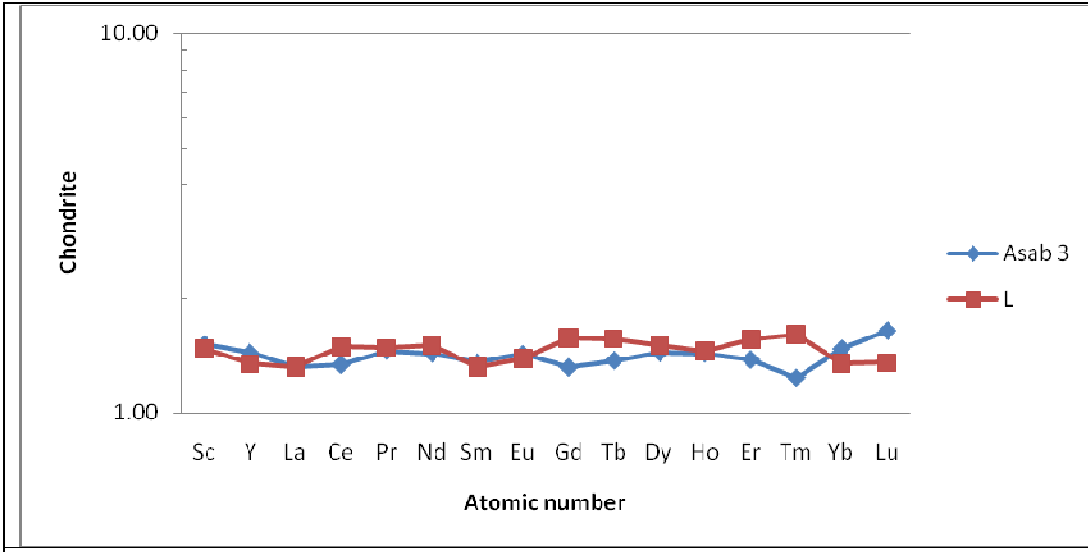


**Figure 6.11: Chondrite-normalised chemical variation of the REE's in the unreported meteorite sample Asab 3 as well as general L-group chondrites (Wasson and Kallemyn, 1988), plotted on a spidergram (normalised after Anders and Grevasse, 1989) to determine its relative enrichment/depletion with respect to chondrite.**

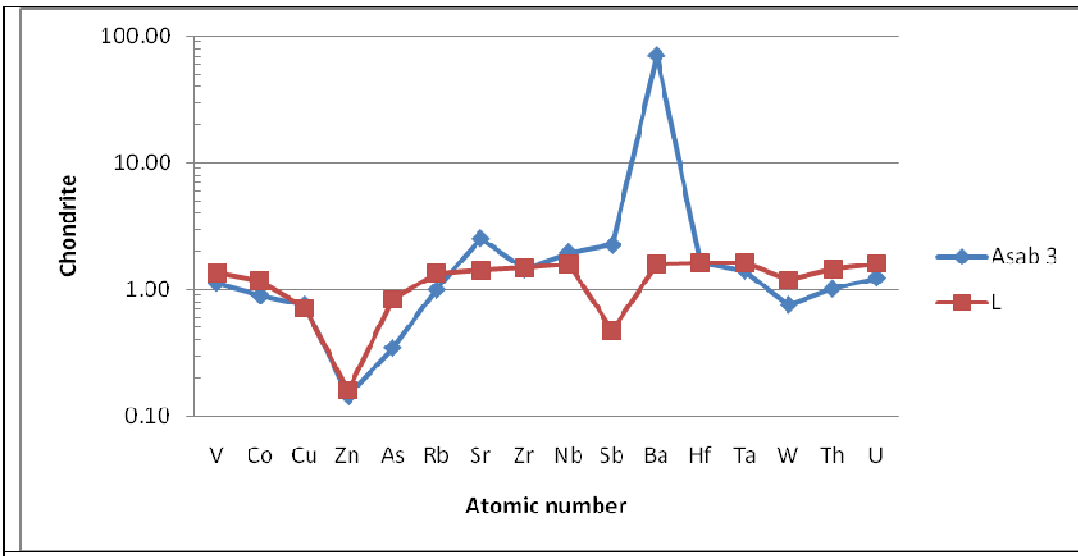


**Figure 6.12: Chondrite-normalised chemical variation of trace elements in the unreported meteorite sample Asab 3 as well as general L-group chondrites (Wasson and Kallemyn, 1988), plotted on a spidergram (normalised after Anders and Grevasse, 1989) to determine its relative enrichment/depletion with respect to chondrite.**

# CHAPTER 7
# CLASSIFICATION

Various different types of classification are used for meteorite identification. The first distinction is made between a fall and a find. A meteorite that is seen to fall is termed a "fall" while a meteorite that was only collected without a sighting and recognised by other methods such as chemical composition, mineralogy and structure is termed a "find" (Mason, 1962; Wasson, 1974; Dodd, 1981 and Zanda and Rotaru, 2001).

The second distinction can be made by making use of major and trace element data (Dodd, 1981). Wasson (1974) and Norton (1998) group meteorites into four broad categories: chondrites, achondrites, irons and stony irons, while Dodd (1981) prefers 3 general categories irons (siderites), stones (aerolites) and stony irons (siderolites) as discussed in the introduction.

Primary classification of meteorites is done making use of bulk chemistry (Wasson, 1974; Dodd, 1981 and Krot *et al*, 2004). Comparison of atomic Mg/Si, Fe/Si and Al/Si ratios are used to distinguish between the different groups and classes of chondritic meteorites (Dodd, 1981). The total metal and silicate ratio is also used to distinguish between the different chondrite groups. H-chondrites contains high total iron and high metallic iron (15 – 20% FeNi metal by mass. L-chondrites contains low total iron (7-11% FeNi metal by mass) and LL-chondrites contains low total iron and low metal (3-5% FeNi metal by mass. Enstatite condrites are the most chemicall reduced chondrites and Fe occurs in the form of metal/sulphides rather than oxides, and is high (Krot *et al*, 2004). Subclassification of iron meteorites are based on the abundance of Ni and several trace elements as well as kamacite bandwidth in octahedrites (Wasson, 1974; Dodd, 1981 and Haack and McCoy, 2003).

Chondrites are furthur subdivided into petrologic types on the basis of textural and mineralogical variations (Dodd, 1981).

Degree of shock is used as an additional classification category for ordinary chondrites and carbonaceous chondrites. Rubin (2003) suggested the use of chromite and plagioclase as a shock indicator for ordinary chondrites. The generally accepted classification is based on the shock effects in olivine and plagioclase (Stöffler *et al*, 1991). The sample is studied microscopically to determine shock charateristics (Stöffler *et al*, 1991).

Weathering classification can be observed in hand specimens or in polished thin sections (Krot *et al*, 2004), of which the latter is seldom used. Weathering categories for hand specimens are a) minor rustiness, b) moderate rustiness, c) severe rustiness and d) evaporite minerals visible to the naked eye (Krot *et al*, 2004).

## 7.1 The Thuathe meteorite

The Thuathe meteorites have been classified as an H-type ordinary chondrite. Major element data are plots and the atomic Mg/Si, Fe/Si and Al/Si ratios were used to determine this classification (**Table 5.1 and Figure 7.1**) (Dodd, 1981). Petrologic type was also determined (after Dodd, 1981) (**Table 1.3)**. The Thuathe meteorites belong to the H4 type as the olivine is essentially homogeneous with a composition of $Fo_{87}$, the pyroxene is nearly homogeneous with an average composition of $En_{85}$ and plagioclase is microcrystalline. Troilite is essentially Ni free (S ~ 36 wt%; Fe ~ 62 wt%; Cu, Pb, Zn ~1.95 wt % and Ni < 0.05 wt%) and chromite is homogeneous ($Cr_2O_3$ ~ 53.8 wt %) (**Appendix A**). Shock features are classified as S2/3 (Stöffler *et al,* 1991) (**Table 1.4**). S2/3 chondrites are very weakly to weakly shocked and show undulatory extinction and irregular fractures in olivine (**Figure 4.2)**. The terrestrial weathering classification after the classification system of Wlotzka (1993) for the Thuathe meteorite is W0 as there is no visible oxidation of metal or sulphides in hand specimen.

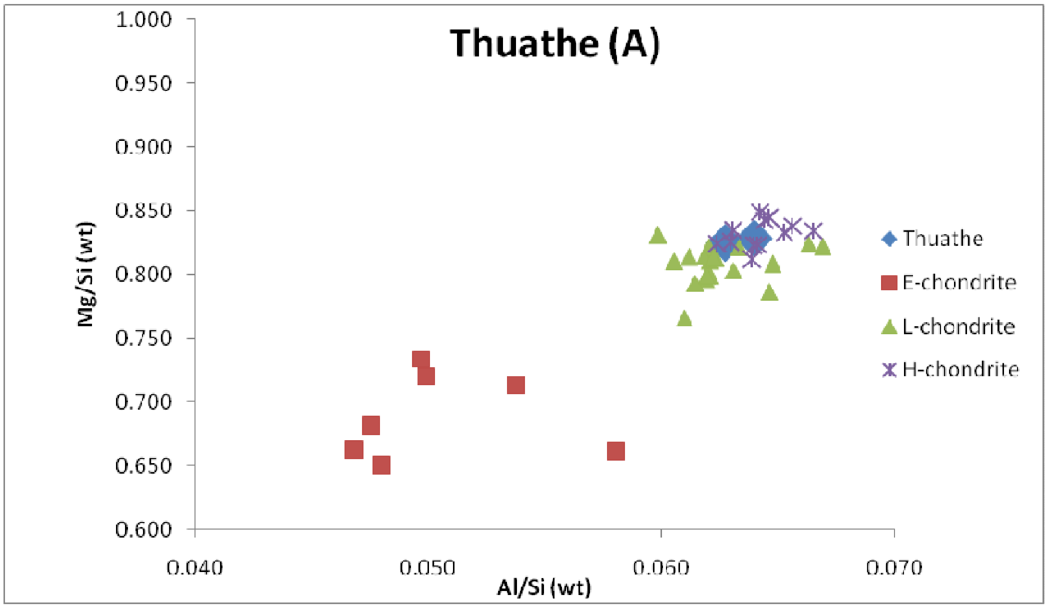


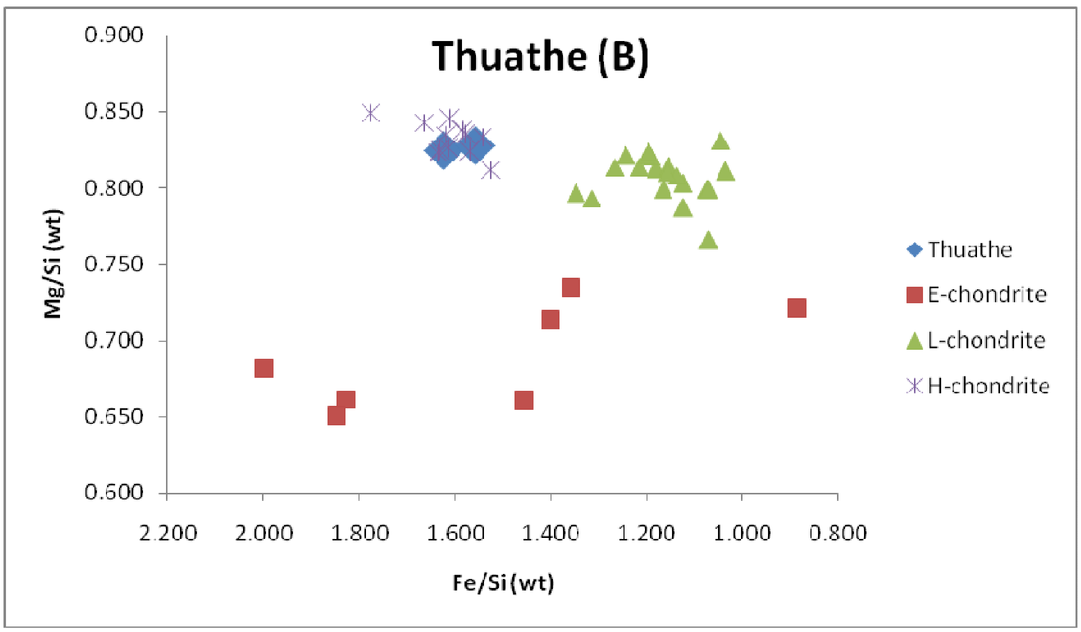


**Figure 7.1: Classification of the Thuathe meteorite using chemical data: A = Al/Si versus Mg/Si, and B = Fe/Si versus Mg/Si. References used: Dodd (1981); von Michaelis *et al* (1969); Mason (1971).**

## 7.2 The Machinga meteorite

Ratio plots of Al/Si, Fe/Si and Mg/Si (**Table 5.1 and Figure 7.2**) reveal that the classifications are ambigious and that the Machinga meteorite might be closer in classification to an E chondrite than a L chondrite (after Dodd, 1981). The presence of only enstatitic pyroxene ($En_{97}$), olivine ($Fo_{95}$), plagioclase ($Ab_{86}$), only kamacite and no taenite indicates an E6 rather than L6 chondrite classification (**Appendix B**). Previously the Machinga meteorite was classified as a L6 type ordinary chondrite with olivine ($Fo_{75}$), clinopyroxene ($En_{54}$), orthopyroxene ($Fs_{22}$), plagioclase ($Ab_{86}$) and chromite ($Cr_2O_3$ ~ 57 wt%) (Graham *et al*, 1984). It was refined to L6d with rare accessory phases of apatite and pentlandite (Koeberl *et al*, 1990), olivine ($Fo_{74-78}$), rare clinopyroxene ($En_{45-47}$), orthopyroxene ($En_{75-78}$) and plagioclase ($Ab_{82-85}$). According to Dodd, 1981 CM type carbonaceous chondrites commonly include calcite and magnetite in the matrix, as found in this meteorite. The Machinga meteorite is moderately shocked (S4) according to the classification system of Stöffler *et al* (1991) and exhibits weak mosaicism and planar fractures in olivine (**Table 1.4**). Shock on this meteorite is described as being in the order of 15 – 20 Gpa pressure maximum as detected in pyroxene (Koeberl *et al*, 1990).

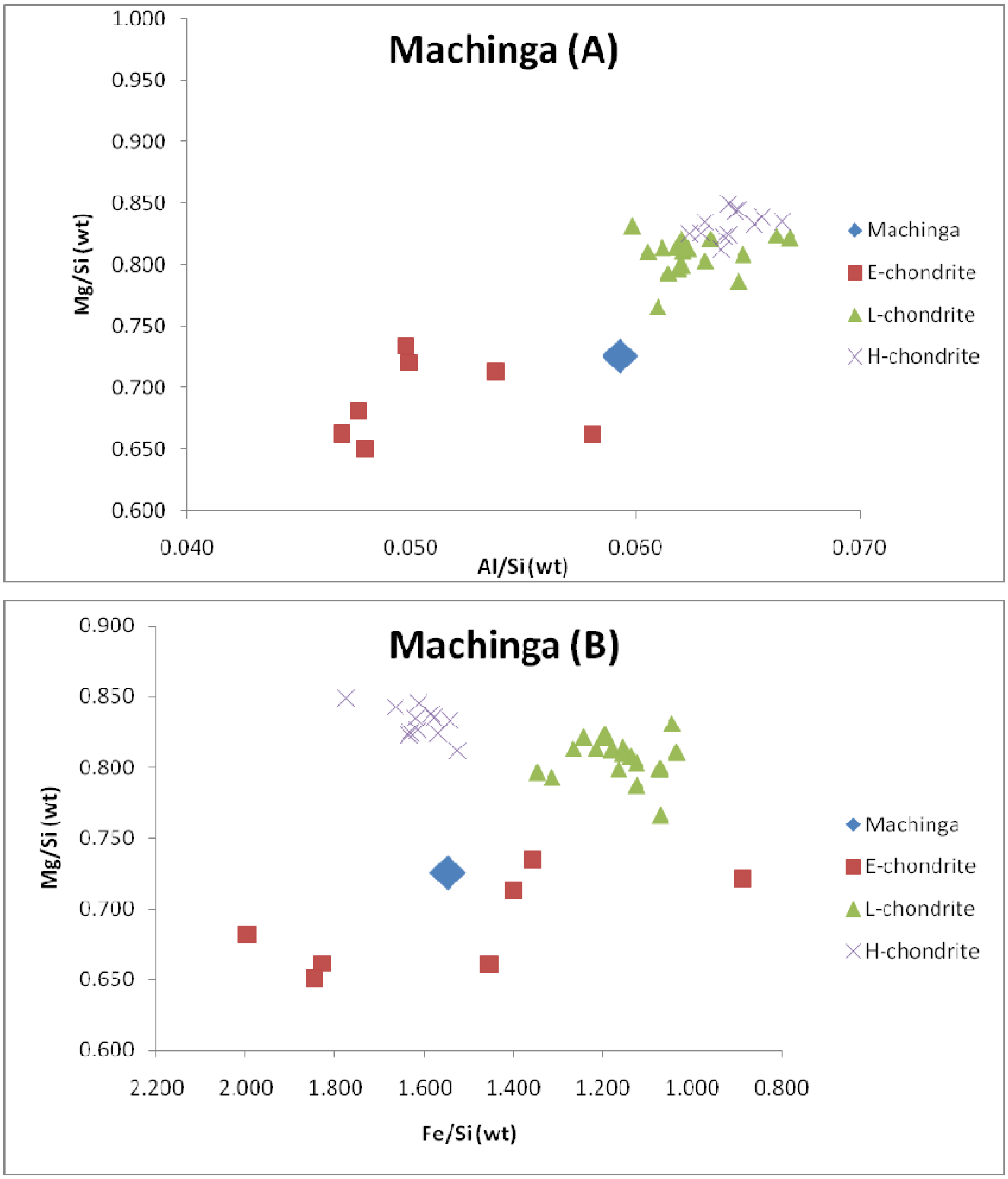


**Figure 7.2: Classification of the Machinga meteorite using chemical data: A = Al/Si versus Mg/Si, and B = Fe/Si versus Mg/Si. References used: Dodd (1981); von Michaelis *et al* (1969); Mason (1971).**

**Table 7.1: Mineralogical comparison of E6 chondrites, L6 ordinary chondrites and the Machinga meteorite. Literature references (1) Brearley and Jones, 1998; (2) Dodd, 1981; (3) Koeberl et al, 1991.**

| Minerals | E6 chondrite | L6 ordinary chondrite | Machinga |
|---|---|---|---|
| Orthopyroxene | Enstatitic (low Ca)[1] | Composition varies[2] | $En_{98}$ Low Ca |
| Olivine | No reported olivine[1] | Most abundant mineral in ordinary chondrites; Composition varies[2] | $Fo_{95}$ but occurs rarely |
| Plagioclase | $An_7$[1] | $An_{86}$[1] | $An_9$ |
| Troilite | Present[1] | Present[1] | Present |
| Fe-Ni phases (kamacite – taenite) | Kamacite only[2] | Kamacite-taenite[2] | Kamacite only |
| Apatite | Rare[3] | Rare[3] | Not encountered in this study, but reported by Koeberl et al. (1991), thus presumably rare |
| Pentlandite | Rare[3] | Rare[3] | Not encountered in this study, but reported by Koeberl et al. (1991), thus presumably rare |
| Chromite | Not reported in literature study | Most abundant accessory mineral in ordinary chondrites[2] | Not encountered in this study, but reported by Koeberl et al. (1991), thus presumably rare |

## 7.3 The Balaka meteorite

The Balaka meteorite proves to be a L-type ordinary chondrite (**Table 5.1 and Figure 6.3**). The petrologic type is 6 according to Dodd, 1981 and Wasson, 1974 (**Table 1.3**). Olivine ($Fo_{78}$) and pyroxene ($En_{79}$) are homogeneous (**Table 4.1**) and plagioclase ($Ab_{83}$) is coarse in texture. Kamacite (Ni ~ 5.8 wt%) and taenite (Ni ~ 33.7 wt%) is present with troilite (S~36 wt%; Fe~63 wt%) as well as chromite ($Cr_2O_3$ ~ 57 wt%) (**Appendix C**). The Balaka meteorite is weakly shocked (S3) showing undulatory extinction and irregular fractures in olivine (after the classification system of Stöffler *et al,* 1991) (**Figure 4.16**).

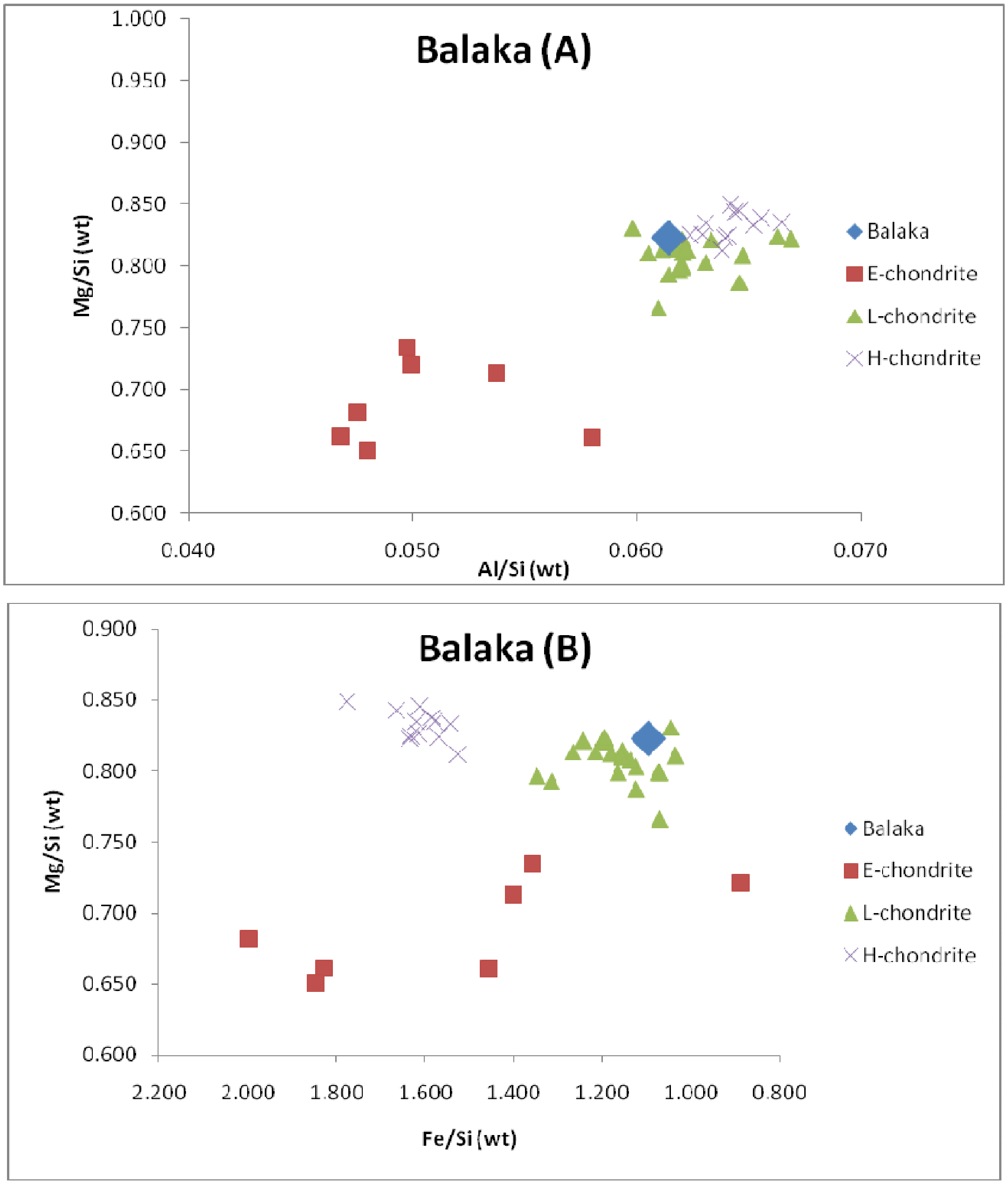


**Figure 7.3: Classification of the Balaka meteorite using chemical data: A = Al/Si versus Mg/Si, and B = Fe/Si versus Mg/Si. References used: Dodd (1981); von Michaelis *et al* (1969); Mason (1971).**

## 7.4 The Chisenga meteorite

Classification of iron meteorites is be based on their chemistry and texture. The Chisenga meteorite was classified as a being close to groups IA and IIB chemically and a coarse octahedrite in texture (Og) by Chapola (1991) and Wlotzka (1992). This classification was reviewed and with further analysis (Grady, 2001) it was classified as a class IIIAB iron meteorite, which is the most common and largest group of iron meteorites (Goldstein, 2009). This classification is based on the fact the the meteorite sample studied contained no silicate inclusions and the chemical composition with regards to Ni (~6.9 wt%), Ga (~21 ppm), Ge (~42 ppm) and Ir (517 ppb). **Table 5.1 and 7.2** corresponds to the values given by Dodd (1981) and Hutchison (2004), for group IIIAB iron meteorites. The coarseness of the Widmanstätten structure in the Chisenga meteorite proves it to be in the medium octahedrite textural group (Om) (after Dodd, 1981) with kamacite band width of on average 1.5mm and taenite bands about 0.1mm, but the texture can also be observed on a sub-millimeter scale as illustrated in **Figure 7.4** and **7.5**.

**Figure 7.4: A Backscattered electron image of kamacite and taenite intergrowth in the Chisenga iron meteorite.**

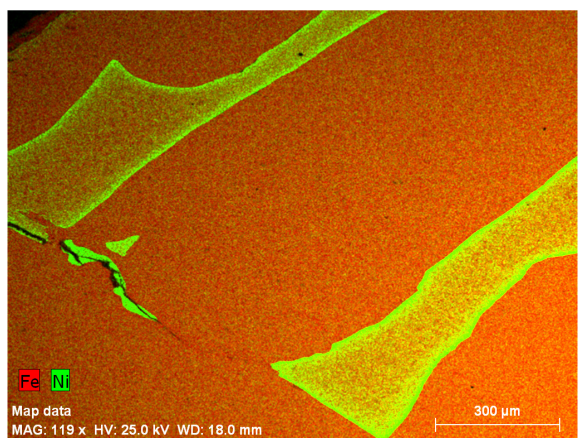


**Figure 7.5: An element map of the backscattered electron image (Figure 6.4) illustrating the concentration of iron (red to orange) and nickel (green) in the Chisenga meteorite.**

**Table 7.2: Classification characteristics of the Chisenga meteorite compared to Group IIIAB iron meteorites.**

| | Group IIIAB | Chisenga |
|---|---|---|
| Ni (wt %) | 7.1 – 10.5 wt% | 6.2 – 8.9 wt% |
| Ga (ppm) | 16 – 23 ppm | 21 ppm |
| Ge (ppm) | 27 – 47 ppm | 42 ppm |
| Ir (ppb) | 10 – 20 000 ppb | 517 ppb |

## 7.5 The unknown meteorite specimens from Asab

The Asab meteorites proves to be L-type ordinary chondrites (**Table 5.1 and Figure 7.6**). The petrologic type is 6 according to Dodd, 1981 and Wasson, 1974 (**Table 1.3**). Olivine ($Fo_{77}$) and pyroxene ($Fs_{76}$) are homogeneous and albitic plagioclase ($Ab_{89}$) is coarse (**Appendix E**). The Asab meteorites are moderately shocked (S4) showing mosaicism and planar fractures in olivine (after the classification system of Stöffler *et al,* 1991) (**Figures 4.25 – 4.30**). Terrestrial weathering is also visible in hand specimens and the weathering stage is W2 after the classification system of Wlotzka (1993). Moderate oxidation of metal is observed.

There are 18 known meteorites from Namibia (**Table 7.3**). Of these 11 are ordinary chondrites and 5 are L-group chondrites. Comparing the localities of these meteorites with that of the unknown specimens from Asab, it is concluded that none of the known L-group chondrites correspond to the studied specimens.

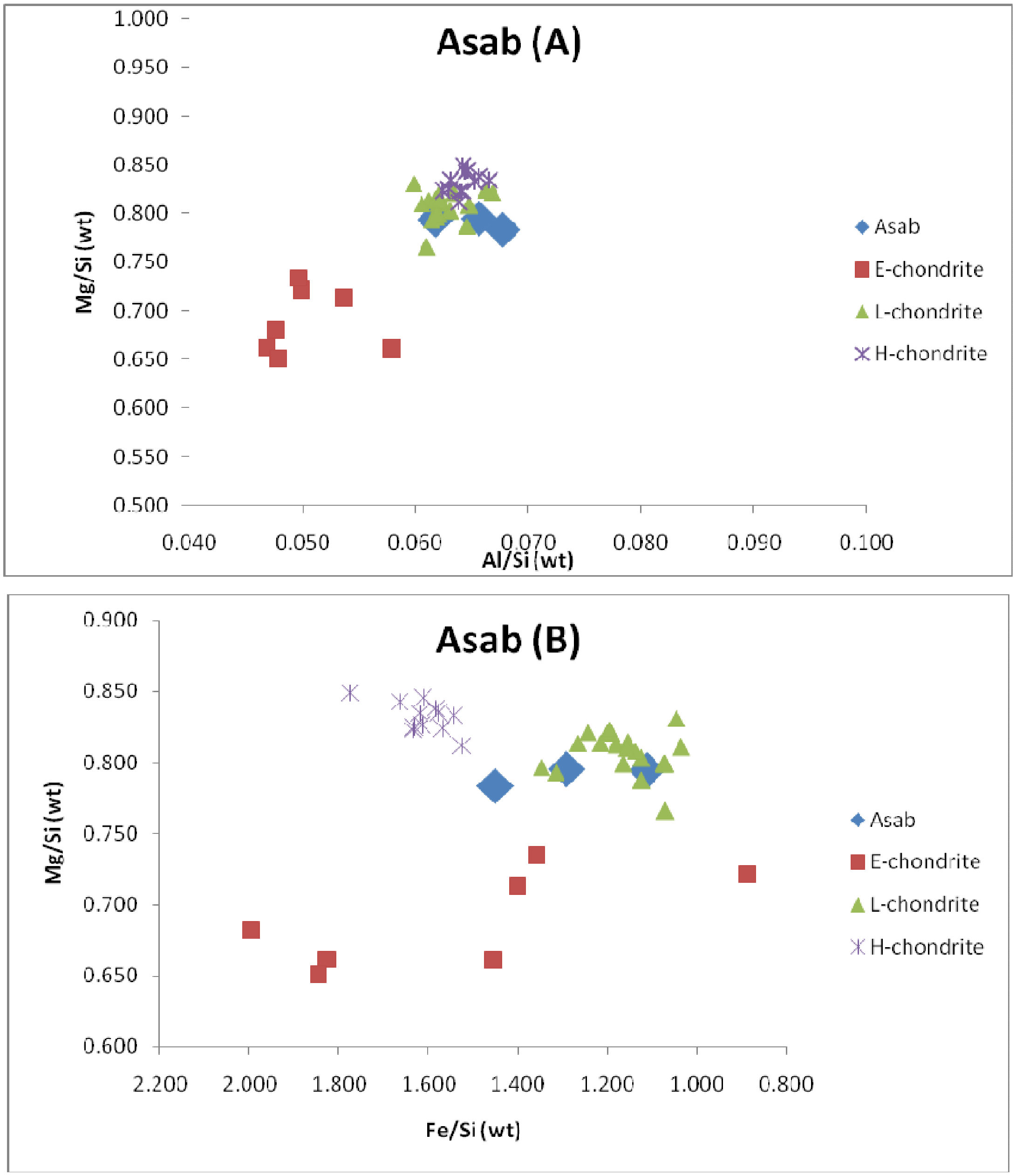


**Figure 7.6: Classification of the Asab meteorites using chemical data: A = Al/Si versus Mg/Si, and B = Fe/Si versus Mg/Si. References used: Dodd (1981); von Michaelis *et al* (1969); Mason (1971).**

**Table 7.3: Recorded meteorites from Namibia.**

| Name | Year | Fall/ Find | Coordinates | Recovered weight | Type | Class | Group | Petrologic / Structural type | Bandwidth | Shock stage | Weathering grade |
|---|---|---|---|---|---|---|---|---|---|---|---|
| Asab | 1999 | Find | 25° 26' S / 17° 55' E | 1.53 kg | Stone | Ordinary | H | 5 | na | S2 | W1 |
| Aus | NR | Find | 26° 40' S / 16° 15' E | NR | Stone | Ordinary | L | NR | na | NR | NR |
| Etosha | NR | Find | 18° 30' S / 16° E | 110.7 kg | Iron | Medium octahedrite | IC | Om | NR | NR | NR |
| Gibeon | 1836 | Find | 25° 30' S / 18° E | NR | Iron | Fine octahedrite | IVA | Of | 0.3 mm | NR | NR |
| Gobabeb | 1969 | Find | 23° 33' S / 15° 2' E | 27 kg | Stone | Ordinary | H | 4 | na | NR | NR |
| Hoba | 1920 | Find | 19° 35' S / 17° 55' E | 60 t | Iron | Ataxite | IVB | D | NR | NR | NR |
| Itzawisis | 1946 | Find | 26° 16' S / 18° 11' E | 0.35 kg | Stony-Iron | Pallasite | PAL | na | NR | NR | NR |
| Karasburg | 1964 | Find | 27° 40' S / 18° 58' E | NR | Iron | Medium octahedrite | IIIAB | Om | 1.2 mm | NR | NR |
| Korra Korrabes | 1996 | Find | 25° 12' S / 18° 5' E | 120 - 130 kg | Stone | Ordinary | H | 3 | na | S1 | W2 |
| Maltahöhe | 1991 | Find | 24° 55' S / 16° 59' E | 22.272 kg | Iron | Fine octahedrite | IIICD | Of | NR | NR | NR |
| Namib desert | 1979 | Find | 24° 45' S / 15° 22' E | 1 kg | Stone | Ordinary | H | 4 | na | NR | NR |
| Okahandja | 1926 | Find | 21° 59' S / 16° 56' E | 6.6 kg | Iron | Hexahedrite | IIAB | H | NR | NR | NR |
| Ovambu | 1900 | Fall | 18° S / 16° E | 0.056 kg | Stone | Ordinary | L | 6 | na | NR | NR |
| Rooikop 001 | 1991 | Find | 23° 5' 00" S / 14° 42' 54" E | 1.039 kg | Stone | Ordinary | H | 5 | na | NR | NR |
| Rooikop 002 | 1991 | Find | 23° 5' 00" S / 14° 42' 54" E | 0.903 kg | Stone | Ordinary | L | 5 | na | NR | NR |
| Rooikop 003 | 1991 | Find | 23° 5' 00" S / 14° 42' 54" E | 0.902 kg | Stone | Ordinary | L | 4 to 5 | na | NR | NR |
| St Francis Bay | 1976 | Find | 25° 4' S / 14° 53' E | 0.531 kg | Stone | Ordinary | L | 6 | na | NR | NR |
| Witsand | 1932 | Find | 28° 40' S / 18° 55' E | NR | Stone | Ordinary | LL | 4 | na | NR | NR |

**not recorded = NR; not applicable = na*

# CHAPTER 8
# DISCUSSION

This project was undertaken to study the mineralogy and geochemistry of seven meteorite specimens from Malawi, Namibia and Lesotho and to classify them. The mineralogy was studied making use of optical microscopy as well as SEM with EDS detector and an electron microprobe for analysis of mineral phases. ICP as well as XRF techniques were used to obtain chemical information for the geochemical study of the meteorites. For classification purposes mineralogical and chemical data were utilised.

The Thuathe meteorite is a H4 ordinary chondrite with shock features classified as S2/3 and a weathering grade of W0. Metal constitutes ~ 7 volume % and silicates 93 volume % of the chondrite, with chondrules making up ~60 volume % of the silicate fraction. Several metal, sulphide, oxide and silicate mineral phases were distinguished: kamacite, troilite, chalcopyrite, chromite, plagioclase ($Ab_{78}$), olivine ($Fo_{87}$) and pyroxene ($En_{85}$). This meteorite is unique as it contains Sb sulphides, which had not been previously reported in any chondritic meteorite. The antimony sulphide minerals berthierite and stibnite was observed under the SEM and confirmed by means of electron microprobe analyses (De Bruyn *et al*, 2004). Pyroxene chondrules dominate, but chondrules composed of olivine were also observed. Chondrules are present but deficient in metal and sulphides compared to the host rock. The chondrite normalised spidergram for the Thuathe meteorite after Anders and Grevasse (1989) shows the REE spectrum is relatively flat with no significant LREE/HREE variation with only slight enrichment of Co, W and U and slightly more marked enrichment of Ta, as well as depletion in Cu, Zn and Pb. The overall trend corresponds with the reference sample after (Wasson and Kallemyn (1988), but the depletion in the reference values for Sb cannot be confirmed as it was not analysed in the Thuathe meteorites. Co, W, Ta and U are enriched, and Cu, Zn and Pb are depleted in H-group chondrites (Von Michaelis, 1964 and Mason, 1966).

The Machinga meteorite is classified as an E6 ordinary chondrite and is moderately shocked (S4). Previously it had been classified as an L6 chondrite (Graham *et al,* 1984 and Koeberl *et al,* 1990). This study demonstrates the heterogeneous nature of meteoritic material and the importance of representative sampling. The Machinga meteorite was examined and ~12 volume % metal and ~88 volume % silicates that contain ~ 70 volume % chondrules were observed. Microscopically the mineral phases identified were: pyroxene ($En_{97}$), olivine ($Fo_{96}$), plagioclase ($Ab_{86}$), troilite, magnetite, calcite and gypsum. Olivine particles were noted under the microscope as part of the matrix as well as in chondrules, but chondrules are dominantly pyroxenitic. The matrix is very fine crystalline and iron staining is evident. Chemical variation in the Machinga meteorite show slight enrichment of P, Co and Ba, more marked enrichment of Ta, W and U, as well as a slight depletion of Zn with respect to ordinary chondrites (Anders and Grevasse, 1989). The trends show similarities, but cannot be conclusively matched to the standard of Wasson and Kallemyn (1988). P is highly variable in chondrites and Co, Ba, Ta, W and U enrichment is the norm for E-group chondrites. It is slightly depleted in Zn (Von Michaelis, 1964 and Mason, 1966).

The Balaka meteorite is a L6 ordinary chondrite and is weakly shocked (S2). It has a very fine matrix with prominent alteration and iron staining and therefore mineral identification is very difficult. In the Balaka meteorite less than 3 volume % metal and ~ 93 volume % silicates are observed with ~50 volume % chondrules in the silicate fraction. Minerals were mainly identified by means of SEM techniques. The mineralogy of the meteorite is simple olivine ($Fo_{78}$), plagioclase ($Ab_{83}$), enstatitic pyroxene ($En_{79}$), chromite, Ti-magnetite, troilite, kamacite and taenite. Olivine chondrules are dominant in this meteorite. Chemical variation in the Balaka meteorite show slight depletion V, Co, Cu and As as well as slightly more marked depletion of Zn and Pb with respect to ordinary chondrites (Anders and Grevasse, 1989). The trends of the two diagrams are very similar with only slight depletions in V, Co, Cu and As that is not noted in the reference diagram (Wasson and Kallemeyn, 1988). V, Co, Cu, As, Zn and Pb depletion is expected for L-group chondrites (Van Michaelis, 1964 and Mason, 1966).

The Chisenga meteorite is classified as an IIIAB medium octahedrite. Kamacite, taenite, trolite and schreibersite were observed. Kamacite is the dominant Fe/Ni phase and Widmanstätten texture is very prominent. A cooling rate of 2.638ºC/Myr was determined for the Chisenga meteorite.

The unreported specimens from Asab prove to be L6 ordinary chondrites that are moderately shocked (S4) with a weathering grade of W2. The three Namibian meteorite specimens were examined microscopically. All three samples showed large mineral grains with prominent iron staining associated with the sulphide and oxide phases. The specimens contain less than 6 volume % metal with ~ 94 volume % silicates of which ~75 volume % constitutes chondrules. The minerals observed were: Olivine ($Fo_{77}$), plagioclase ($Ab_{89}$), enstatitic pyroxene ($En_{65}$), clinopyroxene ($Fs_{76}$), troillite and kamacite. Chondrules consisting of olivine and pyroxene were observed. Shock veins transect chondrules. The similar mineralogy and appearance of these samples confirms that the three samples are part of one event. Chemical variation in these meteorite samples show much more enrichment and depletion that the other meteorites studied. This may be due to more terrestrial weathering observed in these meteorites compared to any of the other studied samples. The rare earth element spectrum for the sample 1 from Asab shows slight enrichment of LREE/HREE, most marked in Ba, La, Ce, Th and U. Slight depletion of Zn is noted. Sample 2 from Asab shows slight Ba, La and U enrichment as well as slight depletion in Zn. Sample 3 from Asab displays a flat plot with nearly no variation between LREE and HREE (Anders and Grevasse, 1989; and Wasson and Kallemeyn, 1988 ). However, slight enrichment in Ba and depletion in Zn is observed. Chemical variation in these meteorite samples show much more enrichment and depletion that the other meteorites studied that can be due to terrestrial weathering. The general trends of the diagrams are similar indicating that the three unknown specimens are of the same fall. The enrichment of Ba, La, Ce, Th and U are not expected as these elements are usually depleted in chondrites, but variation can occur (Von Michaelis, 1964). The depleted values of Zn noted in these samples are as expected for chondrites (Van Michaelis, 1964 and Mason, 1966).

There are 18 known meteorites from Namibia of these 11 are ordinary chondrites and 5 are L-group chondrites. Comparing the localities of these meteorites with that of the unknown specimens from Asab, it is concluded that none of the known L-group chondrites correspond to the studied specimens and that this is new specimens of an uncatalogued meteorite.

## References

Ambrose D.P. (2003). Catalogue of stones from the strewnfield of the Thuathe meteorites of 21 July 2002. House 9 Publications. Lesotho.

Ambrose D.P., Reimold W.U. and Buchanan P.C. (2003). The Thuathe meteorite of 21 July 2002, Lesotho: mapping the strewn field and initial mineralogical classification. *South African Journal of Science.*, **99**, 153-159.

Amelin Y., Ghosh A. And Rotenburg E. (2005). Unraveling the evolution of chondrite parent asteroids by precise U-Pb dating and thermal modelling. *Geochimica et Cosmochima Acta,* **69**, 505-518.

Anders E. and Grevesse N. (1989). Abundances of elements: Meteoritic and solar. *Geochimica et Cosmochima Acta,* **53**, 197-214.

Anon. Lunar and Planetary Institute. **Luna Mission** (online). Available at: http://lpi.usra.edu/lunar/missions/luna/. (Accessed on 18 November 2010).

Anon. Natural History Museum. **The Catalogue of meteorites** (online). Available at: http://www.nhm.ac.uk/jdml/research/projects/metcat/list.dsml/?Country=Namibia&sort=Name. (Accessed on 2 December 2010).

Anon. (2005) National Space Science Data Centre. **Soviet Missions to the Moon** (online). Available at: http://nssdc.nasa.gov/planetary/lunar/lunarussr.html. (Accessed on 18 November 2010).

Baedecker PA. and Wasson JT. (1975). Elemental fractionations among enstatite chondrites. *Geochimica et Cosmochima Acta,* **39**, 735-765.

Bouvier A., Blichert-Toft J., Moynier F., Vervoort J.D. and Albarede F. (2007). Pb-Pb dating constraints on the accretion and cooling history of chondrites.

*Geochimica et Cosmochima Acta,* **71**, 1583-1604.

Brearley A.J. and Jones R.H. (1998). Chondritic meteorites. *Reviews in Mineralogy,* **36**, 398pp.

Bunch T.E., Keil K. and Snetsinger K.G. (1967). Chromite composition in relation to chemistry and texture of ordinary chondrites. *Geochimica et Cosmochima Acta,* **31**, 1569-1582.

Cervantes-de la Cruz K.E., Ortega-Gutierrez F., Reyes-Salas A.M., Alba-Aldave L.A., Angeles-Garcia S., Linares-Lopez C. And Altuzar-Coello P. (2010). Termometria de dos piroxenos en condros de la condrita ordinaria Nuevo Mercurio H5, Mexico. *Revista Mexicana de Ciencias Geologicas*, **27**, 134-147.

Chapola L.S. (1991). A preliminary report of the Chisenga iron meteorite, Malawi. *Journal of African Earth Sciences*, **12**, 533-536.

De Bruiyn H., Lombard A. and Schoch A.E. (2004). Anthimony sulphides in the Thuathe meteorite of Lesotho. *Neues Jahrbuch fur Mineralogie*, **8**, 357-360.

Dodd R.T. (1981). Meteorites, A petrologic-chemical synthesis. Cambridge University Press, Cambridge, 368pp.

Downie N.M. and Heath R.W. (1970). Basic statistical methods. Harper International, New York.

Glass B.P. (1982). Introduction to planetary geology. Cambridge University Press, Cambridge, 469pp.

Goldstein J.J., Scott E.R.D. and Chabot N.L. (2009). Iron meteorites: Crystallization, thermal history, parent bodies, and origin. *Chemie der Erde*, **69**, 293-325.

Grady M.M. (2001). Catalogue of meteorites. Cambridge University Press, Cambridge, 679pp.

Graham A.L., Crow M.J., Chatupa J.C. and Mndala A.T. (1984). The Mashinga, Malawi meteorite: A recent L6 fall. *Meteoritics*, **19**, 85-88.

Haack H. And McCoy T.J. (2004). Treatise on Geochemistry: Meteorites, Comets and Planet: Iron and Stony-iron meteorites. (Exec. Ed. Holland H.D. and Turekian K.K., Vol. Ed. Davis A.M.), Elsevier, New York, 7800pp.

Hamaguchi H., Onuma N., Hirao Y., Yokohama H., Bando S. and Furukawa M. (1969). The abundance of arsenic, tin and antimony in chondritic meteorites. *Geochimica et Cosmochima Acta,* **33**, 507-518.

Hutchison R. (2004). Meteorites: A Petrologic, Chemical and Isotopic Synthesis. Cambridge University press, Cambridge. 506pp.

Jenkins R. (1988). X-Ray Fluorescence Spectrometry. John Wiley and Sons, New York. 175pp.

Keil K. (1968). Mineralogical and chemical relationships among Enstatite chondrites. *Journal of Geophysical Research*, **73**, no 2, 6045-6976.

Kessel R., Beckett J.R. and Stolper E.M. (2007). The thermal history of equilibrated ordinary chondrites and the relationship between textural maturity and temperatures. *Geochimica et Cosmochima Acta,* **71**, 1855-1881.

Koeberl C., Reimold W.U., Horsch H.E. and Merkle R.K.W. (1990). New mineralogical chemical data on the Machinga (L6) chondrite, Malawi. *Meteoritics,* **25**, 23-26.

Krot A.N., Keil K., Goodrich C.A. and Scott E.R.D (2004). Treatise on Geochemistry: Meteorites, Comets and Planet: Classification of meteorites.

(Exec. Ed. Holland H.D. and Turekian K.K., Vol. Ed. Davis A.M.), Elsevier New York, 7800pp.

Lauretta D.S. and Killgore M. (2005). A Color Atlas of Meteorites in Thin Section. Golden Retriever Publications and Southwest Meteorite Press, South- Korea, 301pp.

Lombard A., de Bruiyn H., Scholtz N., Praekelt H.E., Wilson A.H. and Schoch A.E. (2003). The Thuathe meteorite fall of 21 July 2002. *South African Journal of Science*, **99**, 160-162.

Mason B. (1962). Meteorites. John Wiley and Sons, Inc., New York, 274 pp.

Mason B. (1966). Geochemistry and meteorites. *Meteoritics and Planetary Science,* **30**, 365-374.

Mason B. ed (1971). Handbook for Elemental Abundances in Meteorites. Gordon and Breach Publishers, New York, 555pp.

Mueller R.F. and Saxena S.K. (1977). Chemical Petrography with applications to the terrestrial planets and meteorites. Springer-Verlag, New York, 394pp.

Norton O.R. (1998). Rocks from space. Mountain Press Publishing Company, Missoula, 444pp.

Onuma N., Calyton R.N. and Mayeda T.K. (1972). Oxygen isotope temperatures for “equilibrated” ordinary chondrites. *Geochimica et Cosmochima Acta,* **36**, 157-168.

Potts P.J., Bowles J.F.W., Reed S.J.B and Cave M.R. ed (1995). The Mineralogical Society Series 6: Microprobe Techniques in the Earth Sciences. Chapman & Hall, London, pp419.

Pouchou J.L. and Picoir F. (1984). A new model for quantitative X-ray microanalysis. Part I: Application to analysis of homogenous samples. *La Recherche Aérospatiale,* **3**, 13 – 38.

Ramdohr, P. (1973). The opaque minerals in stony meteorites. Elsevier Publishing Company, London, 244pp.

Reimold W.U., Buchanan P.C., Ambrose D., Koeberl C. Franchi I., Lalkhan C., Schultz L., Franke L. And Heusser G. (2004). Thuathe, a new H4/5 chondrite from Lesotho: History of the fall, petrography, and geochemistry. *Meteoritics and Planetary Science*, **39**, 1321-1341.

Ringwood A.E. and Kaufman L. (1962). The influence of high pressure on transformation equilibria in iron meteorites. *Geochimica et Cosmochimica Acta,* **26**, 999-1009.

Rollinson H. (1993). Using geochemical data: evaluation, presentation, interpretation. Chapman & Hall, London, 352pp.

Rubin A.E. (1997). Mineralogy of meteorite groups. *Meteoritics and Planetary Science*, **32**, 231-247.

Rubin A.E. (2000). Petrologic, geochemical and experimental constraints on models of chondrule formation. *Earth-Science Reviews*, **50**, 3-27.

Rubin A.E. (2003). Personal Communication, University of California, Los Angeles.

Rubin A.E. (2003). Chromite-Plagioclase assemblages as a new shock indicator; implications for the shock and thermal histories of ordinary chondrites. *Geochimica et Cosmochimica Acta,* **67**, 2695-2709.

Rubin A.E. and Keil K. (1983). Mineralogy and petrology of the Abee enstatite chondrite breccias and its dark inclusions. *Earth and Planetary Science Letters*, **62**, 118-131.

Scholtz N. (2002). Personal Communication.

Scott E.R.D., Keil K. and Stöffler D. (1992). Shock metamorphism of carbonaceous chondrites. *Geochimica et Cosmochimica Acta,* **56**, 4281-4293.

Sears D. (2004). The Origin of Chondrules and Chondrites. Cambridge University Press, Cambridge, 209pp.

Smitt R.T. and Stöffler D. (1995). Experimental data in support of the 1991 shock classification of chondrites. *Meteoritics*, **30**, 574-575.

Stöffler D., Keil K. and Scott E.R.D. (1991). Shock metamorphism of ordinary chondrites. *Geochimica et Cosmochimica Acta,* **55**, 3845 – 3867.

Tanner J.T. and Ehmann W.D. (1966). The abundance of antimony in meteorites. *Earth and Planetary Science Letters*, **1**, 276-279.

Tanner J.T. and Ehmann W.D. (1967). The abundance of antimony in meteorites, tektites and rocks by neutron activation analysis. *Geochimica et Cosmochimica Acta*, **31**, 2007-2026.

Van Niekerk D. and Keil K. (2006). Classification of five new ordinary chondrites from North West Africa. *Chemie der Erde*, **66**, Issue 2, 153-158.

Van Schmus W.R. and Koffman D.M. (1967). Equilibration temperatures of iron and magnesium in chondritic meteorites. *Science,* **36**, 157-168.

Von Michaelis H. (1969). Fractionation of Lithophile elements in chondritic meteorites. Unpublished M Sc Thesis, University of Cape Town, Cape Town.

Von Michaelis H., Ahrens L.H. and Willis J.P. (1969). The composition of stony meteorites II: Analytical Data and an assessment of their quality. *Earth and Planetary Science Letters,* **5**, 387 – 394.

Wasson J.T. (1974). Meteorites. Classification and properties. Springer-Verlag, Heidelberg. 316pp.

Wasson J.T. and Kallemyn G.W. (1988). Composition of the chondrite groups. Philosophical Transactions of the Royal Society of London, **A325**, 535-544.

Wedepohl K.H. (1971). Geochemistry. Holt Rinehart & Winston Inc, United States of America, 231pp.

Willis J. (1981). Antimony in iron meteorites. *Earth and Planetary Science Letters*, **53**, 1-10.

Wlotzka F. (1992). The Meteoritical Bulletin No 72. *Meteoritics*, **27**, 109-117.

Wlotzka F. (1993). A weathering scale for the ordinary chondrites. *Meteoritics*, **28**, 460.

Zanda B. and Rotaru M. ed (2001). Meteorites, their impact on science and history. Cambridge University Press, Cambridge, 65pp.

Zanda B. (2004). Chondrules. *Earth and Planetary Science Letters*, **224**, 1-17.

# Appendix A
## EDS and electron microprobe data of minerals in the Thuathe meteorite

**Thuathe meteorite EDS data: Olivine**

| | 2 | 3 | 6 | 7 | 8 | Mean |
|---|---|---|---|---|---|---|
| SiO2 | 40.29 | 40.38 | 40.47 | 39.98 | 39.84 | 40.19 |
| Al2O3 | 2.13 | 1.17 | 0.74 | 0.89 | 0.43 | 1.07 |
| FeO | 14.28 | 14.82 | 14.90 | 14.97 | 14.41 | 14.67 |
| MnO | 0.36 | 0.39 | 0.35 | 0.36 | 0.41 | 0.37 |
| MgO | 41.36 | 42.64 | 42.84 | 43.32 | 44.57 | 42.95 |
| CaO | 0.83 | 0.42 | 0.52 | 0.52 | 0.41 | 0.54 |
| Na2O | 0.80 | 0.00 | 0.00 | 0.00 | 0.00 | 0.16 |
| Total | 100.04 | 99.82 | 99.81 | 100.04 | 100.08 | 99.96 |
| **Structural formulae to 4 O** | | | | | | |
| Si | 1.00 | 1.01 | 1.02 | 1.00 | 1.00 | 1.01 |
| Al | 0.06 | 0.03 | 0.02 | 0.03 | 0.01 | 0.03 |
| Fe | 0.30 | 0.31 | 0.31 | 0.31 | 0.30 | 0.31 |
| Mn | 0.01 | 0.01 | 0.01 | 0.01 | 0.01 | 0.01 |
| Mg | 1.53 | 1.59 | 1.60 | 1.62 | 1.66 | 1.60 |
| Ca | 0.02 | 0.01 | 0.01 | 0.01 | 0.01 | 0.01 |
| Na | 0.04 | 0.00 | 0.00 | 0.00 | 0.00 | 0.01 |
| **End-member compositions** | | | | | | |
| fo | 84 | 84 | 84 | 84 | 85 | 84 |
| fa | 16 | 16 | 16 | 16 | 15 | 16 |

**Thuathe meteorite EDS data: Pyroxene**

| | 13 | 14 | 15 | 16 | 17 | Mean |
|---|---|---|---|---|---|---|
| SiO2 | 56.97 | 57.55 | 56.92 | 56.57 | 56.90 | 56.98 |
| TiO2 | 0.00 | 0.00 | 0.48 | 0.27 | 0.00 | 0.15 |
| Al2O3 | 0.32 | 0.00 | 0.25 | 1.02 | 0.62 | 0.44 |
| FeO | 8.75 | 9.33 | 9.58 | 10.24 | 10.29 | 9.64 |
| MnO | 0.39 | 0.39 | 0.49 | 0.37 | 0.44 | 0.42 |
| MgO | 32.50 | 32.47 | 31.69 | 31.01 | 31.09 | 31.75 |
| CaO | 0.55 | 0.57 | 0.66 | 0.54 | 0.57 | 0.58 |
| Total | 99.48 | 100.31 | 100.07 | 100.02 | 99.91 | 99.96 |
| **Structural formulae to 6 O** | | | | | | |
| Si | 2.00 | 2.00 | 1.99 | 1.98 | 2.00 | 2.00 |
| Ti | 0.00 | 0.00 | 0.01 | 0.01 | 0.00 | 0.00 |
| Al | 0.01 | 0.00 | 0.01 | 0.04 | 0.03 | 0.02 |
| Fe | 0.26 | 0.27 | 0.28 | 0.30 | 0.30 | 0.28 |
| Mn | 0.01 | 0.01 | 0.01 | 0.01 | 0.01 | 0.01 |
| Mg | 1.70 | 1.69 | 1.65 | 1.62 | 1.63 | 1.66 |
| Ca | 0.02 | 0.02 | 0.02 | 0.02 | 0.02 | 0.02 |
| **End-member compositions** | | | | | | |
| en | 86 | 85 | 84 | 83 | 83 | 85 |
| wo | 1 | 1 | 1 | 1 | 1 | 1 |
| fs | 13 | 14 | 14 | 15 | 15 | 14 |

**Thuathe meteorite electron microprobe data: Olivine**

Chemical analyses and structural formulae (to 4 oxygen atoms) of olivine from the Thuathe meteorites.

| Analysis # | 1 | 2 | 3 | 4 | 5 | 6 | 7 | 8 | 9 | 10 | 11 |
|---|---|---|---|---|---|---|---|---|---|---|---|
| SiO2 | 40.04 | 40.02 | 40.02 | 39.91 | 40.05 | 40.32 | 39.79 | 39.56 | 39.59 | 38.34 | 38.51 |
| TiO2 | 0.06 | 0.06 | 0.11 | 0.00 | 0.03 | 0.00 | 0.00 | 0.02 | 0.10 | 0.13 | 0.03 |
| Al2O3 | 0.02 | 0.00 | 0.03 | 0.00 | 0.03 | 0.00 | 0.00 | 0.03 | 0.03 | 0.00 | 0.02 |
| FeO | 13.69 | 12.77 | 12.95 | 12.80 | 12.87 | 12.96 | 12.83 | 14.30 | 15.04 | 14.56 | 15.27 |
| Cr2O3 | 0.04 | 0.00 | 0.02 | 0.00 | 0.01 | 0.00 | 0.04 | 0.00 | 0.02 | 0.00 | 0.00 |
| MnO | 0.41 | 0.36 | 0.38 | 0.38 | 0.40 | 0.47 | 0.43 | 0.36 | 0.43 | 0.48 | 0.40 |
| MgO | 46.23 | 46.44 | 46.73 | 46.97 | 46.41 | 45.96 | 46.81 | 46.43 | 44.41 | 46.14 | 45.72 |
| NiO | 0.00 | 0.00 | 0.00 | 0.00 | 0.00 | 0.01 | 0.00 | 0.00 | 0.03 | 0.00 | 0.00 |
| CaO | 0.04 | 0.03 | 0.04 | 0.03 | 0.00 | 0.02 | 0.03 | 0.00 | 0.01 | 0.00 | 0.03 |
| Na2O | 0.00 | 0.38 | 0.21 | 0.13 | 0.00 | 0.17 | 0.04 | 0.00 | 0.00 | 0.30 | 0.00 |
| K2O | 0.00 | 0.00 | 0.02 | 0.00 | 0.00 | 0.00 | 0.03 | 0.00 | 0.03 | 0.00 | 0.00 |
| Total | 100.53 | 100.06 | 100.50 | 100.23 | 99.80 | 99.91 | 100.01 | 100.70 | 99.70 | 99.95 | 99.98 |
| **Structural formulae to 6 O** | | | | | | | | | | | |
| Si | 0.99 | 1.00 | 0.99 | 0.99 | 1.00 | 1.00 | 0.99 | 0.98 | 1.00 | 0.97 | 0.97 |
| Ti | 0.00 | 0.00 | 0.00 | 0.00 | 0.00 | 0.00 | 0.00 | 0.00 | 0.00 | 0.00 | 0.00 |
| Al | 0.00 | 0.00 | 0.00 | 0.00 | 0.00 | 0.00 | 0.00 | 0.00 | 0.00 | 0.00 | 0.00 |
| Fe | 0.28 | 0.27 | 0.27 | 0.27 | 0.27 | 0.27 | 0.27 | 0.30 | 0.32 | 0.31 | 0.32 |
| Cr | 0.01 | 0.01 | 0.01 | 0.01 | 0.01 | 0.01 | 0.01 | 0.01 | 0.01 | 0.01 | 0.01 |
| Mn | 0.01 | 0.01 | 0.01 | 0.01 | 0.01 | 0.01 | 0.01 | 0.01 | 0.01 | 0.01 | 0.01 |
| Mg | 1.71 | 1.72 | 1.73 | 1.74 | 1.72 | 1.71 | 1.74 | 1.72 | 1.67 | 1.74 | 1.72 |
| Ni | 0.00 | 0.00 | 0.00 | 0.00 | 0.00 | 0.00 | 0.00 | 0.00 | 0.00 | 0.00 | 0.00 |
| Ca | 0.00 | 0.00 | 0.00 | 0.00 | 0.00 | 0.00 | 0.00 | 0.00 | 0.00 | 0.00 | 0.00 |
| Na | 0.00 | 0.02 | 0.01 | 0.01 | 0.00 | 0.01 | 0.00 | 0.00 | 0.00 | 0.01 | 0.00 |
| K | 0.00 | 0.00 | 0.00 | 0.00 | 0.00 | 0.00 | 0.00 | 0.00 | 0.00 | 0.00 | 0.00 |
| Total | 3.01 | 3.02 | 3.02 | 3.02 | 3.01 | 3.01 | 3.02 | 3.02 | 3.01 | 3.05 | 3.03 |
| **End-member compositions** | | | | | | | | | | | |
| Mg | 85.4 | 86.3 | 86.2 | 86.4 | 86.2 | 85.9 | 86.3 | 84.9 | 83.6 | 84.5 | 83.9 |
| Fe | 14.2 | 13.3 | 13.4 | 13.2 | 13.4 | 13.6 | 13.3 | 14.7 | 15.9 | 15.0 | 15.7 |
| Mn | 0.4 | 0.4 | 0.4 | 0.4 | 0.4 | 0.5 | 0.5 | 0.4 | 0.5 | 0.5 | 0.4 |

**Thuathe meteorite electron microprobe data: Olivine continued**

Chemical analyses and structural formulae (to 4 oxygen atoms) of olivine from the Thuathe meteorites continued.

| Analysis # | 12 | 13 | 14 | 15 | 16 | 17 | 18 | 19 | 20 | 21 | 22 |
|---|---|---|---|---|---|---|---|---|---|---|---|
| SiO2 | 39.59 | 39.56 | 38.98 | 39.79 | 39.94 | 40.45 | 40.69 | 39.90 | 40.04 | 39.37 | 39.01 |
| TiO2 | 0.05 | 0.00 | 0.06 | 0.00 | 0.05 | 0.05 | 0.00 | 0.02 | 0.07 | 0.03 | 0.03 |
| Al2O3 | 0.10 | 0.02 | 0.05 | 0.04 | 0.02 | 0.03 | 0.02 | 0.00 | 0.01 | 0.02 | 0.00 |
| FeO | 13.91 | 13.64 | 13.24 | 12.14 | 11.96 | 11.87 | 11.69 | 11.76 | 11.61 | 12.44 | 12.32 |
| Cr2O3 | 0.00 | 0.00 | 0.02 | 0.03 | 0.01 | 0.02 | 0.03 | 0.00 | 0.00 | 0.07 | 0.01 |
| MnO | 0.46 | 0.46 | 0.35 | 0.31 | 0.37 | 0.34 | 0.32 | 0.38 | 0.30 | 0.34 | 0.41 |
| MgO | 46.90 | 46.32 | 46.72 | 47.23 | 48.14 | 47.20 | 47.27 | 47.88 | 48.06 | 47.94 | 48.35 |
| NiO | 0.00 | 0.02 | 0.00 | 0.00 | 0.00 | 0.00 | 0.04 | 0.03 | 0.00 | 0.00 | 0.00 |
| CaO | 0.05 | 0.03 | 0.02 | 0.01 | 0.02 | 0.02 | 0.02 | 0.02 | 0.07 | 0.01 | 0.03 |
| Na2O | 0.08 | 0.08 | 0.08 | 0.17 | 0.00 | 0.13 | 0.00 | 0.00 | 0.00 | 0.00 | 0.04 |
| K2O | 0.01 | 0.02 | 0.00 | 0.01 | 0.00 | 0.00 | 0.01 | 0.00 | 0.00 | 0.00 | 0.03 |
| Total | 101.15 | 100.15 | 99.52 | 99.72 | 100.51 | 100.09 | 100.09 | 99.99 | 100.17 | 100.23 | 100.23 |
| **Structural formulae to 6 O** | | | | | | | | | | | |
| Si | 0.98 | 0.99 | 0.98 | 0.99 | 0.99 | 1.00 | 1.00 | 0.99 | 0.99 | 0.98 | 0.97 |
| Ti | 0.00 | 0.00 | 0.00 | 0.00 | 0.00 | 0.00 | 0.00 | 0.00 | 0.00 | 0.00 | 0.00 |
| Al | 0.00 | 0.00 | 0.00 | 0.00 | 0.00 | 0.00 | 0.00 | 0.00 | 0.00 | 0.00 | 0.00 |
| Fe | 0.29 | 0.28 | 0.28 | 0.25 | 0.25 | 0.25 | 0.24 | 0.24 | 0.24 | 0.26 | 0.26 |
| Cr | 0.01 | 0.01 | 0.01 | 0.01 | 0.01 | 0.01 | 0.01 | 0.01 | 0.01 | 0.01 | 0.01 |
| Mn | 0.01 | 0.01 | 0.01 | 0.01 | 0.01 | 0.01 | 0.01 | 0.01 | 0.01 | 0.01 | 0.01 |
| Mg | 1.73 | 1.72 | 1.75 | 1.75 | 1.77 | 1.74 | 1.74 | 1.77 | 1.77 | 1.77 | 1.79 |
| Ni | 0.00 | 0.00 | 0.00 | 0.00 | 0.00 | 0.00 | 0.00 | 0.00 | 0.00 | 0.00 | 0.00 |
| Ca | 0.00 | 0.00 | 0.00 | 0.00 | 0.00 | 0.00 | 0.00 | 0.00 | 0.00 | 0.00 | 0.00 |
| Na | 0.00 | 0.00 | 0.00 | 0.01 | 0.00 | 0.01 | 0.00 | 0.00 | 0.00 | 0.00 | 0.00 |
| K | 0.00 | 0.00 | 0.00 | 0.00 | 0.00 | 0.00 | 0.00 | 0.00 | 0.00 | 0.00 | 0.00 |
| Total | 3.03 | 3.02 | 3.03 | 3.02 | 3.02 | 3.01 | 3.00 | 3.02 | 3.02 | 3.03 | 3.04 |
| **End-member compositions** | | | | | | | | | | | |
| Mg | 85.3 | 85.4 | 86.0 | 87.1 | 87.4 | 87.3 | 87.5 | 87.5 | 87.8 | 87.0 | 87.1 |
| Fe | 14.2 | 14.1 | 13.7 | 12.6 | 12.2 | 12.3 | 12.1 | 12.1 | 11.9 | 12.7 | 12.5 |
| Mn | 0.5 | 0.5 | 0.4 | 0.3 | 0.4 | 0.4 | 0.3 | 0.4 | 0.3 | 0.4 | 0.4 |

**Thuathe meteorite electron microprobe data: Olivine continued**

Chemical analyses and structural formulae (to 4 oxygen atoms) of olivine from the Thuathe meteorites continued.

| Analysis # | 23 | 24 | 25 | 26 | 27 | 28 |
|---|---|---|---|---|---|---|
| SiO2 | 39.26 | 38.63 | 38.13 | 38.91 | 39.85 | 39.98 |
| TiO2 | 0.00 | 0.00 | 0.06 | 0.05 | 0.01 | 0.00 |
| Al2O3 | 0.03 | 0.08 | 0.02 | 0.09 | 0.03 | 0.02 |
| FeO | 12.06 | 13.47 | 13.67 | 13.24 | 12.56 | 11.35 |
| Cr2O3 | 0.00 | 0.05 | 0.08 | 0.29 | 0.00 | 0.00 |
| MnO | 0.35 | 0.37 | 0.48 | 0.36 | 0.46 | 0.33 |
| MgO | 48.22 | 46.91 | 47.86 | 47.21 | 47.32 | 48.12 |
| NiO | 0.00 | 0.00 | 0.08 | 0.09 | 0.00 | 0.00 |
| CaO | 0.00 | 0.03 | 0.03 | 0.02 | 0.01 | 0.07 |
| Na2O | 0.13 | 0.00 | 0.00 | 0.00 | 0.00 | 0.21 |
| K2O | 0.00 | 0.00 | 0.02 | 0.03 | 0.00 | 0.04 |
| Total | 100.04 | 99.56 | 100.42 | 100.28 | 100.25 | 100.12 |
| **Structural formulae to 6 O** | | | | | | |
| Si | 0.98 | 0.97 | 0.95 | 0.97 | 0.99 | 0.99 |
| Ti | 0.00 | 0.00 | 0.00 | 0.00 | 0.00 | 0.00 |
| Al | 0.00 | 0.00 | 0.00 | 0.00 | 0.00 | 0.00 |
| Fe | 0.25 | 0.28 | 0.29 | 0.28 | 0.26 | 0.23 |
| Cr | 0.01 | 0.01 | 0.01 | 0.01 | 0.01 | 0.01 |
| Mn | 0.01 | 0.01 | 0.01 | 0.01 | 0.01 | 0.01 |
| Mg | 1.79 | 1.76 | 1.79 | 1.76 | 1.75 | 1.77 |
| Ni | 0.00 | 0.00 | 0.00 | 0.00 | 0.00 | 0.00 |
| Ca | 0.00 | 0.00 | 0.00 | 0.00 | 0.00 | 0.00 |
| Na | 0.01 | 0.00 | 0.00 | 0.00 | 0.00 | 0.01 |
| K | 0.00 | 0.00 | 0.00 | 0.00 | 0.00 | 0.00 |
| Total | 3.03 | 3.03 | 3.05 | 3.03 | 3.02 | 3.02 |
| **End-member compositions** | | | | | | |
| Mg | 87.4 | 85.8 | 85.8 | 86.1 | 86.6 | 88.0 |
| Fe | 12.3 | 13.8 | 13.7 | 13.5 | 12.9 | 11.7 |
| Mn | 0.4 | 0.4 | 0.5 | 0.4 | 0.5 | 0.3 |

**Thuathe meteorite electron microprobe data: Pyroxene**

Chemical analyses and structural formulae (to 4 cations) of pyroxene from the Thuathe meteorites.

| Analysis # | 1 | 2 | 3 | 4 | 5 | 6 | 7 | 8 | 9 | 10 |
|---|---|---|---|---|---|---|---|---|---|---|
| SiO2 | 57.45 | 56.53 | 57.42 | 57.50 | 56.85 | 57.38 | 57.54 | 57.08 | 56.16 | 57.32 |
| TiO2 | 0.07 | 0.07 | 0.13 | 0.07 | 0.14 | 0.09 | 0.07 | 0.07 | 0.04 | 0.16 |
| Al2O3 | 0.26 | 0.37 | 0.30 | 0.06 | 0.37 | 0.25 | 0.13 | 0.22 | 0.25 | 0.43 |
| FeO | 8.41 | 7.09 | 8.40 | 8.41 | 7.75 | 8.70 | 8.45 | 10.98 | 13.96 | 8.46 |
| Cr2O3 | 0.12 | 0.28 | 0.07 | 0.05 | 0.18 | 0.06 | 0.02 | 0.34 | 0.00 | 0.14 |
| MnO | 0.35 | 0.45 | 0.51 | 0.40 | 0.38 | 0.43 | 0.45 | 0.41 | 0.48 | 0.39 |
| MgO | 33.02 | 27.61 | 32.39 | 32.92 | 28.21 | 32.79 | 32.93 | 30.43 | 28.38 | 32.25 |
| NiO | 0.01 | 0.04 | 0.00 | 0.00 | 0.04 | 0.00 | 0.00 | 0.08 | 0.14 | 0.02 |
| CaO | 0.45 | 7.05 | 0.53 | 0.35 | 6.29 | 0.30 | 0.40 | 0.46 | 0.34 | 0.65 |
| Na2O | 0.00 | 0.49 | 0.00 | 0.00 | 0.33 | 0.49 | 0.04 | 0.04 | 0.00 | 0.00 |
| K2O | 0.00 | 0.00 | 0.00 | 0.01 | 0.00 | 0.04 | 0.03 | 0.04 | 0.01 | 0.01 |
| Total | 100.14 | 99.98 | 99.75 | 99.77 | 100.54 | 100.53 | 100.06 | 100.15 | 99.76 | 99.83 |
| Si | 2.00 | 2.00 | 2.01 | 2.01 | 2.00 | 1.98 | 2.00 | 2.02 | 2.02 | 2.01 |
| Aliv | 0.00 | 0.00 | 0.00 | 0.00 | 0.00 | 0.01 | 0.00 | 0.00 | 0.00 | 0.00 |
| T-site | 2.00 | 2.00 | 2.01 | 2.01 | 2.00 | 1.99 | 2.00 | 2.02 | 2.02 | 2.01 |
| Alvi | 0.01 | 0.02 | 0.01 | 0.00 | 0.02 | 0.00 | 0.01 | 0.01 | 0.01 | 0.02 |
| Ti | 0.00 | 0.00 | 0.00 | 0.00 | 0.00 | 0.00 | 0.00 | 0.00 | 0.00 | 0.00 |
| Fe | 0.24 | 0.21 | 0.25 | 0.25 | 0.23 | 0.25 | 0.25 | 0.32 | 0.42 | 0.25 |
| Cr | 0.00 | 0.01 | 0.00 | 0.00 | 0.00 | 0.00 | 0.00 | 0.01 | 0.00 | 0.00 |
| Mn | 0.01 | 0.01 | 0.02 | 0.01 | 0.01 | 0.01 | 0.01 | 0.01 | 0.01 | 0.01 |
| Mg | 1.71 | 1.45 | 1.69 | 1.71 | 1.48 | 1.69 | 1.71 | 1.60 | 1.52 | 1.68 |
| Ni | 0.00 | 0.00 | 0.00 | 0.00 | 0.00 | 0.00 | 0.00 | 0.00 | 0.00 | 0.00 |
| Ca | 0.02 | 0.27 | 0.02 | 0.01 | 0.24 | 0.01 | 0.01 | 0.02 | 0.01 | 0.02 |
| Na | 0.00 | 0.03 | 0.00 | 0.00 | 0.02 | 0.03 | 0.00 | 0.00 | 0.00 | 0.00 |
| K | 0.00 | 0.00 | 0.00 | 0.00 | 0.00 | 0.00 | 0.00 | 0.00 | 0.00 | 0.00 |
| M1, M2 | 2.00 | 2.00 | 1.99 | 1.99 | 2.00 | 2.00 | 2.00 | 1.98 | 1.98 | 1.99 |
| Mg | 86.8 | 75.3 | 86.4 | 86.9 | 76.1 | 86.5 | 86.8 | 82.4 | 77.8 | 86.1 |
| Fe | 12.4 | 10.9 | 12.6 | 12.5 | 11.7 | 12.9 | 12.5 | 16.7 | 21.5 | 12.7 |
| Ca | 0.8 | 13.8 | 1.0 | 0.7 | 12.2 | 0.6 | 0.7 | 0.9 | 0.7 | 1.3 |
| mg# | 87.0 | 86.7 | 86.6 | 86.9 | 86.1 | 86.5 | 86.8 | 82.6 | 77.8 | 86.7 |

**Thuathe meteorite electron microprobe data: Pyroxene continued**

Chemical analyses and structural formulae (to 4 cations) of pyroxene from the Thuathe meteorites continued.

| Analysis # | 11 | 12 | 13 | 14 | 15 | 16 | 17 | 18 | 19 |
|---|---|---|---|---|---|---|---|---|---|
| SiO2 | 56.48 | 57.11 | 57.22 | 57.53 | 57.73 | 56.95 | 57.96 | 57.50 | 57.17 |
| TiO2 | 0.12 | 0.06 | 0.12 | 0.09 | 0.20 | 0.03 | 0.11 | 0.10 | 0.05 |
| Al2O3 | 0.40 | 0.13 | 0.25 | 0.15 | 0.39 | 0.60 | 0.23 | 0.19 | 0.12 |
| FeO | 8.02 | 9.07 | 8.45 | 8.18 | 7.63 | 8.71 | 6.87 | 7.74 | 8.46 |
| Cr2O3 | 0.73 | 0.05 | 0.42 | 0.08 | 0.11 | 0.13 | 0.11 | 0.05 | 0.08 |
| MnO | 0.33 | 0.45 | 0.43 | 0.44 | 0.34 | 0.45 | 0.30 | 0.41 | 0.43 |
| MgO | 29.45 | 32.76 | 32.42 | 32.48 | 33.45 | 32.84 | 33.57 | 33.66 | 33.14 |
| NiO | 0.00 | 0.00 | 0.08 | 0.00 | 0.04 | 0.00 | 0.00 | 0.04 | 0.05 |
| CaO | 4.50 | 0.39 | 0.41 | 0.42 | 0.33 | 0.40 | 0.70 | 0.34 | 0.49 |
| Na2O | 0.25 | 0.00 | 0.00 | 0.12 | 0.20 | 0.04 | 0.00 | 0.12 | 0.00 |
| K2O | 0.00 | 0.01 | 0.00 | 0.01 | 0.03 | 0.01 | 0.01 | 0.00 | 0.00 |
| Total | 100.27 | 100.02 | 99.80 | 99.49 | 100.45 | 100.17 | 99.86 | 100.16 | 99.99 |
| Si | 1.99 | 1.99 | 2.00 | 2.02 | 1.99 | 1.98 | 2.01 | 1.99 | 1.99 |
| Aliv | 0.01 | 0.01 | 0.00 | 0.00 | 0.01 | 0.02 | 0.00 | 0.01 | 0.01 |
| T-site | 2.00 | 2.00 | 2.00 | 2.02 | 2.00 | 2.00 | 2.01 | 2.00 | 2.00 |
| Alvi | 0.01 | 0.00 | 0.01 | 0.01 | 0.01 | 0.00 | 0.01 | 0.00 | 0.00 |
| Ti | 0.00 | 0.00 | 0.00 | 0.00 | 0.01 | 0.00 | 0.00 | 0.00 | 0.00 |
| Fe | 0.24 | 0.26 | 0.25 | 0.24 | 0.22 | 0.25 | 0.20 | 0.22 | 0.25 |
| Cr | 0.02 | 0.00 | 0.01 | 0.00 | 0.00 | 0.00 | 0.00 | 0.00 | 0.00 |
| Mn | 0.01 | 0.01 | 0.01 | 0.01 | 0.01 | 0.01 | 0.01 | 0.01 | 0.01 |
| Mg | 1.54 | 1.70 | 1.69 | 1.70 | 1.72 | 1.70 | 1.74 | 1.74 | 1.72 |
| Ni | 0.00 | 0.00 | 0.00 | 0.00 | 0.00 | 0.00 | 0.00 | 0.00 | 0.00 |
| Ca | 0.17 | 0.01 | 0.02 | 0.02 | 0.01 | 0.02 | 0.03 | 0.01 | 0.02 |
| Na | 0.02 | 0.00 | 0.00 | 0.01 | 0.01 | 0.00 | 0.00 | 0.01 | 0.00 |
| K | 0.00 | 0.00 | 0.00 | 0.00 | 0.00 | 0.00 | 0.00 | 0.00 | 0.00 |
| M1, M2 | 2.01 | 2.00 | 2.00 | 1.98 | 2.00 | 1.99 | 1.99 | 2.00 | 2.00 |
| Mg | 79.2 | 85.9 | 86.5 | 86.9 | 88.1 | 86.4 | 88.5 | 88.0 | 86.7 |
| Fe | 12.1 | 13.3 | 12.7 | 12.3 | 11.3 | 12.9 | 10.2 | 11.4 | 12.4 |
| Ca | 8.7 | 0.7 | 0.8 | 0.8 | 0.6 | 0.8 | 1.3 | 0.6 | 0.9 |
| mg# | 86.3 | 86.0 | 86.7 | 87.0 | 88.2 | 86.5 | 89.3 | 88.0 | 86.9 |

**Thuathe meteorite electron microprobe data: Plagioclase**

Analyses and structural formulae (to 32 oxygen atoms) of plagioclase of the Thuathe meteorites.

| Analysis # | 1 | 2 | 3 | 4 |
|---|---|---|---|---|
| SiO2 | 64.82 | 63.43 | 58.24 | 58.46 |
| TiO2 | 0.02 | 0.20 | 0.09 | 0.05 |
| Al2O3 | 21.93 | 22.95 | 26.74 | 26.55 |
| FeO | 0.09 | 0.06 | 0.09 | 0.03 |
| MnO | 0.03 | 0.01 | 0.02 | 0.00 |
| MgO | 0.06 | 0.04 | 0.04 | 0.07 |
| CaO | 2.63 | 3.27 | 5.46 | 6.25 |
| Na2O | 10.04 | 9.72 | 8.68 | 8.66 |
| K2O | 0.51 | 0.33 | 0.56 | 0.18 |
| Total | 100.14 | 100.01 | 99.93 | 100.25 |
| **Structural formulae to 24 O** | | | | |
| Si | 11.43 | 11.23 | 10.44 | 10.44 |
| Al | 4.56 | 4.79 | 5.65 | 5.59 |
| T-site | 15.99 | 16.02 | 16.09 | 16.03 |
| Ti | 0.00 | 0.03 | 0.01 | 0.01 |
| Fe | 0.01 | 0.01 | 0.01 | 0.01 |
| Mn | 0.01 | 0.00 | 0.00 | 0.00 |
| Mg | 0.02 | 0.01 | 0.01 | 0.02 |
| Ca | 0.48 | 0.60 | 1.01 | 1.16 |
| Na | 3.43 | 3.34 | 3.02 | 3.00 |
| K | 0.12 | 0.07 | 0.13 | 0.04 |
| Total | 4.06 | 4.06 | 4.20 | 4.22 |
| **End-member compositions** | | | | |
| ab | 85 | 83 | 73 | 71 |
| an | 12 | 15 | 24 | 28 |
| or | 3 | 2 | 3 | 1 |

**Thuathe meteorite electron microprobe data: Chromite**

Spinel composition and structural formulae
(to 24 cations, $Fe^{3+}$ stoichiometrically calculated)
of the Thuathe meteorite.

| Analysis # | 1 | 2 | 3 |
|---|---|---|---|
| $SiO_2$ | 0.46 | 0.62 | 0.20 |
| $TiO_2$ | 0.46 | 0.52 | 0.53 |
| $Al_2O_3$ | 8.49 | 9.06 | 11.42 |
| $Fe_2O_3$ | 4.89 | 4.59 | 0.88 |
| $Cr_2O_3$ | 53.87 | 52.97 | 54.43 |
| $V_2O_5$ | 0.35 | 0.49 | 0.50 |
| FeO | 25.78 | 27.35 | 26.61 |
| MnO | 0.35 | 0.63 | 0.39 |
| NiO | 1.08 | 0.13 | 0.31 |
| ZnO | 0.21 | 0.21 | 0.2 |
| MgO | 3.98 | 4.00 | 4.27 |
| Total | 99.92 | 100.57 | 99.74 |
| Si | 0.13 | 0.17 | 0.05 |
| Ti | 0.10 | 0.11 | 0.11 |
| Al | 2.79 | 2.95 | 3.69 |
| $Fe^{3+}$ | 1.03 | 0.95 | 0.18 |
| Cr | 11.87 | 11.56 | 11.81 |
| V | 0.06 | 0.09 | 0.09 |
| $Fe^{2+}$ | 6.01 | 6.31 | 6.11 |
| Mn | 0.08 | 0.15 | 0.09 |
| Ni | 0.24 | 0.03 | 0.07 |
| Zn | 0.04 | 0.04 | 0.04 |
| Mg | 1.65 | 1.65 | 1.75 |
| Cations | 24 | 24 | 24 |

**Thuathe meteorite electron microprobe data: Troilite**

Troilite analyses and structural formulae of minerals from the Thuathe meteorite.

| Analysis # | 1 | 2 | 3 | 4 | 5 | 6 | 7 | 8 | 9 | 10 | 11 | 12 | Mean |
|---|---|---|---|---|---|---|---|---|---|---|---|---|---|
| S | 36.45 | 36.39 | 36.58 | 36.35 | 37.25 | 36.67 | 36.52 | 36.83 | 36.43 | 36.91 | 35.90 | 36.07 | 36.53 |
| Fe | 63.16 | 63.74 | 62.92 | 63.54 | 62.62 | 63.51 | 63.25 | 63.87 | 59.00 | 60.59 | 59.84 | 56.90 | 61.91 |
| Cu | 0.15 | 0.04 | 0.10 | 0.10 | 0.08 | 0.00 | 0.06 | 0.08 | 4.87 | 2.42 | 2.74 | 6.38 | 1.42 |
| Ni | 0.01 | 0.03 | 0.06 | 0.03 | 0.02 | 0.00 | 0.03 | 0.02 | 0.00 | 0.03 | 0.07 | 0.15 | 0.04 |
| Zn | 0.00 | 0.00 | 0.05 | 0.00 | 0.00 | 0.04 | 0.07 | 0.06 | 0.00 | 0.03 | 0.06 | 0.00 | 0.03 |
| Pb | 0.00 | 0.00 | 0.00 | 0.00 | 0.00 | 0.00 | 0.00 | 0.00 | 0.00 | 0.00 | 1.57 | 1.05 | 0.22 |
| Total | 99.76 | 100.20 | 99.70 | 100.01 | 99.97 | 100.22 | 99.92 | 100.86 | 100.30 | 99.98 | 100.18 | 100.55 | 100.14 |
| **Structural formulae** | | | | | | | | | | | | | |
| S | 1.00 | 1.00 | 1.00 | 1.00 | 1.02 | 1.00 | 1.00 | 1.00 | 1.00 | 1.01 | 1.00 | 1.00 | 1.00 |
| Fe | 1.00 | 1.00 | 0.99 | 1.00 | 0.98 | 1.00 | 1.00 | 1.00 | 0.93 | 0.95 | 0.96 | 0.90 | 0.98 |
| Cu | 0.00 | 0.00 | 0.00 | 0.00 | 0.00 | 0.00 | 0.00 | 0.00 | 0.07 | 0.03 | 0.04 | 0.09 | 0.02 |
| Ni | 0.00 | 0.00 | 0.00 | 0.00 | 0.00 | 0.00 | 0.00 | 0.00 | 0.00 | 0.00 | 0.00 | 0.00 | 0.00 |
| Zn | 0.00 | 0.00 | 0.00 | 0.00 | 0.00 | 0.00 | 0.00 | 0.00 | 0.00 | 0.00 | 0.00 | 0.00 | 0.00 |
| Pb | 0.00 | 0.00 | 0.00 | 0.00 | 0.00 | 0.00 | 0.00 | 0.00 | 0.00 | 0.00 | 0.01 | 0.01 | 0.00 |
| Atoms | 2 | 2 | 2 | 2 | 2 | 2 | 2 | 2 | 2 | 2 | 2 | 2 | 2 |

**Thuathe meteorite electron microprobe data: Chalcopyrite**

Chalocpyrite analysis and structural formulae of minerals from the Thuathe meteorite.

| | |
|---|---|
| S | 34.85 |
| Fe | 30.88 |
| Cu | 33.81 |
| Ni | 0.50 |
| Zn | 0.05 |
| Pb | 0.00 |
| Total | 100.10 |
| **Structural formulae** | |
| S | 2.02 |
| Fe | 1.02 |
| Cu | 0.98 |
| Ni | 0.01 |
| Zn | 0.00 |
| Pb | 0.00 |
| Atoms | 3 |

**Thuathe meteorite electron microprobe data: Kamacite**

Microprobe analyses of kamacite from the Thuathe meteorites in weight percentage.

| Analysis# | 1 | 2 | 3 | 4 | 5 | 6 | Mean |
|---|---|---|---|---|---|---|---|
| Fe | 94.73 | 94.49 | 94.83 | 94.39 | 94.46 | 93.98 | 94.48 |
| Ni | 5.46 | 5.17 | 5.4 | 5.55 | 5.04 | 5.93 | 5.42 |
| V | 0 | 0 | 0 | 0 | 0 | 0 | 0 |
| Ti | 0.04 | 0.03 | 0 | 0 | 0 | 0 | 0.01 |
| Zn | 0 | 0 | 0.02 | 0.03 | 0 | 0 | 0.01 |
| Cr | 0 | 0 | 0 | 0 | 0.02 | 0.02 | 0.01 |
| Mn | 0.07 | 0 | 0 | 0 | 0.02 | 0 | 0.01 |
| Total | 100.3 | 99.69 | 100.25 | 99.97 | 99.55 | 99.93 | 99.95 |

**Thuathe meteorite electron microprobe data: Antimony sulphides.**

| | Berthierite | | | | | | | | | |
|---|---|---|---|---|---|---|---|---|---|---|
| Analysis# | 1 | 2 | 3 | 4 | 5 | 6 | 7 | 8 | 9 | Mean |
| Sb | 56.75 | 57.1 | 56.89 | 56.87 | 57.15 | 56.82 | 56.98 | 57.37 | 57.16 | 57.01 |
| Fe | 12.85 | 12.94 | 12.98 | 12.97 | 12.99 | 12.94 | 13.13 | 12.75 | 13.11 | 12.96 |
| S | 29.85 | 29.94 | 29.75 | 29.95 | 30.04 | 29.51 | 29.98 | 30.23 | 29.88 | 29.90 |
| Ni | 0.12 | 0.13 | 0.06 | 0.09 | 0.14 | 0.07 | 0.00 | 0.44 | 0.16 | 0.13 |
| Total | 99.57 | 100.11 | 99.68 | 99.88 | 100.32 | 99.34 | 100.09 | 100.79 | 100.31 | 100.01 |
| Structural Formulae | | | | | | | | | | |
| Sb | 2.01 | 2.00 | 2.00 | 2.00 | 2.00 | 2.00 | 1.99 | 2.00 | 2.01 | 2.00 |
| Fe | 0.99 | 0.99 | 1.00 | 0.99 | 0.99 | 0.99 | 1.00 | 0.97 | 1.00 | 0.99 |
| S | 4.01 | 3.99 | 3.97 | 4.00 | 3.99 | 3.95 | 3.98 | 4.00 | 3.98 | 3.99 |
| Ni | 0.01 | 0.01 | 0.00 | 0.01 | 0.01 | 0.01 | 0.00 | 0.03 | 0.01 | 0.01 |

| | Stibnite | | | | | | | | | |
|---|---|---|---|---|---|---|---|---|---|---|
| Analysis# | 1 | 2 | 3 | 4 | 5 | 6 | 7 | 8 | 9 | Mean |
| Sb | 69.58 | 69.63 | 69.95 | 69.84 | 69.66 | 69.86 | 69.77 | 69.59 | 69.94 | 69.76 |
| Fe | 1.37 | 1.30 | 1.25 | 1.32 | 1.04 | 1.11 | 0.96 | 1.16 | 0.89 | 1.16 |
| S | 29.15 | 29.07 | 28.65 | 29.03 | 29.11 | 28.92 | 29.13 | 29.20 | 29.15 | 29.05 |
| Ni | 0.00 | 0.08 | 0.05 | 0.06 | 0.04 | 0.07 | 0.04 | 0.02 | 0.08 | 0.05 |
| Total | 100.10 | 100.08 | 99.90 | 100.25 | 99.85 | 99.96 | 99.90 | 99.97 | 100.06 | 100.01 |
| Structural Formulae | | | | | | | | | | |
| Sb | 1.92 | 1.92 | 1.92 | 1.91 | 1.91 | 1.92 | 1.91 | 1.90 | 1.91 | 1.91 |
| Fe | 0.08 | 0.08 | 0.07 | 0.08 | 0.06 | 0.07 | 0.06 | 0.07 | 0.05 | 0.07 |
| S | 3.05 | 3.04 | 2.99 | 3.01 | 3.03 | 3.01 | 3.03 | 3.03 | 3.03 | 3.02 |
| Ni | 0.00 | 0.00 | 0.00 | 0.00 | 0.00 | 0.00 | 0.00 | 0.00 | 0.00 | 0.00 |

# Appendix B
## EDS and electron microprobe data of minerals in the Machinga meteorite

**Machinga meteorite EDS data: Olivine**

| | |
|---|---|
| Si | 39.98 |
| Fe | 16.08 |
| Mg | 42.73 |
| Ni | 1.28 |
| Ca | 0.39 |
| Total | 100.45 |
| Structural formulae to 4 O | |
| Si | 1.01 |
| Fe | 0.34 |
| Mg | 1.61 |
| Ni | 0.03 |
| Ca | 0.01 |
| End-members | |
| fo | 83 |
| fa | 17 |

**Machinga meteorite EDS data: Pyroxene**

| Analysis# | 1 | 2 | 3 |
|---|---|---|---|
| $SiO_2$ | 57.35 | 57.25 | 59.07 |
| $Al_2O_3$ | 1.24 | 0.83 | 0.00 |
| FeO | 4.81 | 5.52 | 2.53 |
| MgO | 35.45 | 35.40 | 38.04 |
| NiO | 0.00 | 0.28 | 0.00 |
| CaO | 0.73 | 0.69 | 0.40 |
| $Na_2O$ | 0.46 | 0.00 | 0.00 |
| Total | 100.04 | 99.97 | 100.04 |
| **Structural formulae to 6 oxygen atoms** | | | |
| $Si^{iv}$ | 1.97 | 1.97 | 2.00 |
| $Al^{iv}$ | 0.03 | 0.03 | 0.00 |
| T site | 2.00 | 2.00 | 2.00 |
| $Al^{vi}$ | 0.02 | 0.00 | 0.00 |
| $Fe^{2+}$ | 0.14 | 0.16 | 0.07 |
| Ni | 0.00 | 0.01 | 0.00 |
| Mg | 1.81 | 1.82 | 1.92 |
| Ca | 0.03 | 0.03 | 0.01 |
| Na | 0.03 | 0.00 | 0.00 |
| $M_1$, $M_2$ | 2.02 | 2.01 | 2.00 |
| **End-member compositions** | | | |
| en | 91.4 | 90.5 | 96.0 |
| fs | 7.1 | 8.0 | 3.5 |
| wo | 1.5 | 1.5 | 0.5 |

**Machinga meteorite EDS data: Gypsum**

| | |
|---|---|
| FeO | 4.00 |
| MnO | 0.75 |
| MgO | 3.50 |
| CaO | 28.10 |
| $SO_3$ | 52.32 |
| $H_2O$ | 11.33 |
| Total | 100.00 |
| **Structural Formula** | |
| Fe | 0.34 |
| Mn | 0.06 |
| Mg | 0.53 |
| Ca | 3.06 |
| S | 3.99 |
| $H_2O$ | 7.68 |

$H_2O$ calculated by difference

**Machinga meteorite EDS data: Magnetite**

| | |
|---|---|
| $SiO_2$ | 9.31 |
| $Fe_2O_3$ | 51.16 |
| FeO | 25.91 |
| MgO | 7.59 |
| CaO | 0.31 |
| NiO | 5.66 |
| **Structural formula** | |
| Si | 2.61 |
| $Fe^{3+}$ | 10.78 |
| $Fe^{2+}$ | 6.07 |
| Mg | 3.17 |
| Ca | 0.09 |
| Ni | 1.28 |
| Cations | 24 |
| Oxygens | 32 |

$Fe_2O_3$ determined stoichiometrically

**Machinga meteorite EDS data: Troilite**

| Analysis# | 1 | 2 | dark bands | light bands |
|---|---|---|---|---|
| Fe | 58.85 | 47.40 | 31.61 | 53.07 |
| Cr | 2.78 | 14.29 | 28.43 | 9.32 |
| Mn | 1.06 | 1.45 | 2.66 | 1.00 |
| Ni | 0.74 | 0.00 | 0.00 | 0.00 |
| S | 36.55 | 36.84 | 37.28 | 36.64 |
| Total | 99.97 | 99.98 | 99.97 | 100.03 |
| **Structural Formula** | | | | |
| Fe | 1.05 | 0.85 | 0.57 | 0.95 |
| Cr | 0.05 | 0.27 | 0.55 | 0.18 |
| Mn | 0.02 | 0.03 | 0.05 | 0.02 |
| Ni | 0.01 | 0.00 | 0.00 | 0.00 |
| Cations | 1.14 | 1.15 | 1.16 | 1.15 |
| S | 1.14 | 1.15 | 1.16 | 1.14 |

**Machinga meteorite electron microprobe data: Olivine**

Chemical analyses and structural formulae (to 3 cations) of olivine from the Machinga meteorite.

| Analysis # | 1 | 2 | Mean |
|---|---|---|---|
| $SiO_2$ | 40.91 | 41.03 | 40.97 |
| $TiO_2$ | 0.00 | 0.00 | 0.00 |
| $Al_2O_3$ | 0.15 | 0.14 | 0.15 |
| FeO | 4.87 | 3.27 | 4.07 |
| $Cr_2O_3$ | 0.00 | 0.02 | 0.01 |
| MnO | 0.02 | 0.05 | 0.03 |
| MgO | 53.50 | 53.08 | 53.29 |
| NiO | 0.33 | 2.38 | 1.36 |
| CaO | 0.41 | 0.28 | 0.35 |
| $Na_2O$ | 0.03 | 0.04 | 0.03 |
| $K_2O$ | 0.03 | 0.01 | 0.02 |
| Total | 100.25 | 100.31 | 100.28 |
| **Structural formulae** | | | |
| Si | 0.98 | 0.98 | 0.98 |
| Fe | 0.10 | 0.07 | 0.08 |
| Mn | 0.00 | 0.00 | 0.00 |
| Mg | 1.90 | 1.89 | 1.90 |
| Ni | 0.01 | 0.05 | 0.03 |
| Ca | 0.01 | 0.01 | 0.01 |
| $[Y]^6$ | 2.02 | 2.02 | 2.02 |
| **End-member compositions** | | | |
| Mg | 95.1 | 96.6 | 95.9 |
| Fe | 4.9 | 3.3 | 4.1 |
| Mn | 0.0 | 0.1 | 0.0 |

**Machinga meteorite electron microprobe data: Pyroxene**

Chemical analyses and structural formulae (to 4 cations) of the orthopyroxene from the Machinga meteorite.

| Analysis # | 1 | 2 | 3 | 4 | 5 | 6 | 7 | 8 | 9 | 10 | 11 |
|---|---|---|---|---|---|---|---|---|---|---|---|
| SiO2 | 59.86 | 59.31 | 59.73 | 59.80 | 59.51 | 59.55 | 59.99 | 59.65 | 59.61 | 59.71 | 59.49 |
| TiO2 | 0.01 | 0.01 | 0.00 | 0.01 | 0.04 | 0.04 | 0.03 | 0.01 | 0.00 | 0.00 | 0.00 |
| Al2O3 | 0.38 | 0.25 | 0.41 | 0.19 | 0.18 | 0.14 | 0.14 | 0.26 | 0.18 | 0.28 | 0.13 |
| Cr2O3 | 0.05 | 0.01 | 0.00 | 0.00 | 0.00 | 0.00 | 0.00 | 0.04 | 0.02 | 0.00 | 0.00 |
| Fe2O3 | 0.00 | 0.23 | 0.00 | 0.00 | 0.01 | 0.00 | 0.00 | 0.00 | 0.00 | 0.00 | 0.00 |
| FeO | 0.25 | 2.31 | 0.31 | 0.32 | 1.35 | 0.91 | 0.74 | 0.60 | 0.38 | 0.16 | 1.54 |
| MnO | 0.00 | 0.00 | 0.00 | 0.00 | 0.02 | 0.00 | 0.00 | 0.03 | 0.00 | 0.06 | 0.00 |
| NiO | 0.03 | 0.02 | 0.00 | 0.05 | 0.00 | 0.24 | 0.00 | 0.02 | 0.12 | 0.06 | 0.02 |
| MgO | 39.26 | 37.59 | 39.25 | 39.45 | 38.44 | 38.47 | 39.33 | 38.91 | 39.39 | 39.29 | 38.31 |
| CaO | 0.40 | 0.53 | 0.42 | 0.42 | 0.45 | 0.41 | 0.43 | 0.44 | 0.37 | 0.41 | 0.42 |
| Na2O | 0.00 | 0.19 | 0.00 | 0.00 | 0.15 | 0.19 | 0.04 | 0.00 | 0.00 | 0.00 | 0.11 |
| K2O | 0.00 | 0.01 | 0.01 | 0.01 | 0.01 | 0.01 | 0.00 | 0.01 | 0.01 | 0.02 | 0.03 |
| Total | 100.24 | 100.46 | 100.13 | 100.25 | 100.16 | 99.96 | 100.70 | 99.97 | 100.08 | 99.99 | 100.05 |
| Si IV | 2 | 2 | 2 | 2 | 2 | 2 | 2 | 2 | 2 | 2 | 2 |
| T site | 2 | 2 | 2 | 2 | 2 | 2 | 2 | 2 | 2 | 2 | 2 |
| Al VI | 0.01 | 0.01 | 0.02 | 0.01 | 0.01 | 0.01 | 0.01 | 0.01 | 0 | 0.01 | 0.01 |
| Fe +3 | 0 | 0.01 | 0 | 0 | 0 | 0 | 0 | 0 | 0 | 0 | 0 |
| Fe +2 | 0.01 | 0.07 | 0.01 | 0.01 | 0.04 | 0.03 | 0.02 | 0.02 | 0.01 | 0 | 0.04 |
| Mg | 1.96 | 1.89 | 1.96 | 1.97 | 1.93 | 1.93 | 1.95 | 1.95 | 1.97 | 1.96 | 1.92 |
| Ca | 0.01 | 0.02 | 0.02 | 0.02 | 0.02 | 0.01 | 0.02 | 0.02 | 0.01 | 0.01 | 0.02 |
| Na | 0 | 0.01 | 0 | 0 | 0.01 | 0.01 | 0 | 0 | 0 | 0 | 0.01 |
| M1,M2 | 2 | 2 | 2 | 2 | 2 | 2 | 2 | 2 | 2 | 2 | 2 |
| O | 6.01 | 6 | 6.01 | 6 | 6 | 6 | 6 | 6.01 | 6 | 6.01 | 6 |
| En | 98.9 | 95.4 | 98.8 | 98.8 | 97.3 | 97.9 | 98.2 | 98.3 | 98.8 | 99 | 97 |
| Fs | 0.4 | 3.6 | 0.4 | 0.4 | 1.9 | 1.3 | 1 | 0.9 | 0.5 | 0.2 | 2.2 |
| Wo | 0.7 | 1 | 0.8 | 0.8 | 0.8 | 0.8 | 0.8 | 0.8 | 0.7 | 0.7 | 0.8 |
| Mg# | 99.6 | 96.4 | 99.6 | 99.5 | 98 | 98.7 | 99 | 99.1 | 99.5 | 99.7 | 97.8 |

**Machinga meteorite electron microprobe data: Pyroxene continued**

Chemical analyses and structural formulae (to 4 cations) of the orthopyroxene from the Machinga meteorite (continued).

| Analysis # | 12 | 13 | 14 | 15 | 16 | 17 | 18 | 19 | 20 | 21 | 22 |
|---|---|---|---|---|---|---|---|---|---|---|---|
| SiO2 | 59.51 | 59.62 | 59.45 | 59.53 | 59.69 | 59.72 | 59.1 | 58.45 | 59.04 | 59.62 | 58.94 |
| TiO2 | 0.02 | 0 | 0 | 0.01 | 0 | 0.06 | 0.02 | 0.03 | 0 | 0 | 0 |
| Al2O3 | 0.14 | 0.09 | 0.07 | 0.14 | 0.17 | 0.11 | 0.22 | 0.23 | 0.21 | 0.17 | 0.31 |
| Cr2O3 | 0.02 | 0.01 | 0.01 | 0.03 | 0 | 0.03 | 0.05 | 0 | 0 | 0 | 0.03 |
| Fe2O3 | 0 | 0.11 | 0 | 0 | 0.4 | 0 | 0 | 0 | 0 | 0.58 | 0 |
| FeO | 1.09 | 0.84 | 0.89 | 1.08 | 0.52 | 0.24 | 3.42 | 5.08 | 3.14 | 0.04 | 2.51 |
| MnO | 0.01 | 0 | 0 | 0 | 0.01 | 0.02 | 0.03 | 0 | 0 | 0 | 0.02 |
| NiO | 0 | 0.05 | 0.09 | 0.04 | 0.06 | 0.05 | 0.21 | 0.15 | 0 | 0.06 | 0.04 |
| MgO | 38.81 | 38.89 | 38.93 | 38.59 | 38.7 | 39.43 | 36.81 | 35.76 | 37.3 | 38.93 | 37.66 |
| CaO | 0.46 | 0.25 | 0.32 | 0.39 | 0.42 | 0.38 | 0.4 | 0.44 | 0.4 | 0.4 | 0.42 |
| Na2O | 0.04 | 0.15 | 0 | 0.15 | 0.26 | 0 | 0 | 0.04 | 0.04 | 0.27 | 0 |
| K2O | 0.02 | 0.02 | 0.02 | 0 | 0.02 | 0 | 0.05 | 0.03 | 0.03 | 0.01 | 0.01 |
| Total | 100.12 | 100.03 | 99.78 | 99.96 | 100.25 | 100.04 | 100.31 | 100.21 | 100.16 | 100.08 | 99.94 |
| Si IV | 2 | 2 | 2 | 2 | 2 | 2 | 2.01 | 2 | 2 | 2 | 2 |
| T site | 2 | 2 | 2 | 2 | 2 | 2 | 2.01 | 2 | 2 | 2 | 2 |
| Al VI | 0 | 0 | 0 | 0.01 | 0.01 | 0 | 0.01 | 0.01 | 0.01 | 0.01 | 0.01 |
| Fe +3 | 0 | 0 | 0 | 0 | 0.01 | 0 | 0 | 0 | 0 | 0.01 | 0 |
| Fe +2 | 0.03 | 0.02 | 0.03 | 0.03 | 0.01 | 0.01 | 0.1 | 0.15 | 0.09 | 0 | 0.07 |
| Mg | 1.94 | 1.95 | 1.95 | 1.94 | 1.93 | 1.97 | 1.86 | 1.82 | 1.88 | 1.95 | 1.9 |
| Ca | 0.02 | 0.01 | 0.01 | 0.01 | 0.02 | 0.01 | 0.01 | 0.02 | 0.01 | 0.01 | 0.02 |
| Na | 0 | 0.01 | 0 | 0.01 | 0.02 | 0 | 0 | 0 | 0 | 0.02 | 0 |
| M1,M2 | 2 | 2 | 2 | 2 | 2 | 2 | 1.99 | 2 | 2 | 2 | 2 |
| O | 6 | 6 | 6 | 6 | 6 | 6.01 | 6.01 | 6 | 6 | 6 | 6 |
| En | 97.6 | 98.2 | 98.2 | 97.8 | 98 | 99 | 94.3 | 91.9 | 94.8 | 98.5 | 95.7 |
| Fs | 1.5 | 1.3 | 1.3 | 1.5 | 1.2 | 0.3 | 4.9 | 7.3 | 4.5 | 0.8 | 3.6 |
| Wo | 0.8 | 0.5 | 0.6 | 0.7 | 0.8 | 0.7 | 0.7 | 0.8 | 0.7 | 0.7 | 0.8 |
| Mg# | 98.4 | 98.7 | 98.7 | 98.5 | 98.7 | 99.6 | 95 | 92.6 | 95.5 | 99.2 | 96.4 |

**Machinga meteorite electron microprobe data: Pyroxene continued**

Chemical analyses and structural formulae (to 4 cations) of the orthopyroxene from the Machinga meteorite (continued).

| Analysis # | 23 | 24 | 25 | 26 | 27 | Mean |
|---|---|---|---|---|---|---|
| SiO2 | 59.94 | 59.51 | 59.59 | 59.79 | 59.41 | 59.52 |
| TiO2 | 0 | 0 | 0.01 | 0 | 0.06 | 0.01 |
| Al2O3 | 0.14 | 0.14 | 0.15 | 0.17 | 0.17 | 0.19 |
| Cr2O3 | 0.01 | 0.01 | 0 | 0 | 0 | 0.01 |
| Fe2O3 | 0.29 | 0 | 0 | 0 | 0 | 0.06 |
| FeO | 0.77 | 0.91 | 0.92 | 0.16 | 0.99 | 1.17 |
| MnO | 0 | 0 | 0 | 0 | 0.02 | 0.01 |
| NiO | 0.04 | 0.05 | 0 | 0.05 | 0.03 | 0.05 |
| MgO | 38.7 | 38.93 | 38.83 | 38.53 | 38.84 | 38.57 |
| CaO | 0.38 | 0.34 | 0.47 | 0.5 | 0.45 | 0.41 |
| Na2O | 0.3 | 0 | 0.04 | 0.37 | 0 | 0.09 |
| K2O | 0 | 0.03 | 0.03 | 0.04 | 0.04 | 0.02 |
| Total | 100.57 | 99.92 | 100.04 | 99.61 | 100.01 | 100.11 |
| Si IV | 2 | 2 | 2 | 2.01 | 2 | 2 |
| T site | 2 | 2 | 2 | 2.01 | 2 | 2 |
| Al VI | 0.01 | 0.01 | 0.01 | 0.01 | 0 | 0.01 |
| Fe +3 | 0.01 | 0 | 0 | 0 | 0 | 0 |
| Fe +2 | 0.02 | 0.03 | 0.03 | 0 | 0.03 | 0.03 |
| Mg | 1.93 | 1.95 | 1.94 | 1.93 | 1.95 | 1.93 |
| Ca | 0.01 | 0.01 | 0.02 | 0.02 | 0.02 | 0.01 |
| Na | 0.02 | 0 | 0 | 0.02 | 0 | 0.01 |
| M1,M2 | 2 | 2 | 2 | 1.99 | 2 | 2 |
| O | 6 | 6 | 6 | 6 | 6 | 6 |
| En | 97.8 | 98.1 | 97.8 | 98.8 | 97.8 | 97.51 |
| Fs | 1.5 | 1.3 | 1.3 | 0.2 | 1.4 | 1.74 |
| Wo | 0.7 | 0.6 | 0.9 | 0.9 | 0.8 | 0.75 |
| Mg# | 98.5 | 98.7 | 98.7 | 99.8 | 98.6 | 98.24 |

**Machinga meteorite electron microprobe data: Plagioclase**

Chemical analyses and structural formulae (to 32 oxygen atoms) of plagioclase from the Machinga meteorite.

| Analysis # | 1 | 2 | 3 | 4 | Mean |
|---|---|---|---|---|---|
| $SiO_2$ | 64.76 | 65.09 | 65.04 | 65.63 | 65.13 |
| $TiO_2$ | 0.00 | 0.00 | 0.03 | 0.00 | 0.01 |
| $Al_2O_3$ | 22.06 | 22.23 | 22.04 | 21.25 | 21.90 |
| FeO | 0.24 | 0.20 | 0.16 | 0.17 | 0.19 |
| $Cr_2O_3$ | 0.00 | 0.06 | 0.00 | 0.00 | 0.02 |
| MnO | 0.08 | 0.04 | 0.04 | 0.02 | 0.04 |
| MgO | 0.08 | 0.06 | 0.07 | 0.04 | 0.06 |
| NiO | 0.03 | 0.02 | 0.02 | 0.00 | 0.02 |
| CaO | 2.02 | 2.07 | 1.37 | 2.04 | 1.87 |
| $Na_2O$ | 10.29 | 10.01 | 10.08 | 9.90 | 10.07 |
| $K_2O$ | 0.43 | 0.88 | 1.04 | 1.00 | 0.84 |
| Total | 99.98 | 100.68 | 99.89 | 100.06 | 100.15 |
| **Structural formulae** | | | | | |
| Si | 11.38 | 11.38 | 11.44 | 11.56 | 11.44 |
| $Al^{IV}$ | 4.57 | 4.58 | 4.57 | 4.41 | 4.53 |
| Z | 15.95 | 15.96 | 16.02 | 15.97 | 15.97 |
| Fe | 0.03 | 0.03 | 0.02 | 0.03 | 0.03 |
| Cr | 0.00 | 0.01 | 0.00 | 0.00 | 0.00 |
| Mn | 0.01 | 0.01 | 0.01 | 0.00 | 0.01 |
| Mg | 0.02 | 0.02 | 0.02 | 0.01 | 0.02 |
| Ca | 0.38 | 0.39 | 0.26 | 0.38 | 0.35 |
| Na | 3.51 | 3.39 | 3.44 | 3.38 | 3.43 |
| K | 0.10 | 0.20 | 0.23 | 0.23 | 0.19 |
| X | 3.98 | 3.98 | 3.93 | 3.99 | 3.97 |
| **End-member compositions** | | | | | |
| ab | 88 | 85 | 87 | 85 | 86 |
| an | 10 | 10 | 7 | 10 | 9 |
| or | 2 | 5 | 6 | 6 | 5 |

**Machinga meteorite electron microprobe data: Calcite**

Analyses of probable carbonate and ideal calcite
in the Machinga meteorite.

| Analysis # | 1 | 2 | Ideal |
|---|---|---|---|
| Fe | 0.86 | 0.83 | 0 |
| Mn | 1.05 | 1.07 | 0 |
| Mg | 1.05 | 1.01 | 0 |
| Ca | 37.09 | 37.08 | 40.04 |
| Total | 40.06 | 39.99 | 40.04 |

**Machinga meteorite electron microprobe data: Magnetite**

Chemical composition and structural formulae (to 24 cations) of magnetite from the Machinga meteorite ($Fe^{3+}$ stoichiometrically calculated).

| Analysis # | 1 | 2 | 3 | 4 | 5 | Mean |
|---|---|---|---|---|---|---|
| $TiO_2$ | 0.42 | 0.36 | 0.40 | 0.40 | 0.41 | 0.40 |
| $Cr_2O_3$ | 2.24 | 2.10 | 2.34 | 2.52 | 2.09 | 2.26 |
| $Fe_2O_3$ | 66.56 | 66.38 | 66.59 | 66.15 | 66.18 | 66.37 |
| FeO | 30.05 | 29.35 | 29.76 | 30.02 | 30.09 | 29.85 |
| MnO | 1.49 | 1.85 | 1.77 | 1.34 | 1.28 | 1.55 |
| NiO | 0.10 | 0.12 | 0.17 | 0.31 | 0.09 | 0.16 |
| ZnO | 0.12 | 0.18 | 0.08 | 0.00 | 0.03 | 0.08 |
| Total | 100.98 | 100.34 | 101.11 | 100.74 | 100.17 | 100.67 |
| Ti | 0.10 | 0.08 | 0.09 | 0.09 | 0.09 | 0.09 |
| Cr | 0.54 | 0.51 | 0.56 | 0.61 | 0.51 | 0.55 |
| $Fe^{+3}$ | 15.27 | 15.32 | 15.25 | 15.21 | 15.30 | 15.27 |
| $Fe^{+2}$ | 7.66 | 7.53 | 7.58 | 7.67 | 7.73 | 7.63 |
| Mn | 0.38 | 0.48 | 0.46 | 0.35 | 0.33 | 0.40 |
| Ni | 0.02 | 0.03 | 0.04 | 0.08 | 0.02 | 0.04 |
| Zn | 0.03 | 0.04 | 0.02 | 0.00 | 0.01 | 0.02 |
| Cations | 24 | 24 | 24 | 24 | 24 | 24 |
| O | 32 | 32 | 32 | 32 | 32 | 32 |

**Machinga meteorite electron microprobe data: Troilite**

Chemical analyses and structural formulae (to 2 atoms) of troilite from the Machinga meteorite.

| Analysis # | 1 | 2 | 3 | 4 | 5 | 6 | 7 | Mean |
|---|---|---|---|---|---|---|---|---|
| S | 36.54 | 36.44 | 36.43 | 36.84 | 36.42 | 36.33 | 36.54 | 36.51 |
| Fe | 63.18 | 63.29 | 63.21 | 63.55 | 63.27 | 63.06 | 63.43 | 63.28 |
| Cu | 0.07 | 0.10 | 0.10 | 0.14 | 0.11 | 0.03 | 0.10 | 0.09 |
| Ni | 0.13 | 0.14 | 0.11 | 0.12 | 0.22 | 0.31 | 0.08 | 0.16 |
| Zn | 0.00 | 0.05 | 0.05 | 0.02 | 0.03 | 0.04 | 0.05 | 0.03 |
| Total | 99.92 | 100.01 | 99.90 | 100.68 | 100.05 | 99.77 | 100.20 | 100.07 |
| S | 1.00 | 1.00 | 1.00 | 1.00 | 1.00 | 1.00 | 1.00 | 1.00 |
| Fe | 0.99 | 1.00 | 1.00 | 0.99 | 1.00 | 1.00 | 1.00 | 1.00 |

**Machinga meteorite electron microprobe data: Fe-Ni phases**

Chemical analyses of nickel-iron phases in the Machinga meteorite.

| Analysis # | 1 | 2 | 3 | 4 | 5 | 6 | 7 | 8 | 9 | 10 | 11 | 12 | 13 |
|---|---|---|---|---|---|---|---|---|---|---|---|---|---|
| Ti | 0.03 | 0.00 | 0.00 | 0.01 | 0.04 | 0.00 | 0.00 | 0.00 | 0.02 | 0.00 | 0.01 | 0.00 | 0.00 |
| V | 0.03 | 0.02 | 0.00 | 0.02 | 0.00 | 0.02 | 0.01 | 0.00 | 0.00 | 0.00 | 0.01 | 0.00 | 0.01 |
| Cr | 0.03 | 0.01 | 0.00 | 0.02 | 0.00 | 0.03 | 0.00 | 0.04 | 0.01 | 0.00 | 0.03 | 0.05 | 0.02 |
| Mn | 0.00 | 0.00 | 0.08 | 0.09 | 0.02 | 0.00 | 0.10 | 0.00 | 0.00 | 0.06 | 0.02 | 0.01 | 0.03 |
| Fe | 91.64 | 91.10 | 91.68 | 91.49 | 91.32 | 92.87 | 91.93 | 91.66 | 91.82 | 91.20 | 92.17 | 92.97 | 91.85 |
| Co | 0.35 | 0.26 | 0.41 | 0.35 | 0.30 | 0.28 | 0.26 | 0.27 | 0.28 | 0.27 | 0.39 | 0.34 | 0.26 |
| Ni | 7.74 | 7.58 | 7.79 | 7.80 | 7.79 | 7.75 | 7.80 | 7.98 | 7.42 | 7.79 | 7.79 | 7.92 | 7.86 |
| Zn | 0.00 | 0.28 | 0.11 | 0.05 | 0.04 | 0.04 | 0.01 | 0.06 | 0.00 | 0.07 | 0.00 | 0.07 | 0.14 |
| Total | 99.83 | 99.25 | 100.07 | 99.82 | 99.52 | 100.99 | 100.11 | 100.01 | 99.55 | 99.39 | 100.42 | 101.35 | 100.18 |

**Machinga meteorite electron microprobe data: Fe-Ni phases continued**

Chemical analyses of nickel-iron phases in the Machinga meteorite continued.

| 14 | 15 | 16 | 17 | 18 |
|---|---|---|---|---|
| 0.00 | 0.02 | 0.00 | 0.00 | 0.00 |
| 0.01 | 0.03 | 0.00 | 0.00 | 0.00 |
| 0.02 | 0.00 | 0.01 | 0.04 | 0.00 |
| 0.03 | 0.00 | 0.04 | 0.00 | 0.09 |
| 91.65 | 92.18 | 91.93 | 91.83 | 91.91 |
| 0.39 | 0.21 | 0.27 | 0.30 | 0.29 |
| 7.76 | 7.88 | 7.84 | 8.09 | 7.84 |
| 0.02 | 0.16 | 0.00 | 0.11 | 0.00 |
| 99.88 | 100.47 | 100.09 | 100.36 | 100.13 |

# Appendix C
## EDS and electron microprobe data of minerals in the Balaka meteorite

**Balaka meteorite EDS data: Olivine**

| | |
|---|---|
| $SiO_2$ | 39.49 |
| FeO | 18.48 |
| MnO | 0.41 |
| MgO | 41.50 |
| CaO | 0.31 |
| Total | 100.19 |
| **Structural formula** | |
| Si | 1.01 |
| Fe | 0.39 |
| Mn | 0.01 |
| Mg | 1.58 |
| Ca | 0.01 |
| **End-member** | |
| fo | 80 |
| fa | 20 |

**Balaka meteorite EDS data: Pyroxene**

| | |
|---|---|
| SiO2 | 54.68 |
| Al2O3 | 1.01 |
| FeO | 15.27 |
| Cr2O3 | 0.35 |
| MnO | 0.29 |
| MgO | 27.29 |
| CaO | 1.01 |
| Total | 99.89 |
| **Structural formula** | |
| Si | 1.97 |
| Al | 0.04 |
| Fe | 0.46 |
| Cr | 0.01 |
| Mn | 0.01 |
| Mg | 1.47 |
| Ca | 0.04 |
| **End-member** | |
| en | 75 |
| fs | 23 |
| wo | 2 |

**Balaka meteorite EDS data: Chromite**

| | |
|---|---|
| $SiO_2$ | 8.75 |
| $TiO_2$ | 2.77 |
| $Al_2O_3$ | 5.37 |
| FeO | 26.53 |
| $Cr_2O_3$ | 46.07 |
| MnO | 0.75 |
| MgO | 8.09 |
| CaO | 0.32 |
| $Na_2O$ | 0.81 |
| Total | 99.45 |
| **Structural formula** | |
| Si | 2.32 |
| Ti | 0.55 |
| Al | 1.68 |
| Fe | 5.89 |
| Cr | 9.67 |
| Mn | 0.17 |
| Mg | 3.20 |
| Ca | 0.09 |
| Na | 0.42 |
| Cats | 24 |
| Oxygens | 32.18 |

**Balaka meteorite EDS data: Troilite**

| | |
|---|---|
| Fe | 63.71 |
| S | 36.23 |
| Total | 99.94 |
| **Structural formulae** | |
| Fe | 1.00 |
| S | 0.99 |

**Balaka meteorite EDS data: Fe-Ni phases**

| | | |
|---|---|---|
| Si | 3.91 | 6.66 |
| Al | 0.47 | 0.82 |
| Fe | 67.47 | 68.78 |
| Ni | 23.91 | 16.08 |
| Mg | 4.30 | 7.65 |
| Total | 100.05 | 99.98 |

**Balaka meteorite electron microprobe data: Olivine**

Chemical analyses and structural formulae (to 3 cations) of olivine from the Balaka meteorite.

| Analysis # | 1 | 2 | 3 | 4 | 5 | 6 | 7 | 8 | 9 | 10 |
|---|---|---|---|---|---|---|---|---|---|---|
| SiO2 | 38.25 | 38.25 | 38.29 | 38.31 | 38.22 | 38.76 | 38.15 | 38.23 | 38.15 | 38.28 |
| TiO2 | 0.01 | 0 | 0 | 0.01 | 0 | 0 | 0.01 | 0 | 0 | 0.03 |
| Al2O3 | 0.1 | 0.01 | 0 | 0 | 0.02 | 0.04 | 0.03 | 0 | 0.02 | 0.03 |
| FeO | 20.57 | 20.6 | 20.37 | 20.25 | 20.72 | 20.52 | 21.12 | 20.71 | 21.1 | 20.43 |
| Cr2O3 | 1.43 | 0.05 | 0.01 | 0.03 | 0 | 0.08 | 0.06 | 0 | 0 | 0.01 |
| MnO | 0.45 | 0.47 | 0.42 | 0.33 | 0.4 | 0.51 | 0.46 | 0.53 | 0.49 | 0.45 |
| MgO | 39.53 | 39.51 | 39.72 | 39.82 | 39.4 | 40.08 | 39.06 | 39.42 | 39.07 | 39.66 |
| NiO | 0.04 | 0.05 | 0.09 | 0 | 0 | 0 | 0.01 | 0.06 | 0.03 | 0 |
| CaO | 0.04 | 0.04 | 0.03 | 0.05 | 0.01 | 0.02 | 0.03 | 0.01 | 0.05 | 0 |
| Na2O | 0 | 0 | 0.21 | 0 | 0 | 0.13 | 0 | 0 | 0.04 | 0.04 |
| Total | 100.44 | 98.98 | 99.14 | 98.8 | 98.77 | 100.13 | 98.93 | 98.94 | 98.96 | 98.93 |
| **Structural formula** | | | | | | | | | | |
| Si | 0.99 | 1.00 | 1.00 | 1.00 | 1.00 | 1.00 | 1.00 | 1.00 | 1.00 | 1.00 |
| T-site | 0.99 | 1.00 | 1.00 | 1.00 | 1.00 | 1.00 | 1.00 | 1.00 | 1.00 | 1.00 |
| Fe | 0.44 | 0.45 | 0.44 | 0.44 | 0.45 | 0.44 | 0.46 | 0.45 | 0.46 | 0.45 |
| Cr | 0.03 | 0.00 | 0.00 | 0.00 | 0.00 | 0.00 | 0.00 | 0.00 | 0.00 | 0.00 |
| Mn | 0.01 | 0.01 | 0.01 | 0.01 | 0.01 | 0.01 | 0.01 | 0.01 | 0.01 | 0.01 |
| Mg | 1.52 | 1.54 | 1.54 | 1.55 | 1.54 | 1.54 | 1.52 | 1.54 | 1.52 | 1.54 |
| Ca | 0.00 | 0.00 | 0.00 | 0.00 | 0.00 | 0.00 | 0.00 | 0.00 | 0.00 | 0.00 |
| Na | 0.00 | 0.00 | 0.01 | 0.00 | 0.00 | 0.01 | 0.00 | 0.00 | 0.00 | 0.00 |
| Sum | 2.00 | 2.00 | 2.00 | 2.00 | 2.00 | 2.00 | 1.99 | 2.00 | 1.99 | 2.00 |
| **End-member** | | | | | | | | | | |
| Mg | 77.0 | 77.0 | 77.3 | 77.5 | 76.9 | 77.2 | 76.3 | 76.8 | 76.3 | 77.2 |
| Fe | 22.5 | 22.5 | 22.2 | 22.1 | 22.7 | 22.2 | 23.2 | 22.6 | 23.1 | 22.3 |
| Mn | 0.5 | 0.5 | 0.5 | 0.4 | 0.4 | 0.6 | 0.5 | 0.6 | 0.5 | 0.5 |

**Balaka meteorite electron microprobe data: Olivine continued**

Chemical analyses and structural formulae (to 3 cations) of olivine from the Balaka meteorite continued.

| Analysis # | 11 | 12 | 13 | 14 | 15 | 16 | 17 | 18 | 19 | 20 | 21 |
|---|---|---|---|---|---|---|---|---|---|---|---|
| SiO2 | 38.35 | 38.31 | 38.36 | 38.92 | 38.83 | 38.93 | 38.84 | 38.81 | 38.73 | 38.79 | 38.82 |
| TiO2 | 0.01 | 0.02 | 0.02 | 0 | 0 | 0 | 0.03 | 0 | 0 | 0.02 | 0 |
| Al2O3 | 0 | 0.01 | 0.02 | 0 | 0.01 | 0.01 | 0.03 | 0 | 0.01 | 0 | 0 |
| FeO | 20.04 | 20.26 | 19.98 | 19.65 | 20.13 | 19.59 | 20.11 | 20.29 | 20.67 | 20.37 | 20.2 |
| Cr2O3 | 0.03 | 0 | 0 | 0.04 | 0 | 0 | 0.05 | 0 | 0.01 | 0 | 0.01 |
| MnO | 0.39 | 0.47 | 0.45 | 0.42 | 0.47 | 0.54 | 0.41 | 0.52 | 0.45 | 0.37 | 0.46 |
| MgO | 40.01 | 39.81 | 40.06 | 40.35 | 39.93 | 40.4 | 39.94 | 39.79 | 39.45 | 39.71 | 39.86 |
| NiO | 0.02 | 0.02 | 0 | 0 | 0 | 0.01 | 0.01 | 0.02 | 0 | 0 | 0 |
| CaO | 0 | 0.03 | 0.03 | 0.01 | 0.03 | 0.02 | 0.02 | 0.44 | 0.05 | 0.01 | 0.02 |
| Na2O | 0.08 | 0 | 0 | 0 | 0 | 0.08 | 0 | 0 | 0 | 0.13 | 0 |
| Total | 98.93 | 98.93 | 98.92 | 99.39 | 99.4 | 99.58 | 99.44 | 99.86 | 99.38 | 99.41 | 99.37 |
| **Structural formula** | | | | | | | | | | | |
| Si | 1.00 | 1.00 | 1.00 | 1.01 | 1.01 | 1.01 | 1.01 | 1 | 1.01 | 1.01 | 1.01 |
| T-site | 1.00 | 1.00 | 1.00 | 1.01 | 1.01 | 1.01 | 1.01 | 1 | 1.01 | 1.01 | 1.01 |
| Fe | 0.44 | 0.44 | 0.44 | 0.43 | 0.44 | 0.42 | 0.44 | 0.44 | 0.45 | 0.44 | 0.44 |
| Cr | 0.00 | 0.00 | 0.00 | 0.00 | 0.00 | 0.00 | 0 | 0 | 0 | 0 | 0 |
| Mn | 0.01 | 0.01 | 0.01 | 0.01 | 0.01 | 0.01 | 0.01 | 0.01 | 0.01 | 0.01 | 0.01 |
| Mg | 1.55 | 1.55 | 1.55 | 1.56 | 1.54 | 1.55 | 1.54 | 1.53 | 1.53 | 1.54 | 1.54 |
| Ca | 0.00 | 0.00 | 0.00 | 0.00 | 0.00 | 0.00 | 0 | 0.01 | 0 | 0 | 0 |
| Na | 0.00 | 0.00 | 0.00 | 0.00 | 0.00 | 0.00 | 0 | 0 | 0 | 0.01 | 0 |
| Sum | 2.00 | 2.00 | 2.00 | 2.00 | 1.99 | 1.98 | 1.99 | 1.99 | 1.99 | 2 | 1.99 |
| **End-member** | | | | | | | | | | | |
| Mg | 77.7 | 77.4 | 77.7 | 78.2 | 77.5 | 78.1 | 77.6 | 77.3 | 76.9 | 77.3 | 77.5 |
| Fe | 21.8 | 22.1 | 21.8 | 21.4 | 21.9 | 21.3 | 21.9 | 22.1 | 22.6 | 22.3 | 22 |
| Mn | 0.4 | 0.5 | 0.5 | 0.5 | 0.5 | 0.6 | 0.4 | 0.6 | 0.5 | 0.4 | 0.5 |

**Balaka meteorite electron microprobe data: Olivine continued**

Chemical analyses and structural formulae (to 3 cations) of olivine from the Balaka meteorite continued.

| Analysis # | 22 | 23 | 24 | 25 | 26 | 27 | 28 | 29 | 30 | Mean |
|---|---|---|---|---|---|---|---|---|---|---|
| SiO2 | 38.57 | 38.77 | 38.77 | 38.81 | 38.71 | 38.77 | 38.9 | 38.82 | 38.78 | 38.58 |
| TiO2 | 0 | 0.02 | 0.01 | 0 | 0 | 0.02 | 0.04 | 0.02 | 0.04 | 0.01 |
| Al2O3 | 0 | 0.03 | 0.02 | 0.03 | 0 | 0.03 | 0.04 | 0 | 0 | 0.02 |
| FeO | 21.57 | 20.45 | 20.46 | 20.28 | 20.81 | 20.47 | 19.77 | 20.21 | 20.42 | 20.40 |
| Cr2O3 | 0.03 | 0 | 0 | 0.02 | 0 | 0.03 | 0.04 | 0 | 0.01 | 0.06 |
| MnO | 0.42 | 0.48 | 0.47 | 0.44 | 0.39 | 0.4 | 0.55 | 0.42 | 0.44 | 0.45 |
| MgO | 38.66 | 39.64 | 39.64 | 39.79 | 39.33 | 39.62 | 40.24 | 39.85 | 39.67 | 39.70 |
| NiO | 0.07 | 0 | 0.01 | 0.03 | 0 | 0 | 0 | 0 | 0.04 | 0.02 |
| CaO | 0 | 0.04 | 0.03 | 0.03 | 0.01 | 0.04 | 0.04 | 0.04 | 0.01 | 0.04 |
| Na2O | 0.08 | 0 | 0 | 0 | 0.17 | 0.21 | 0 | 0 | 0 | 0.04 |
| Total | 99.4 | 99.45 | 99.39 | 99.43 | 99.43 | 99.59 | 99.61 | 99.35 | 99.41 | 99.32 |
| **Structural formula** | | | | | | | | | | |
| Si | 1.01 | 1.01 | 1.01 | 1.01 | 1.01 | 1 | 1.01 | 1.01 | 1.01 | 1.00 |
| T-site | 1.01 | 1.01 | 1.01 | 1.01 | 1.01 | 1 | 1.01 | 1.01 | 1.01 | 1.00 |
| Fe | 0.47 | 0.44 | 0.44 | 0.44 | 0.45 | 0.44 | 0.43 | 0.44 | 0.44 | 0.44 |
| Cr | 0 | 0 | 0 | 0 | 0 | 0 | 0 | 0 | 0 | 0.00 |
| Mn | 0.01 | 0.01 | 0.01 | 0.01 | 0.01 | 0.01 | 0.01 | 0.01 | 0.01 | 0.01 |
| Mg | 1.51 | 1.54 | 1.54 | 1.54 | 1.52 | 1.53 | 1.55 | 1.54 | 1.54 | 1.54 |
| Ca | 0 | 0 | 0 | 0 | 0 | 0 | 0 | 0 | 0 | 0.00 |
| Na | 0 | 0 | 0 | 0 | 0.01 | 0.01 | 0 | 0 | 0 | 0.00 |
| Sum | 1.99 | 1.99 | 1.99 | 1.99 | 1.99 | 1.99 | 1.99 | 1.99 | 1.99 | 1.99 |
| **End-member** | | | | | | | | | | |
| Mg | 75.8 | 77.1 | 77.1 | 77.4 | 76.8 | 77.2 | 77.9 | 77.5 | 77.2 | 77.2 |
| Fe | 23.7 | 22.3 | 22.3 | 22.1 | 22.8 | 22.4 | 21.5 | 22.1 | 22.3 | 22.3 |
| Mn | 0.5 | 0.5 | 0.5 | 0.5 | 0.4 | 0.4 | 0.6 | 0.5 | 0.5 | 0.5 |

**Balaka meteorite electron microprobe data: Pyroxene**

Chemical analyses and structural formulae (to 4 cations) of pyroxene from the Balaka meteorite.

| Analysis # | 1 | 2 | 3 | 4 | 5 | 6 | 7 | 8 | 9 | 10 | 11 |
|---|---|---|---|---|---|---|---|---|---|---|---|
| SiO2 | 54.97 | 55.04 | 55.09 | 55.16 | 55.17 | 55.06 | 55.12 | 55.08 | 54.69 | 55.19 | 55.12 |
| TiO2 | 0.12 | 0.12 | 0.06 | 0.07 | 0.16 | 0.07 | 0.05 | 0.09 | 0.06 | 0.1 | 0.08 |
| Al2O3 | 0.14 | 0.17 | 0.12 | 0.16 | 0.16 | 0.2 | 0.2 | 0.23 | 0.2 | 0.17 | 0.17 |
| Cr2O3 | 0.12 | 0.08 | 0.11 | 0.12 | 0.05 | 0 | 0.08 | 0.09 | 0.1 | 0.03 | 0.01 |
| Fe2O3 | 0.86 | 0.76 | 1.51 | 0.94 | 2.17 | 2.15 | 1.08 | 1.82 | 0.85 | 1.61 | 0.98 |
| FeO | 12.16 | 11.99 | 11.17 | 11.42 | 10.28 | 10.67 | 11.44 | 10.93 | 13.15 | 10.72 | 11.51 |
| MnO | 0.52 | 0.4 | 0.6 | 0.47 | 0.52 | 0.47 | 0.52 | 0.55 | 0.52 | 0.5 | 0.42 |
| NiO | 0 | 0 | 0.02 | 0 | 0 | 0 | 0.06 | 0 | 0.08 | 0 | 0.1 |
| MgO | 29.12 | 29.34 | 29.47 | 29.68 | 29.72 | 29.4 | 29.57 | 29.44 | 28.29 | 29.78 | 29.58 |
| CaO | 0.97 | 0.96 | 0.96 | 0.95 | 0.95 | 0.96 | 0.95 | 0.96 | 0.99 | 0.95 | 0.95 |
| Na2O | 0 | 0 | 0.08 | 0 | 0.24 | 0.24 | 0 | 0.16 | 0 | 0.12 | 0 |
| K2O | 0 | 0 | 0 | 0 | 0 | 0 | 0 | 0 | 0 | 0 | 0 |
| Total | 98.98 | 98.86 | 99.19 | 98.97 | 99.42 | 99.23 | 99.07 | 99.35 | 98.92 | 99.17 | 98.93 |
| $Si^{IV}$ | 1.98 | 1.98 | 1.98 | 1.98 | 1.97 | 1.97 | 1.98 | 1.97 | 1.98 | 1.98 | 1.98 |
| $Al^{IV}$ | 0.01 | 0.01 | 0.01 | 0.01 | 0.01 | 0.01 | 0.01 | 0.01 | 0.01 | 0.01 | 0.01 |
| T site | 1.99 | 1.99 | 1.98 | 1.99 | 1.98 | 1.98 | 1.99 | 1.98 | 1.99 | 1.98 | 1.99 |
| $Fe^{+3}$ | 0.02 | 0.02 | 0.04 | 0.03 | 0.06 | 0.06 | 0.03 | 0.05 | 0.02 | 0.04 | 0.03 |
| $Fe^{+2}$ | 0.37 | 0.36 | 0.34 | 0.34 | 0.31 | 0.32 | 0.34 | 0.33 | 0.4 | 0.32 | 0.35 |
| Mn | 0.02 | 0.01 | 0.02 | 0.01 | 0.02 | 0.01 | 0.02 | 0.02 | 0.02 | 0.02 | 0.01 |
| Mg | 1.56 | 1.57 | 1.58 | 1.59 | 1.58 | 1.57 | 1.58 | 1.57 | 1.53 | 1.59 | 1.58 |
| Ca | 0.04 | 0.04 | 0.04 | 0.04 | 0.04 | 0.04 | 0.04 | 0.04 | 0.04 | 0.04 | 0.04 |
| Na | 0 | 0 | 0.01 | 0 | 0.02 | 0.02 | 0 | 0.01 | 0 | 0.01 | 0 |
| M1,M2 | 2.01 | 2.01 | 2.02 | 2.01 | 2.02 | 2.02 | 2.01 | 2.02 | 2.01 | 2.02 | 2.01 |
| Mg | 78.6 | 79 | 79.2 | 79.7 | 79.8 | 79.1 | 79.5 | 79.2 | 76.9 | 79.9 | 79.5 |
| Fe | 19.6 | 19.1 | 18.9 | 18.5 | 18.4 | 19 | 18.7 | 19 | 21.2 | 18.3 | 18.7 |
| Ca | 1.9 | 1.9 | 1.9 | 1.8 | 1.8 | 1.9 | 1.8 | 1.9 | 1.9 | 1.8 | 1.8 |
| mg# | 79.4 | 80 | 80 | 80.6 | 80.6 | 80 | 80.3 | 80 | 77.7 | 80.7 | 80.4 |

**Balaka meteorite electron microprobe data: Pyroxene continued**

Chemical analyses and structural formulae (to 4 cations) of pyroxene from the Balaka meteorite continued.

| Analysis # | 12 | 13 | 14 | 15 | 16 | 17 | 18 | 19 | 20 | 21 | 22 |
|---|---|---|---|---|---|---|---|---|---|---|---|
| $SiO_2$ | 55.21 | 55.28 | 55.16 | 54.98 | 55.08 | 55.09 | 55.03 | 54.89 | 55.16 | 55.15 | 55.14 |
| $TiO_2$ | 0.1 | 0.12 | 0.13 | 0.1 | 0.11 | 0.09 | 0.09 | 0.13 | 0.18 | 0.1 | 0.06 |
| $Al_2O_3$ | 0.18 | 0.19 | 0.28 | 0.23 | 0.16 | 0.28 | 0.16 | 0.15 | 0.18 | 0.14 | 0.18 |
| $Cr_2O_3$ | 0.14 | 0.03 | 0 | 0.02 | 0.07 | 0.05 | 0.05 | 0.13 | 0.07 | 0.04 | 0.04 |
| $Fe_2O_3$ | 2.48 | 2.52 | 1.55 | 1.89 | 0.92 | 2.6 | 0.88 | 0.7 | 0.91 | 1.81 | 0.93 |
| FeO | 9.85 | 9.93 | 10.88 | 11.19 | 11.71 | 10.18 | 11.95 | 12.57 | 11.45 | 10.68 | 11.52 |
| MnO | 0.51 | 0.48 | 0.51 | 0.51 | 0.46 | 0.46 | 0.41 | 0.37 | 0.45 | 0.46 | 0.46 |
| NiO | 0.03 | 0.08 | 0 | 0 | 0.04 | 0.07 | 0.08 | 0.07 | 0.07 | 0.08 | 0 |
| MgO | 29.84 | 29.74 | 29.68 | 29.16 | 29.46 | 29.57 | 29.29 | 28.89 | 29.69 | 29.65 | 29.61 |
| CaO | 0.95 | 0.95 | 0.95 | 0.95 | 0.96 | 0.96 | 0.96 | 0.97 | 0.95 | 0.95 | 0.95 |
| $Na_2O$ | 0.28 | 0.32 | 0.12 | 0.2 | 0 | 0.28 | 0 | 0 | 0 | 0.16 | 0 |
| $K_2O$ | 0 | 0 | 0 | 0 | 0 | 0 | 0 | 0 | 0 | 0 | 0 |
| Total | 99.58 | 99.64 | 99.26 | 99.23 | 98.97 | 99.63 | 98.9 | 98.87 | 99.11 | 99.22 | 98.89 |
| $Si^{IV}$ | 1.97 | 1.97 | 1.97 | 1.97 | 1.98 | 1.97 | 1.98 | 1.98 | 1.98 | 1.97 | 1.98 |
| $Al^{IV}$ | 0.01 | 0.01 | 0.01 | 0.01 | 0.01 | 0.01 | 0.01 | 0.01 | 0.01 | 0.01 | 0.01 |
| T site | 1.98 | 1.98 | 1.99 | 1.98 | 1.99 | 1.98 | 1.99 | 1.99 | 1.99 | 1.98 | 1.99 |
| $Fe^{+3}$ | 0.07 | 0.07 | 0.04 | 0.05 | 0.02 | 0.07 | 0.02 | 0.02 | 0.02 | 0.05 | 0.03 |
| $Fe^{+2}$ | 0.29 | 0.3 | 0.33 | 0.34 | 0.35 | 0.3 | 0.36 | 0.38 | 0.34 | 0.32 | 0.35 |
| Mn | 0.02 | 0.01 | 0.02 | 0.02 | 0.01 | 0.01 | 0.01 | 0.01 | 0.01 | 0.01 | 0.01 |
| Mg | 1.59 | 1.58 | 1.58 | 1.56 | 1.58 | 1.57 | 1.57 | 1.56 | 1.59 | 1.58 | 1.59 |
| Ca | 0.04 | 0.04 | 0.04 | 0.04 | 0.04 | 0.04 | 0.04 | 0.04 | 0.04 | 0.04 | 0.04 |
| Na | 0.02 | 0.02 | 0.01 | 0.01 | 0 | 0.02 | 0 | 0 | 0 | 0.01 | 0 |
| M1,M2 | 2.02 | 2.02 | 2.01 | 2.02 | 2.01 | 2.02 | 2.01 | 2.01 | 2.01 | 2.02 | 2.01 |
| Mg | 80 | 79.8 | 79.7 | 78.7 | 79.2 | 79.3 | 78.9 | 78.1 | 79.7 | 79.6 | 79.5 |
| Fe | 18.2 | 18.4 | 18.5 | 19.5 | 18.9 | 18.8 | 19.2 | 20 | 18.5 | 18.5 | 18.6 |
| Ca | 1.8 | 1.8 | 1.8 | 1.8 | 1.9 | 1.9 | 1.9 | 1.9 | 1.8 | 1.8 | 1.8 |
| mg# | 80.8 | 80.7 | 80.5 | 79.5 | 80.2 | 80.2 | 79.9 | 79.1 | 80.6 | 80.5 | 80.5 |

**Balaka meteorite electron microprobe data: Plagioclase**

Chemical analyses and structural formulae (to 32 oxygen atoms) of plagioclase from the Balaka meteorite.

| Analysis # | 1 | 2 | 3 | 4 | 5 | 6 | 7 | 8 | 9 | 10 | 11 | Mean |
|---|---|---|---|---|---|---|---|---|---|---|---|---|
| SiO2 | 66.95 | 66.56 | 66.94 | 66.84 | 66.48 | 66.1 | 66.12 | 65.11 | 65.8 | 65.45 | 62.09 | 65.86 |
| TiO2 | 0.04 | 0 | 0 | 0.07 | 0.06 | 0.03 | 0.04 | 0.02 | 0.02 | 0.03 | 0 | 0.03 |
| Al2O3 | 20.68 | 20.74 | 20.64 | 20.5 | 20.45 | 20.67 | 20.39 | 21.18 | 20.83 | 21.09 | 23.89 | 21.01 |
| FeO | 0.4 | 0.44 | 0.26 | 0.36 | 0.41 | 0.5 | 0.52 | 0.55 | 0.31 | 0.23 | 0.32 | 0.39 |
| MnO | 0 | 0.03 | 0 | 0 | 0.01 | 0.04 | 0.06 | 0.03 | 0.01 | 0 | 0 | 0.02 |
| MgO | 0.03 | 0.02 | 0.07 | 0 | 0 | 0.08 | 0.03 | 0.01 | 0.08 | 0.06 | 0.12 | 0.05 |
| CaO | 2.03 | 2.26 | 2.09 | 1.71 | 2.06 | 2.03 | 1.83 | 2.44 | 2.28 | 2.13 | 4.56 | 2.31 |
| Na2O | 9.39 | 9.37 | 10.02 | 10.15 | 10.01 | 9.88 | 10.12 | 9.78 | 9.84 | 9.58 | 8.31 | 9.68 |
| K2O | 1.02 | 1.1 | 0.97 | 1.11 | 0.88 | 1.08 | 0.96 | 0.99 | 0.98 | 1.35 | 1.25 | 1.06 |
| Total | 100.55 | 100.53 | 100.99 | 100.73 | 100.36 | 100.4 | 100.08 | 100.1 | 100.16 | 99.91 | 100.52 | 100.39 |
| **Structural formula** | | | | | | | | | | | | |
| Si | 11.72 | 11.68 | 11.69 | 11.71 | 11.69 | 11.63 | 11.67 | 11.52 | 11.6 | 11.58 | 11 | 11.59 |
| Al | 4.27 | 4.29 | 4.25 | 4.23 | 4.24 | 4.29 | 4.24 | 4.42 | 4.33 | 4.4 | 4.99 | 4.36 |
| T-site | 15.98 | 15.96 | 15.94 | 15.94 | 15.92 | 15.92 | 15.91 | 15.93 | 15.93 | 15.97 | 15.99 | 15.94 |
| Ti | 0.01 | 0 | 0 | 0.01 | 0.01 | 0 | 0.01 | 0 | 0 | 0 | 0 | 0.00 |
| Fe | 0.06 | 0.06 | 0.04 | 0.05 | 0.06 | 0.07 | 0.08 | 0.08 | 0.05 | 0.03 | 0.05 | 0.06 |
| Mn | 0 | 0.01 | 0 | 0 | 0 | 0.01 | 0.01 | 0 | 0 | 0 | 0 | 0.00 |
| Mg | 0.01 | 0.01 | 0.02 | 0 | 0 | 0.02 | 0.01 | 0 | 0.02 | 0.02 | 0.03 | 0.01 |
| Ca | 0.38 | 0.42 | 0.39 | 0.32 | 0.39 | 0.38 | 0.35 | 0.46 | 0.43 | 0.4 | 0.87 | 0.44 |
| Na | 3.19 | 3.19 | 3.39 | 3.45 | 3.41 | 3.37 | 3.47 | 3.35 | 3.36 | 3.28 | 2.86 | 3.30 |
| K | 0.23 | 0.25 | 0.22 | 0.25 | 0.2 | 0.24 | 0.22 | 0.22 | 0.22 | 0.3 | 0.28 | 0.24 |
| Sum | 3.88 | 3.94 | 4.06 | 4.08 | 4.07 | 4.09 | 4.15 | 4.11 | 4.08 | 4.03 | 4.09 | 4.05 |
| **End-member** | | | | | | | | | | | | |
| ab | 84 | 83 | 85 | 86 | 85 | 84 | 86 | 83 | 84 | 82 | 71 | 83 |
| an | 10 | 11 | 10 | 8 | 10 | 10 | 9 | 11 | 11 | 10 | 22 | 11 |
| or | 6 | 6 | 5 | 6 | 5 | 6 | 5 | 6 | 5 | 8 | 7 | 6 |

**Balaka meteorite electron microprobe data: Chromite**

Spinel analyses and structural formulae (to 24 cations, $Fe_2O_3$ calculated stoichiometrically) of chromite in the Balaka meteorite.

| Analysis # | 1 | 2 | 3 | 4 | 5 | 6 | 7 | 8 | 9 | 10 | 11 | 12 | Mean |
|---|---|---|---|---|---|---|---|---|---|---|---|---|---|
| $SiO_2$ | 0.07 | 0.61 | 0.33 | 0.48 | 0.17 | 0.35 | 0.47 | 0.08 | 0.16 | 0.13 | 0.14 | 0.44 | 0.28 |
| $TiO_2$ | 0.06 | 1.26 | 1.20 | 1.13 | 1.24 | 1.29 | 1.22 | 1.28 | 1.27 | 1.66 | 1.48 | 0.74 | 1.15 |
| $Al_2O_3$ | 23.24 | 6.31 | 6.38 | 5.98 | 6.68 | 6.41 | 5.49 | 6.14 | 6.23 | 5.83 | 5.96 | 6.90 | 7.63 |
| $Fe_2O_3$ | 5.91 | 1.65 | 2.65 | 1.38 | 3.42 | 3.76 | 1.82 | 2.23 | 3.64 | 4.46 | 3.92 | 3.07 | 3.16 |
| $Cr_2O_3$ | 45.08 | 57.55 | 57.58 | 58.14 | 57.14 | 56.71 | 59.47 | 59.28 | 57.32 | 57.94 | 58.42 | 57.51 | 56.84 |
| $V_2O_5$ | 0.14 | 0.68 | 0.75 | 0.83 | 0.64 | 0.67 | 0.51 | 0.70 | 0.65 | 0.67 | 0.59 | 0.57 | 0.62 |
| FeO | 7.46 | 28.45 | 28.42 | 28.40 | 28.36 | 27.69 | 27.97 | 26.83 | 26.59 | 25.68 | 25.99 | 26.18 | 25.67 |
| MnO | 0.16 | 0.52 | 0.49 | 0.48 | 0.46 | 0.41 | 0.44 | 0.43 | 0.47 | 0.46 | 0.52 | 0.70 | 0.46 |
| NiO | 0.11 | 0.01 | 0.02 | 0.01 | 0.08 | 0.06 | 0.08 | 0.08 | 0.02 | 0.04 | 0.12 | 0.06 | 0.06 |
| ZnO | 0.00 | 0.49 | 0.29 | 0.27 | 0.10 | 0.29 | 0.41 | 0.32 | 0.48 | 0.26 | 0.40 | 0.31 | 0.30 |
| MgO | 18.55 | 2.27 | 2.48 | 2.58 | 2.36 | 2.79 | 2.40 | 3.12 | 3.09 | 3.53 | 3.31 | 4.21 | 4.22 |
| Total | 100.77 | 99.81 | 100.59 | 99.67 | 100.65 | 100.44 | 100.26 | 100.50 | 99.91 | 100.66 | 100.84 | 100.68 | 100.40 |
| Si | 0.02 | 0.17 | 0.09 | 0.14 | 0.05 | 0.10 | 0.13 | 0.02 | 0.04 | 0.04 | 0.04 | 0.12 | 0.08 |
| Ti | 0.01 | 0.27 | 0.26 | 0.24 | 0.26 | 0.27 | 0.26 | 0.27 | 0.27 | 0.35 | 0.31 | 0.16 | 0.24 |
| Al | 6.46 | 2.12 | 2.13 | 2.01 | 2.23 | 2.13 | 1.84 | 2.04 | 2.08 | 1.94 | 1.98 | 2.26 | 2.43 |
| $Fe^{3+}$ | 1.05 | 0.35 | 0.56 | 0.30 | 0.73 | 0.80 | 0.39 | 0.47 | 0.78 | 0.95 | 0.83 | 0.64 | 0.65 |
| Cr | 8.40 | 12.97 | 12.87 | 13.11 | 12.77 | 12.67 | 13.39 | 13.23 | 12.86 | 12.90 | 13.00 | 12.64 | 12.57 |
| V | 0.02 | 0.13 | 0.14 | 0.16 | 0.12 | 0.13 | 0.10 | 0.13 | 0.12 | 0.13 | 0.11 | 0.11 | 0.11 |
| $Fe^{2+}$ | 1.47 | 6.78 | 6.72 | 6.77 | 6.70 | 6.54 | 6.66 | 6.33 | 6.31 | 6.05 | 6.12 | 6.09 | 6.05 |
| Mn | 0.03 | 0.13 | 0.12 | 0.12 | 0.11 | 0.10 | 0.11 | 0.10 | 0.11 | 0.11 | 0.12 | 0.16 | 0.11 |
| Ni | 0.02 | 0.00 | 0.00 | 0.00 | 0.02 | 0.01 | 0.02 | 0.02 | 0.01 | 0.01 | 0.03 | 0.01 | 0.01 |
| Zn | 0.00 | 0.10 | 0.06 | 0.06 | 0.02 | 0.06 | 0.09 | 0.07 | 0.10 | 0.05 | 0.08 | 0.06 | 0.06 |
| Mg | 6.52 | 0.96 | 1.04 | 1.10 | 0.99 | 1.18 | 1.02 | 1.31 | 1.31 | 1.48 | 1.39 | 1.75 | 1.67 |
| Cations | 24 | 24 | 24 | 24 | 24 | 24 | 24 | 24 | 24 | 24 | 24 | 24 | 24 |

**Balaka meteorite electron microprobe data: Ti-magnetite**

Spinel analyses and structural formulae (to 24 cations, $Fe_2O_3$ calculated stoichiometrically) of Ti-magnetite in the Balaka meteorite.

| **Analysis #** | 1 |
|---|---|
| $SiO_2$ | 0.06 |
| $TiO_2$ | 34.89 |
| $Al_2O_3$ | 0.00 |
| $Fe_2O_3$ | 36.96 |
| $Cr_2O_3$ | 0.06 |
| $V_2O_5$ | 0.31 |
| FeO | 20.48 |
| MnO | 1.02 |
| NiO | 0.19 |
| ZnO | 0.01 |
| MgO | 6.07 |
| Total | 100.04 |
| Si | 0.02 |
| Ti | 7.72 |
| Al | 0.00 |
| $Fe^{3+}$ | 8.18 |
| Cr | 0.01 |
| V | 0.06 |
| $Fe^{2+}$ | 5.04 |
| Mn | 0.26 |
| Ni | 0.04 |
| Zn | 0.00 |
| Mg | 2.66 |
| Cations | 24 |

**Balaka meteorite electron microprobe data: Troilite**

**Sulphide, troilite chemical analyses and structural formulae (to 2 atoms) from the Balaka meteorite.**

| Analysis# | 1 | 2 | 3 | 4 | 5 | Mean |
|---|---|---|---|---|---|---|
| S | 36.04 | 35.88 | 36.24 | 36.18 | 36.28 | 36.12 |
| Fe | 63.26 | 63.14 | 63.71 | 63.84 | 63.21 | 63.43 |
| Cu | 0.03 | 0.02 | 0.03 | 0.00 | 0.04 | 0.02 |
| Ni | 0.01 | 0.04 | 0.10 | 0.04 | 0.00 | 0.04 |
| Zn | 0.00 | 0.05 | 0.00 | 0.02 | 0.00 | 0.01 |
| Pb | 0.00 | 0.53 | 0.00 | 0.00 | 0.53 | 0.21 |
| Total | 99.34 | 99.65 | 100.09 | 100.08 | 100.08 | 99.85 |
| **Structural formula to two atoms** | | | | | | |
| S | 1.00 | 0.99 | 1.00 | 1.00 | 1.00 | 1.00 |
| Fe | 1.00 | 1.00 | 1.01 | 1.01 | 1.00 | 1.01 |
| Cu | 0.00 | 0.00 | 0.00 | 0.00 | 0.00 | 0.00 |
| Ni | 0.00 | 0.00 | 0.00 | 0.00 | 0.00 | 0.00 |
| Zn | 0.00 | 0.00 | 0.00 | 0.00 | 0.00 | 0.00 |
| Pb | 0.00 | 0.00 | 0.00 | 0.00 | 0.00 | 0.00 |

**Balaka meteorite electron microprobe data: Fe-Ni phases**

Metals analyses of Fe-Ni for the Balaka meteorite.

| Analysis # | Si | Ti | Al | Fe | Cr | V | Mn | Ni | Zn | Mg | Total |
|---|---|---|---|---|---|---|---|---|---|---|---|
| 1 | 0.15 | 0.05 | 0.01 | 94.24 | 0.02 | 0.02 | 0.03 | 5.22 | 0.00 | 0.09 | 99.82 |
| 2 | 0.10 | 0.00 | 0.00 | 92.97 | 0.04 | 0.00 | 0.07 | 6.39 | 0.00 | 0.07 | 99.63 |
| 3 | 0.05 | 0.00 | 0.00 | 76.56 | 0.00 | 0.00 | 0.04 | 23.31 | 0.04 | 0.00 | 99.99 |
| 4 | 0.11 | 0.02 | 0.02 | 76.00 | 0.00 | 0.00 | 0.02 | 23.86 | 0.00 | 0.02 | 100.04 |
| 5 | 0.10 | 0.00 | 0.03 | 66.35 | 0.02 | 0.04 | 0.00 | 33.29 | 0.02 | 0.01 | 99.86 |
| 6 | 0.13 | 0.00 | 0.01 | 64.90 | 0.04 | 0.00 | 0.03 | 34.51 | 0.05 | 0.02 | 99.68 |
| 7 | 0.08 | 0.02 | 0.01 | 66.45 | 0.00 | 0.04 | 0.00 | 33.46 | 0.02 | 0.00 | 100.08 |
| 8 | 0.09 | 0.04 | 0.01 | 65.34 | 0.00 | 0.01 | 0.00 | 34.62 | 0.00 | 0.00 | 100.12 |
| 9 | 0.07 | 0.00 | 0.01 | 65.83 | 0.00 | 0.02 | 0.06 | 33.88 | 0.05 | 0.00 | 99.92 |
| 10 | 0.07 | 0.03 | 0.00 | 66.59 | 0.00 | 0.06 | 0.02 | 33.44 | 0.00 | 0.00 | 100.20 |
| 11 | 0.21 | 0.01 | 0.03 | 56.69 | 0.01 | 0.00 | 0.02 | 43.04 | 0.06 | 0.08 | 100.16 |
| 12 | 0.09 | 0.00 | 0.00 | 55.95 | 0.05 | 0.00 | 0.04 | 43.88 | 0.09 | 0.00 | 100.09 |
| Mean #1 | 0.12 | 0.02 | 0.00 | 93.60 | 0.03 | 0.01 | 0.05 | 5.81 | 0.00 | 0.08 | 99.73 |
| Mean #2 | 0.08 | 0.01 | 0.01 | 76.28 | 0.00 | 0.00 | 0.03 | 23.59 | 0.02 | 0.01 | 100.02 |
| Mean #3 | 0.09 | 0.02 | 0.01 | 65.91 | 0.01 | 0.03 | 0.02 | 33.87 | 0.02 | 0.00 | 99.98 |
| Mean #4 | 0.15 | 0.01 | 0.01 | 56.32 | 0.03 | 0.00 | 0.03 | 43.46 | 0.07 | 0.04 | 100.12 |

# Appendix D
# EDS and electron microprobe data of minerals in the Chisenga meteorite

**Chisenga meteorite EDS data: Fe-Ni phases**

| Analysis# | 1 | 2 | 3 | 4 | 5 |
|---|---|---|---|---|---|
| Fe | 92.81 | 90.75 | 92.93 | 93.51 | 73.15 |
| Ni | 7.06 | 9.09 | 7.03 | 6.69 | 26.87 |
| P | 0.12 | 0.00 | 0.00 | 0.00 | 0.00 |
| Total | 99.99 | 99.84 | 99.95 | 100.20 | 100.02 |

**Chisenga meteorite EDS data: Schreibersite**

| Analysis# | 1 | 2 | 3 | Mean |
|---|---|---|---|---|
| Fe | 63.93 | 54.18 | 54.78 | 57.63 |
| Ni | 20.75 | 30.78 | 30.19 | 27.24 |
| P | 15.52 | 15.48 | 15.29 | 15.43 |
| Total | 100.19 | 100.44 | 100.26 | 100.30 |
| **Structural formulae** | | | | |
| Fe | 2.29 | 1.94 | 1.96 | 2.06 |
| Ni | 0.71 | 1.05 | 1.03 | 0.93 |
| P | 1.00 | 1.00 | 0.99 | 1.00 |

**Chisenga meteorite normalised EDS data: Kamacite and taenite**

| Kamacite | 1 | 2 | 3 | 4 | 5 | 6 | 7 |
|---|---|---|---|---|---|---|---|
| Size in µm | 1200 | 3000 | 2200 | 1900 | 2200 | 2500 | 1000 |
| Ni | 7.17 | 7.35 | 7.79 | 6.98 | 6.23 | 7.10 | 7.53 |
| Fe | 92.83 | 92.65 | 92.21 | 93.02 | 93.77 | 92.90 | 92.47 |
| Total | 100.00 | 100.00 | 100.00 | 100.00 | 100.00 | 100.00 | 100.00 |

| Taenite | 1 | 2 | 3 | 4 | 5 | 6 | 7 | 8 | 9 | 10 |
|---|---|---|---|---|---|---|---|---|---|---|
| Size in µm | 100 | 150 | 200 | 170 | 120 | 300 | 200 | 100 | 100 | 100 |
| Ni | 20.18 | 10.63 | 12.96 | 16.03 | 25.64 | 16.42 | 20.67 | 22.45 | 19.60 | 13.07 |
| Fe | 79.82 | 89.37 | 87.04 | 83.97 | 74.36 | 83.58 | 79.33 | 77.55 | 80.40 | 86.93 |
| | 100.00 | 100.00 | 100.00 | 100.00 | 100.00 | 100.00 | 100.00 | 100.00 | 100.00 | 100.00 |

# Appendix E
## EDS and electron microprobe data of minerals in the unknown meteorite specimens from Asab

**Asab meteorites EDS data: Olivine**

| Analysis# | Asab 2 |
|---|---|
| $SiO_2$ | 42.21 |
| $Al_2O_3$ | 1.06 |
| FeO | 20.1 |
| MgO | 36.16 |
| CaO | 0.48 |
| Total | 100.01 |
| **Structural Formula** | |
| Si | 1.07 |
| Al | 0.03 |
| Fe | 0.43 |
| Mg | 1.37 |
| Ca | 0.01 |
| **End-member** | |
| fo | 76 |
| fa | 24 |

**Asab meteorites EDS data: Olivine**

| Analysis# | Asab 3A | Asab 3B |
|---|---|---|
| $SiO_2$ | 40.50 | 40.52 |
| $Al_2O_3$ | 0.51 | 0.89 |
| FeO | 22.02 | 21.21 |
| MnO | 0.43 | 0.40 |
| MgO | 35.69 | 35.21 |
| CaO | 0.00 | 0.57 |
| Total | 99.14 | 98.80 |
| **Structural Formulae** | | |
| Si | 1.05 | 1.05 |
| Al | 0.02 | 0.03 |
| Fe | 0.48 | 0.46 |
| Mn | 0.01 | 0.01 |
| Mg | 1.38 | 1.37 |
| Ca | 0.00 | 0.02 |
| **End-members** | | |
| fo | 74 | 75 |
| fa | 26 | 25 |

**Asab meteorites EDS data: Pyroxene**

| Analysis# | Asab 2A | Asab 2B |
|---|---|---|
| $SiO_2$ | 54.24 | 55.41 |
| $Al_2O_3$ | 0.00 | 0.96 |
| $Fe_2O_3$ | 0.95 | 0.00 |
| FeO | 17.88 | 14.05 |
| MnO | 0.44 | 0.41 |
| MgO | 25.85 | 27.66 |
| CaO | 0.30 | 0.71 |
| Total | 99.72 | 99.20 |
| **Structural Formulae** | | |
| Si | 1.99 | 2.00 |
| $Al^{iv}$ | 0.00 | 0.00 |
| T-site | 1.99 | 2.00 |
| $Al^{vi}$ | 0.00 | 0.04 |
| $Fe^{3+}$ | 0.03 | 0.00 |
| $Fe^{2+}$ | 0.55 | 0.42 |
| Mn | 0.01 | 0.01 |
| Mg | 1.41 | 1.49 |
| Ca | 0.01 | 0.03 |
| M1, M2 | 2.01 | 2.00 |
| **End-members** | | |
| en | 72 | 77 |
| fs | 28 | 22 |
| wo | 1 | 1 |

**Asab meteorites EDS data: Pyroxene**

| Analysis# | Asab 3A | Asab 3B |
|---|---|---|
| $SiO_2$ | 51.69 | 52.78 |
| $TiO_2$ | 0.00 | 0.23 |
| $Al_2O_3$ | 1.93 | 1.89 |
| $Cr_2O_3$ | 0.39 | 0.42 |
| $Fe_2O_3$ | 5.84 | 3.61 |
| FeO | 7.07 | 8.09 |
| MnO | 0.00 | 0.28 |
| NiO | 0.00 | 0.33 |
| MgO | 21.59 | 20.96 |
| CaO | 9.42 | 10.06 |
| $Na_2O$ | 0.90 | 0.94 |
| Total | 98.83 | 99.60 |
| **Structural formulae** | | |
| Si | 1.91 | 1.93 |
| $Al^{iv}$ | 0.88 | 0.07 |
| T-site | 1.99 | 2.00 |
| $Al^{vi}$ | 0.00 | 0.01 |
| Ti | 0.00 | 0.01 |
| Cr | 0.01 | 0.01 |
| $Fe^{3+}$ | 0.16 | 0.10 |
| $Fe^{2+}$ | 0.22 | 0.25 |
| Mn | 0.00 | 0.01 |
| Ni | 0.00 | 0.01 |
| Mg | 1.19 | 1.14 |
| Ca | 0.37 | 0.39 |
| Na | 0.06 | 0.07 |
| M1, M2 | 2.01 | 2.00 |

| **End-member** | | |
|---|---|---|
| en | 67 | 64 |
| fs | 12 | 14 |
| wo | 21 | 22 |

**Asab meteorites EDS data: Plagioclase**

| Analysis# | Asab 2 |
|---|---|
| $SiO_2$ | 66.73 |
| $Al_2O_3$ | 20.35 |
| FeO | 0.75 |
| CaO | 1.75 |
| $Na_2O$ | 10.06 |
| $K_2O$ | 0.53 |
| Total | 100.17 |
| **Structural formula** | |
| Si | 11.73 |
| Al | 4.22 |
| Sum Tet | 15.95 |
| Fe | 0.11 |
| Ca | 0.33 |
| Na | 3.43 |
| K | 0.12 |
| **End-member composition** | |
| ab | 88 |
| an | 9 |
| or | 3 |

**Asab meteorites EDS data: Troilite**

| Analysis# | Asab 3 |
|---|---|
| Fe | 60.92 |
| Co | 0.19 |
| Mg | 1.84 |
| S | 36.96 |
| Total | 99.92 |
| **Structural Formula** | |
| Fe | 1.09 |
| Co | 0.00 |
| Mg | 0.08 |
| S | 1.15 |

**Asab meteorites electron microprobe data: Olivine**

Olivine (Asab 1)

| Analysis # | 1 | 4 | 6 | 9 | 10 | 12 | 13 | 14 | 15 | 17 | Mean |
|---|---|---|---|---|---|---|---|---|---|---|---|
| SiO2 | 38.66 | 38.91 | 39.17 | 38.65 | 38.93 | 38.91 | 38.85 | 38.89 | 38.69 | 39.14 | 38.88 |
| TiO2 | 0.01 | 0.09 | 0.00 | 0.00 | 0.00 | 0.02 | 0.00 | 0.01 | 0.02 | 0.09 | 0.02 |
| Al2O3 | 0.00 | 0.00 | 0.00 | 0.00 | 0.01 | 0.01 | 0.00 | 0.00 | 0.04 | 0.00 | 0.01 |
| FeO | 19.46 | 19.33 | 19.00 | 20.46 | 19.42 | 19.38 | 20.52 | 19.23 | 19.62 | 18.84 | 19.53 |
| Cr2O3 | 0.06 | 0.01 | 0.06 | 0.01 | 0.08 | 0.03 | 0.01 | 0.03 | 0.25 | 0.00 | 0.05 |
| MnO | 0.53 | 0.50 | 0.48 | 0.41 | 0.54 | 0.50 | 0.51 | 0.47 | 0.44 | 0.51 | 0.49 |
| MgO | 41.25 | 41.38 | 41.55 | 39.87 | 41.29 | 40.37 | 40.07 | 40.68 | 40.12 | 41.38 | 40.80 |
| CaO | 0.04 | 0.02 | 0.00 | 0.01 | 0.02 | 0.02 | 0.04 | 0.01 | 0.04 | 0.04 | 0.02 |
| Na2O | 0.00 | 0.04 | 0.07 | 0.21 | 0.00 | 0.25 | 0.00 | 0.00 | 0.07 | 0.00 | 0.06 |
| K2O | 0.00 | 0.00 | 0.00 | 0.00 | 0.00 | 0.00 | 0.02 | 0.01 | 0.00 | 0.01 | 0.00 |
| Total | 100.01 | 100.27 | 100.33 | 99.62 | 100.29 | 99.48 | 100.02 | 99.33 | 99.29 | 100.03 | 99.87 |
| **Number of ions to 4 oxygens** | | | | | | | | | | | |
| Si | 0.99 | 1.00 | 1.00 | 1.00 | 1.00 | 1.00 | 1.00 | 1.00 | 1.00 | 1.00 | 1.00 |
| Ti | 0.00 | 0.00 | 0.00 | 0.00 | 0.00 | 0.00 | 0.00 | 0.00 | 0.00 | 0.00 | 0.00 |
| Al | 0.00 | 0.00 | 0.00 | 0.00 | 0.00 | 0.00 | 0.00 | 0.00 | 0.00 | 0.00 | 0.00 |
| Fe | 0.42 | 0.41 | 0.41 | 0.44 | 0.42 | 0.42 | 0.44 | 0.42 | 0.42 | 0.40 | 0.42 |
| Cr | 0.00 | 0.00 | 0.00 | 0.00 | 0.00 | 0.00 | 0.00 | 0.00 | 0.01 | 0.00 | 0.00 |
| Mn | 0.01 | 0.01 | 0.01 | 0.01 | 0.01 | 0.01 | 0.01 | 0.01 | 0.01 | 0.01 | 0.01 |
| Mg | 1.58 | 1.58 | 1.58 | 1.54 | 1.58 | 1.55 | 1.54 | 1.57 | 1.55 | 1.58 | 1.56 |
| Ca | 0.00 | 0.00 | 0.00 | 0.00 | 0.00 | 0.00 | 0.00 | 0.00 | 0.00 | 0.00 | 0.00 |
| Na | 0.00 | 0.00 | 0.00 | 0.01 | 0.00 | 0.01 | 0.00 | 0.00 | 0.00 | 0.00 | 0.00 |
| K | 0.00 | 0.00 | 0.00 | 0.00 | 0.00 | 0.00 | 0.00 | 0.00 | 0.00 | 0.00 | 0.00 |
| Sum | 3.01 | 3.00 | 3.00 | 3.00 | 3.00 | 3.00 | 3.00 | 3.00 | 3.00 | 3.00 | 3.00 |
| **End-member compositions** | | | | | | | | | | | |
| fo | 79.1 | 79.2 | 79.6 | 77.6 | 79.1 | 78.8 | 77.7 | 79.0 | 78.5 | 79.7 | 78.8 |
| fa | 20.9 | 20.8 | 20.4 | 22.4 | 20.9 | 21.2 | 22.3 | 21.0 | 21.5 | 20.3 | 21.2 |

**Asab meteorites electron microprobe data: Olivine**

Olivine (Asab 2)

| Analysis# | 1 | 2 | 4 | 5 | 6 | 11 | 12 | 14 | 18 |
|---|---|---|---|---|---|---|---|---|---|
| SiO2 | 38.75 | 38.68 | 38.38 | 38.62 | 38.67 | 38.27 | 37.72 | 37.72 | 38.64 |
| TiO2 | 0.00 | 0.00 | 0.06 | 0.04 | 0.00 | 0.01 | 0.12 | 0.06 | 0.01 |
| Al2O3 | 0.04 | 0.33 | 0.06 | 0.05 | 0.02 | 0.03 | 0.40 | 0.27 | 0.00 |
| FeO | 21.64 | 21.36 | 21.66 | 21.60 | 21.92 | 23.31 | 22.87 | 23.09 | 21.41 |
| Cr2O3 | 0.09 | 0.01 | 0.02 | 0.00 | 0.03 | 0.06 | 0.19 | 0.03 | 0.00 |
| MnO | 0.49 | 0.37 | 0.50 | 0.42 | 0.46 | 0.48 | 0.37 | 0.23 | 0.42 |
| MgO | 38.45 | 39.16 | 39.19 | 39.11 | 38.88 | 37.99 | 37.63 | 37.28 | 39.38 |
| CaO | 0.03 | 0.10 | 0.04 | 0.08 | 0.01 | 0.03 | 0.52 | 0.59 | 0.03 |
| Na2O | 0.50 | 0.00 | 0.29 | 0.04 | 0.04 | 0.00 | 0.00 | 0.01 | 0.07 |
| K2O | 0.00 | 0.00 | 0.00 | 0.01 | 0.00 | 0.00 | 0.03 | 0.28 | 0.02 |
| Total | 99.98 | 100.02 | 100.20 | 99.96 | 100.02 | 100.17 | 99.85 | 99.57 | 99.99 |
| **Number of ions to 4 oxygens** | | | | | | | | | |
| Si | 1.01 | 1.00 | 1.00 | 1.00 | 1.00 | 1.00 | 1.00 | 1.00 | 1.00 |
| Ti | 0.00 | 0.00 | 0.00 | 0.00 | 0.00 | 0.00 | 0.00 | 0.00 | 0.00 |
| Al | 0.00 | 0.01 | 0.00 | 0.00 | 0.00 | 0.00 | 0.01 | 0.01 | 0.00 |
| Fe | 0.47 | 0.46 | 0.47 | 0.47 | 0.48 | 0.51 | 0.51 | 0.51 | 0.46 |
| Cr | 0.00 | 0.00 | 0.00 | 0.00 | 0.00 | 0.00 | 0.00 | 0.00 | 0.00 |
| Mn | 0.01 | 0.01 | 0.01 | 0.01 | 0.01 | 0.01 | 0.01 | 0.01 | 0.01 |
| Mg | 1.49 | 1.51 | 1.51 | 1.51 | 1.50 | 1.48 | 1.48 | 1.47 | 1.52 |
| Ca | 0.00 | 0.00 | 0.00 | 0.00 | 0.00 | 0.00 | 0.01 | 0.02 | 0.00 |
| Na | 0.03 | 0.00 | 0.01 | 0.00 | 0.00 | 0.00 | 0.00 | 0.00 | 0.00 |
| K | 0.00 | 0.00 | 0.00 | 0.00 | 0.00 | 0.00 | 0.00 | 0.01 | 0.00 |
| Sum | 3.00 | 2.99 | 3.01 | 3.00 | 3.00 | 3.00 | 3.03 | 3.03 | 3.00 |
| **End-member compositions** | | | | | | | | | |
| fo | 76.0 | 76.6 | 76.3 | 76.3 | 76.0 | 74.4 | 74.6 | 74.2 | 76.6 |
| fa | 24.0 | 23.4 | 23.7 | 23.7 | 24.0 | 25.6 | 25.4 | 25.8 | 23.4 |

**Asab meteorites electron microprobe data: Olivine continued**

Olivine (Asab 2) continued

| Analysis# | 19 | 20 | 25 | 26 | 27 | 28 | 29 | 30 | Mean |
|---|---|---|---|---|---|---|---|---|---|
| SiO2 | 38.46 | 38.13 | 38.04 | 38.50 | 38.67 | 38.58 | 38.45 | 38.55 | 38.40 |
| TiO2 | 0.00 | 0.03 | 0.00 | 0.04 | 0.00 | 0.00 | 0.00 | 0.00 | 0.02 |
| Al2O3 | 0.00 | 0.04 | 0.04 | 0.08 | 0.01 | 0.00 | 0.02 | 0.00 | 0.08 |
| FeO | 22.37 | 21.88 | 25.39 | 23.36 | 21.83 | 22.06 | 22.59 | 22.47 | 22.40 |
| Cr2O3 | 0.01 | 0.05 | 0.02 | 0.00 | 0.00 | 0.00 | 0.01 | 0.00 | 0.03 |
| MnO | 0.42 | 0.48 | 0.38 | 0.43 | 0.46 | 0.41 | 0.45 | 0.44 | 0.42 |
| MgO | 38.40 | 38.50 | 36.41 | 37.96 | 38.99 | 38.33 | 38.47 | 38.59 | 38.40 |
| CaO | 0.03 | 0.00 | 0.04 | 0.06 | 0.02 | 0.04 | 0.01 | 0.00 | 0.10 |
| Na2O | 0.18 | 0.18 | 0.00 | 0.00 | 0.15 | 0.62 | 0.00 | 0.00 | 0.12 |
| K2O | 0.00 | 0.00 | 0.02 | 0.01 | 0.02 | 0.02 | 0.00 | 0.01 | 0.03 |
| Total | 99.88 | 99.29 | 100.36 | 100.44 | 100.15 | 100.06 | 99.99 | 100.05 | 100.00 |
| **Number of ions to 4 oxygens** | | | | | | | | | |
| Si | 1.00 | 1.00 | 1.00 | 1.00 | 1.00 | 1.00 | 1.00 | 1.00 | 1.00 |
| Ti | 0.00 | 0.00 | 0.00 | 0.00 | 0.00 | 0.00 | 0.00 | 0.00 | 0.00 |
| Al | 0.00 | 0.00 | 0.00 | 0.00 | 0.00 | 0.00 | 0.00 | 0.00 | 0.00 |
| Fe | 0.49 | 0.48 | 0.56 | 0.51 | 0.47 | 0.48 | 0.49 | 0.49 | 0.49 |
| Cr | 0.00 | 0.00 | 0.00 | 0.00 | 0.00 | 0.00 | 0.00 | 0.00 | 0.00 |
| Mn | 0.01 | 0.01 | 0.01 | 0.01 | 0.01 | 0.01 | 0.01 | 0.01 | 0.01 |
| Mg | 1.49 | 1.50 | 1.43 | 1.47 | 1.51 | 1.49 | 1.49 | 1.50 | 1.49 |
| Ca | 0.00 | 0.00 | 0.00 | 0.00 | 0.00 | 0.00 | 0.00 | 0.00 | 0.00 |
| Na | 0.01 | 0.01 | 0.00 | 0.00 | 0.01 | 0.03 | 0.00 | 0.00 | 0.01 |
| K | 0.00 | 0.00 | 0.00 | 0.00 | 0.00 | 0.00 | 0.00 | 0.00 | 0.00 |
| Sum | 3.00 | 3.00 | 3.00 | 3.00 | 3.00 | 3.01 | 3.00 | 3.00 | 3.00 |
| **End-member compositions** | | | | | | | | | |
| fo | 75.4 | 75.8 | 71.9 | 74.3 | 76.1 | 75.6 | 75.2 | 75.4 | 75.3 |
| fa | 24.6 | 24.2 | 28.1 | 25.7 | 23.9 | 24.4 | 24.8 | 24.6 | 24.7 |

**Asab meteorites electron microprobe data: Olivine**

Olivine (Asab 3)

| Analysis# | 1 | 2 | 9 | 10 | 11 | 12 | 13 |
|---|---|---|---|---|---|---|---|
| SiO2 | 38.91 | 39.18 | 38.99 | 38.87 | 39.07 | 38.80 | 38.72 |
| TiO2 | 0.09 | 0.03 | 0.00 | 0.09 | 0.00 | 0.02 | 0.00 |
| Al2O3 | 0.00 | 0.18 | 0.06 | 0.09 | 0.07 | 0.03 | 0.06 |
| FeO | 18.84 | 18.42 | 18.49 | 18.46 | 20.25 | 20.30 | 20.28 |
| Cr2O3 | 0.00 | 0.02 | 0.03 | 0.03 | 0.06 | 0.00 | 0.03 |
| MnO | 0.25 | 0.29 | 0.30 | 0.28 | 0.15 | 0.15 | 0.05 |
| MgO | 41.82 | 41.48 | 41.78 | 41.68 | 40.67 | 40.62 | 40.64 |
| CaO | 0.04 | 0.36 | 0.19 | 0.14 | 0.13 | 0.16 | 0.04 |
| Na2O | 0.00 | 0.02 | 0.07 | 0.06 | 0.07 | 0.00 | 0.07 |
| K2O | 0.01 | 0.02 | 0.08 | 0.10 | 0.02 | 0.01 | 0.02 |
| Total | 99.98 | 99.99 | 99.99 | 99.79 | 100.49 | 100.09 | 99.89 |
| **Number of ions to 4 oxygens** | | | | | | | |
| Si | 1.00 | 1.00 | 1.00 | 1.00 | 1.00 | 1.00 | 1.00 |
| Ti | 0.00 | 0.00 | 0.00 | 0.00 | 0.00 | 0.00 | 0.00 |
| Al | 0.00 | 0.01 | 0.00 | 0.00 | 0.00 | 0.00 | 0.00 |
| Fe | 0.40 | 0.39 | 0.40 | 0.40 | 0.43 | 0.44 | 0.44 |
| Cr | 0.00 | 0.00 | 0.00 | 0.00 | 0.00 | 0.00 | 0.00 |
| Mn | 0.01 | 0.01 | 0.01 | 0.01 | 0.00 | 0.00 | 0.00 |
| Mg | 1.60 | 1.58 | 1.59 | 1.59 | 1.55 | 1.56 | 1.56 |
| Ca | 0.00 | 0.01 | 0.01 | 0.00 | 0.00 | 0.00 | 0.00 |
| Na | 0.00 | 0.00 | 0.00 | 0.00 | 0.00 | 0.00 | 0.00 |
| K | 0.00 | 0.00 | 0.00 | 0.00 | 0.00 | 0.00 | 0.00 |
| Sum | 3.00 | 3.00 | 3.01 | 3.00 | 3.00 | 3.00 | 3.00 |
| **End-member compositions** | | | | | | | |
| fo | 79.8 | 80.1 | 80.1 | 80.1 | 78.2 | 78.1 | 78.1 |
| fa | 20.2 | 19.9 | 19.9 | 19.9 | 21.8 | 21.9 | 21.9 |

**Asab meteorites electron microprobe data: Olivine continued**

Olivine (Asab 3) continued

| Analysis# | 14 | 17 | 18 | 23 | 24 | 27 | Mean |
|---|---|---|---|---|---|---|---|
| SiO2 | 39.08 | 38.93 | 38.71 | 38.97 | 38.94 | 38.87 | 38.92 |
| TiO2 | 0.09 | 0.04 | 0.13 | 0.06 | 0.19 | 0.04 | 0.06 |
| Al2O3 | 0.02 | 0.11 | 0.15 | 0.04 | 0.11 | 0.06 | 0.08 |
| FeO | 20.40 | 20.24 | 20.20 | 20.07 | 20.14 | 20.63 | 19.75 |
| Cr2O3 | 0.14 | 0.07 | 0.08 | 0.07 | 0.07 | 0.00 | 0.05 |
| MnO | 0.05 | 0.04 | 0.28 | 0.15 | 0.45 | 0.35 | 0.21 |
| MgO | 40.38 | 40.43 | 40.04 | 40.58 | 40.11 | 39.40 | 40.74 |
| CaO | 0.01 | 0.38 | 0.45 | 0.06 | 0.29 | 0.29 | 0.20 |
| Na2O | 0.05 | 0.10 | 0.00 | 0.00 | 0.09 | 0.08 | 0.05 |
| K2O | 0.00 | 0.01 | 0.03 | 0.00 | 0.04 | 0.23 | 0.04 |
| Total | 100.22 | 100.35 | 100.07 | 99.99 | 100.42 | 99.94 | 100.09 |
| **Number of ions to 4 oxygens** | | | | | | | |
| Si | 1.00 | 1.00 | 1.00 | 1.00 | 1.00 | 1.00 | 1.00 |
| Ti | 0.00 | 0.00 | 0.00 | 0.00 | 0.00 | 0.00 | 0.00 |
| Al | 0.00 | 0.00 | 0.00 | 0.00 | 0.00 | 0.00 | 0.00 |
| Fe | 0.44 | 0.43 | 0.44 | 0.43 | 0.43 | 0.45 | 0.42 |
| Cr | 0.00 | 0.00 | 0.00 | 0.00 | 0.00 | 0.00 | 0.00 |
| Mn | 0.00 | 0.00 | 0.01 | 0.00 | 0.01 | 0.01 | 0.00 |
| Mg | 1.55 | 1.55 | 1.54 | 1.55 | 1.53 | 1.52 | 1.56 |
| Ca | 0.00 | 0.01 | 0.01 | 0.00 | 0.01 | 0.01 | 0.01 |
| Na | 0.00 | 0.00 | 0.00 | 0.00 | 0.00 | 0.00 | 0.00 |
| K | 0.00 | 0.00 | 0.00 | 0.00 | 0.00 | 0.01 | 0.00 |
| Sum | 2.99 | 3.00 | 3.00 | 3.00 | 3.00 | 3.00 | 3.00 |
| **End-member compositions** | | | | | | | |
| fo | 77.9 | 78.1 | 77.9 | 78.3 | 78.0 | 77.3 | 78.6 |
| fa | 22.1 | 21.9 | 22.1 | 21.7 | 22.0 | 22.7 | 21.4 |

**Asab meteorites electron microprobe data: Pyroxene**

Pyroxene (Asab 1)

| Analysis # | 1 | 2 | 3 | 4 | 5 | 6 | 7 | Mean |
|---|---|---|---|---|---|---|---|---|
| SiO2 | 55.30 | 55.15 | 55.56 | 55.75 | 55.63 | 55.64 | 55.63 | 55.52 |
| TiO2 | 0.05 | 0.26 | 0.16 | 0.31 | 0.17 | 0.14 | 0.15 | 0.18 |
| Al2O3 | 0.05 | 0.34 | 2.73 | 0.32 | 0.20 | 0.18 | 0.18 | 0.57 |
| FeO | 14.94 | 14.97 | 11.73 | 14.29 | 14.20 | 14.24 | 14.06 | 14.06 |
| Cr2O3 | 0.13 | 0.37 | 1.16 | 0.54 | 0.27 | 0.19 | 0.15 | 0.40 |
| MnO | 0.52 | 0.57 | 0.46 | 0.57 | 0.52 | 0.54 | 0.48 | 0.52 |
| MgO | 27.83 | 27.47 | 26.28 | 27.79 | 27.94 | 28.79 | 28.18 | 27.76 |
| CaO | 0.76 | 0.83 | 1.42 | 0.48 | 0.50 | 0.79 | 0.88 | 0.81 |
| Na2O | 0.07 | 0.30 | 1.17 | 0.00 | 0.00 | 0.00 | 0.20 | 0.25 |
| K2O | 0.00 | 0.00 | 0.07 | 0.01 | 0.00 | 0.00 | 0.00 | 0.01 |
| Total | 99.65 | 100.28 | 100.74 | 100.05 | 99.43 | 100.51 | 99.91 | 100.08 |
| **Number of ions to 4 oxygens** | | | | | | | | |
| Si | 2.00 | 1.98 | 1.97 | 2.00 | 2.00 | 1.99 | 2.00 | 1.99 |
| $Al^{iv}$ | 0.00 | 0.01 | 0.03 | 0.00 | 0.00 | 0.01 | 0.00 | 0.01 |
| T-site | 2.00 | 1.99 | 2.00 | 2.00 | 2.00 | 2.00 | 2.00 | 2.00 |
| $Al^{vi}$ | 0.00 | 0.00 | 0.08 | 0.01 | 0.01 | 0.00 | 0.01 | 0.02 |
| Ti | 0.00 | 0.01 | 0.00 | 0.01 | 0.00 | 0.00 | 0.00 | 0.00 |
| Cr | 0.00 | 0.01 | 0.03 | 0.02 | 0.01 | 0.01 | 0.00 | 0.01 |
| Fe | 0.45 | 0.45 | 0.35 | 0.43 | 0.43 | 0.42 | 0.42 | 0.42 |
| Mn | 0.02 | 0.02 | 0.01 | 0.02 | 0.02 | 0.02 | 0.01 | 0.02 |
| Mg | 1.50 | 1.47 | 1.39 | 1.48 | 1.50 | 1.53 | 1.51 | 1.48 |
| Ca | 0.03 | 0.03 | 0.05 | 0.02 | 0.02 | 0.03 | 0.03 | 0.03 |
| Na | 0.00 | 0.00 | 0.00 | 0.00 | 0.00 | 0.00 | 0.00 | 0.00 |
| K | 0.00 | 0.00 | 0.00 | 0.00 | 0.00 | 0.00 | 0.00 | 0.00 |
| M1, M2 | 2.0 | 2.0 | 1.9 | 2.0 | 2.0 | 2.0 | 2.0 | 2.0 |
| **End-member compositions** | | | | | | | | |
| wo | 1 | 2 | 3 | 1 | 1 | 2 | 2 | 2 |
| en | 76 | 75 | 78 | 77 | 77 | 77 | 77 | 77 |
| fs | 23 | 23 | 19 | 22 | 22 | 21 | 21 | 22 |

**Asab meteorites electron microprobe data: Pyroxene**

Pyroxene (Asab 2)

| Analysis# | 1 | 2 | 3 | 4 | Mean (opx) | 5 |
|---|---|---|---|---|---|---|
| SiO2 | 55.41 | 55.89 | 55.25 | 55.13 | 55.42 | 55.40 |
| TiO2 | 0.11 | 0.14 | 0.12 | 0.06 | 0.11 | 0.11 |
| Al2O3 | 0.13 | 0.18 | 0.30 | 0.18 | 0.20 | 0.46 |
| FeO | 14.21 | 13.40 | 17.21 | 14.97 | 14.95 | 14.68 |
| Cr2O3 | 0.09 | 0.08 | 0.20 | 0.11 | 0.12 | 0.21 |
| MnO | 0.51 | 0.53 | 0.34 | 0.52 | 0.47 | 0.36 |
| MgO | 28.18 | 28.46 | 25.86 | 27.50 | 27.50 | 24.03 |
| CaO | 0.59 | 0.64 | 0.64 | 0.44 | 0.58 | 4.99 |
| Na2O | 0.07 | 0.20 | 0.00 | 0.21 | 0.12 | 0.39 |
| K2O | 0.00 | 0.00 | 0.02 | 0.02 | 0.01 | 0.01 |
| Total | 99.28 | 99.53 | 99.93 | 99.14 | 99.47 | 100.64 |
| **Number of ions to 6 oxygens** | | | | | | |
| Si | 2.00 | 2.00 | 2.00 | 2.00 | 2.00 | 2.00 |
| Aliv | 0.00 | 0.00 | 0.00 | 0.00 | 0.00 | 0.00 |
| T-site | 2.00 | 2.00 | 2.00 | 2.00 | 2.00 | 2.00 |
| Alvi | 0.01 | 0.01 | 0.01 | 0.01 | 0.01 | 0.02 |
| Ti | 0.00 | 0.00 | 0.00 | 0.00 | 0.00 | 0.00 |
| Cr | 0.00 | 0.00 | 0.01 | 0.00 | 0.00 | 0.01 |
| Fe | 0.43 | 0.40 | 0.52 | 0.45 | 0.45 | 0.44 |
| Mn | 0.02 | 0.02 | 0.01 | 0.02 | 0.01 | 0.01 |
| Mg | 1.52 | 1.52 | 1.40 | 1.49 | 1.48 | 1.29 |
| Ca | 0.02 | 0.02 | 0.02 | 0.02 | 0.02 | 0.19 |
| Na | 0.00 | 0.01 | 0.00 | 0.01 | 0.01 | 0.03 |
| K | 0.00 | 0.00 | 0.00 | 0.00 | 0.00 | 0.00 |
| M1, M2 | 6.00 | 5.99 | 5.98 | 6.00 | 5.99 | 2.00 |
| **End-member compositions** | | | | | | |
| wo | 1 | 1 | 1 | 1 | 1 | 10 |
| en | 77 | 78 | 72 | 76 | 76 | 67 |
| fs | 22 | 21 | 27 | 23 | 23 | 23 |

**Asab meteorites electron microprobe data: Pyroxene**

Pyroxene (Asab 3)

| Analysis # | 6 | 7 | 8 | 9 | 10 | 11 | 12 | 13 | 14 | 15 | Mean opx |
|---|---|---|---|---|---|---|---|---|---|---|---|
| SiO2 | 54.28 | 54.94 | 55.42 | 55.28 | 54.98 | 54.01 | 54.88 | 54.69 | 54.74 | 55.33 | 54.86 |
| TiO2 | 0.14 | 0.13 | 0.17 | 0.02 | 0.12 | 0.14 | 0.19 | 0.12 | 0.16 | 0.12 | 0.13 |
| Al2O3 | 0.70 | 1.67 | 0.19 | 0.10 | 0.22 | 0.35 | 0.12 | 0.28 | 0.28 | 0.52 | 0.44 |
| FeO | 15.32 | 10.58 | 16.44 | 15.74 | 15.33 | 15.03 | 14.47 | 14.99 | 15.00 | 14.53 | 14.74 |
| Cr2O3 | 0.69 | 0.17 | 0.29 | 0.06 | 0.09 | 0.12 | 0.10 | 0.16 | 0.23 | 0.05 | 0.20 |
| MnO | 0.51 | 0.25 | 0.15 | 0.50 | 0.54 | 0.42 | 0.57 | 0.51 | 0.53 | 0.44 | 0.44 |
| MgO | 27.28 | 31.00 | 26.62 | 27.24 | 27.57 | 27.27 | 27.01 | 27.10 | 27.36 | 27.70 | 27.62 |
| CaO | 0.63 | 1.08 | 0.56 | 0.73 | 0.84 | 0.64 | 0.77 | 0.71 | 0.66 | 0.57 | 0.72 |
| Na2O | 0.00 | 0.11 | 0.11 | 0.21 | 0.17 | 0.17 | 0.10 | 0.28 | 0.25 | 0.52 | 0.19 |
| K2O | 0.01 | 0.01 | 0.02 | 0.01 | 0.00 | 0.01 | 0.03 | 0.05 | 0.03 | 0.03 | 0.02 |
| Total | 99.55 | 99.94 | 99.96 | 99.90 | 99.87 | 98.17 | 98.25 | 98.89 | 99.22 | 99.79 | 99.36 |
| **Number of ions to 6 oxygens** | | | | | | | | | | | |
| Si | 1.97 | 1.94 | 2.00 | 2.00 | 1.99 | 1.98 | 2.01 | 1.99 | 1.99 | 1.99 | 1.99 |
| Aliv | 0.03 | 0.06 | 0.00 | 0.00 | 0.01 | 0.02 | | 0.01 | 0.01 | 0.01 | 0.01 |
| T-site | 2.00 | 2.00 | 2.00 | 2.00 | 2.00 | 2.00 | 2.01 | 2.00 | 2.00 | 2.00 | 2.00 |
| Alvi | 0.00 | 0.01 | 0.01 | 0.00 | 0.00 | 0.00 | 0.01 | 0.00 | 0.00 | 0.01 | 0.00 |
| Ti | 0.00 | 0.00 | 0.00 | 0.00 | 0.00 | 0.00 | 0.01 | 0.00 | 0.00 | 0.00 | 0.00 |
| Cr | 0.02 | 0.00 | 0.01 | 0.00 | 0.00 | 0.00 | 0.00 | 0.00 | 0.01 | 0.00 | 0.01 |
| Fe | 0.46 | 0.31 | 0.50 | 0.48 | 0.46 | 0.46 | 0.44 | 0.46 | 0.46 | 0.44 | 0.45 |
| Mn | 0.02 | 0.01 | 0.00 | 0.02 | 0.02 | 0.01 | 0.02 | 0.02 | 0.02 | 0.01 | 0.01 |
| Mg | 1.48 | 1.63 | 1.43 | 1.47 | 1.48 | 1.49 | 1.47 | 1.47 | 1.48 | 1.49 | 1.49 |
| Ca | 0.02 | 0.04 | 0.02 | 0.03 | 0.03 | 0.03 | 0.03 | 0.03 | 0.03 | 0.02 | 0.03 |
| Na | 0.00 | 0.01 | 0.01 | 0.01 | 0.01 | 0.01 | 0.01 | 0.02 | 0.02 | 0.04 | 0.01 |
| K | 0.00 | 0.00 | 0.00 | 0.00 | 0.00 | 0.00 | 0.00 | 0.00 | 0.00 | 0.00 | 0.00 |
| M1, M2 | 2.00 | 2.02 | 1.99 | 2.01 | 2.01 | 2.01 | 1.99 | 2.01 | 2.01 | 2.01 | 2.01 |
| **End-member compositions** | | | | | | | | | | | |
| wo | 1 | 2 | 1 | 1 | 2 | 1 | 2 | 1 | 1 | 1 | 1 |
| en | 75 | 82 | 73 | 74 | 75 | 75 | 76 | 75 | 75 | 76 | 76 |
| fs | 24 | 16 | 25 | 24 | 23 | 23 | 23 | 23 | 23 | 22 | 23 |

**Asab meteorites electron microprobe data: Pyroxene continued**

Pyroxene (Asab 3) continued

| Analysis # | 16 | 17 | 18 | 19 | 20 | 21 | Mean cpx |
|---|---|---|---|---|---|---|---|
| SiO2 | 53.67 | 52.41 | 53.39 | 54.35 | 54.60 | 54.69 | 53.85 |
| TiO2 | 0.18 | 0.13 | 0.19 | 0.22 | 0.11 | 0.21 | 0.17 |
| Al2O3 | 0.31 | 0.22 | 1.65 | 0.43 | 0.69 | 0.68 | 0.66 |
| FeO | 15.35 | 24.11 | 11.78 | 11.23 | 14.12 | 13.79 | 15.06 |
| Cr2O3 | 0.26 | 0.28 | 0.49 | 0.46 | 0.17 | 0.34 | 0.33 |
| MnO | 0.25 | 0.19 | 0.41 | 0.33 | 0.31 | 0.38 | 0.31 |
| MgO | 23.84 | 15.84 | 23.85 | 23.54 | 23.53 | 23.44 | 22.34 |
| CaO | 4.44 | 6.47 | 7.54 | 7.37 | 5.15 | 5.73 | 6.12 |
| Na2O | 0.15 | 0.33 | 0.33 | 0.38 | 0.49 | 0.62 | 0.38 |
| K2O | 0.08 | 0.05 | 0.09 | 0.32 | 0.03 | 0.05 | 0.10 |
| Total | 98.52 | 100.05 | 99.70 | 98.63 | 99.21 | 99.93 | 99.34 |
| **Number of ions to 6 oxygens** | | | | | | | |
| Si | 1.99 | 2.00 | 1.94 | 1.99 | 2.00 | 1.99 | 1.99 |
| Aliv | 0.01 | 0.00 | 0.06 | 0.01 | 0.00 | 0.01 | 0.01 |
| T-site | 2.00 | 2.00 | 2.00 | 2.00 | 2.00 | 2.00 | 2.00 |
| Alvi | 0.00 | 0.01 | 0.02 | 0.01 | 0.03 | 0.02 | 0.01 |
| Ti | 0.01 | 0.00 | 0.01 | 0.01 | 0.00 | 0.01 | 0.00 |
| Cr | 0.01 | 0.01 | 0.01 | 0.01 | 0.00 | 0.01 | 0.01 |
| Fe | 0.48 | 0.77 | 0.36 | 0.34 | 0.43 | 0.42 | 0.47 |
| Mn | 0.01 | 0.01 | 0.01 | 0.01 | 0.01 | 0.01 | 0.01 |
| Mg | 1.32 | 0.90 | 1.29 | 1.29 | 1.28 | 1.27 | 1.23 |
| Ca | 0.18 | 0.27 | 0.29 | 0.29 | 0.20 | 0.22 | 0.24 |
| Na | 0.01 | 0.02 | 0.02 | 0.03 | 0.03 | 0.04 | 0.03 |
| K | 0.00 | 0.00 | 0.00 | 0.01 | 0.00 | 0.00 | 0.00 |
| M1, M2 | 2.00 | 2.00 | 2.02 | 2.01 | 2.00 | 2.01 | 2.01 |
| **End-member compositions** | | | | | | | |
| wo | 9 | 14 | 15 | 15 | 11 | 12 | 13 |
| en | 67 | 47 | 66 | 67 | 67 | 66 | 63 |
| fs | 24 | 40 | 18 | 18 | 23 | 22 | 24 |

**Asab meteorites electron microprobe data: Plagioclase**

Plagioclase (Asab 2)

| Analysis# | 1 | 2 | 3 | 4 | 5 | 6 | 7 | 8 | Mean |
|---|---|---|---|---|---|---|---|---|---|
| SiO2 | 64.92 | 65.08 | 64.83 | 66.03 | 64.82 | 64.62 | 64.60 | 64.58 | 64.94 |
| TiO2 | 0.00 | 0.00 | 0.00 | 0.06 | 0.07 | 0.07 | 0.04 | 0.00 | 0.03 |
| Al2O3 | 22.47 | 20.91 | 21.88 | 20.07 | 21.90 | 22.18 | 22.44 | 22.67 | 21.82 |
| FeO | 0.14 | 0.14 | 0.68 | 0.50 | 0.16 | 0.16 | 0.13 | 0.14 | 0.25 |
| Cr2O3 | 0.02 | 0.02 | 0.01 | 0.01 | 0.00 | 0.01 | 0.02 | 0.00 | 0.01 |
| MnO | 0.03 | 0.03 | 0.06 | 0.01 | 0.02 | 0.15 | 0.00 | 0.00 | 0.04 |
| MgO | 0.12 | 0.10 | 0.13 | 0.23 | 0.11 | 0.08 | 0.05 | 0.03 | 0.11 |
| CaO | 1.77 | 1.47 | 1.30 | 1.53 | 1.68 | 1.41 | 1.66 | 1.60 | 1.55 |
| Na2O | 10.08 | 11.55 | 10.90 | 10.54 | 10.20 | 10.64 | 10.59 | 10.08 | 10.57 |
| K2O | 0.68 | 0.78 | 0.56 | 0.65 | 0.95 | 0.58 | 0.91 | 1.07 | 0.77 |
| Total | 100.22 | 100.10 | 100.35 | 99.63 | 99.91 | 99.90 | 100.45 | 100.16 | 100.09 |
| **Numbers of ions to 32 oxygens** | | | | | | | | | |
| Si | 11.41 | 11.52 | 11.43 | 11.69 | 11.46 | 11.41 | 11.37 | 11.38 | 11.46 |
| Al | 4.66 | 4.36 | 4.55 | 4.19 | 4.56 | 4.62 | 4.66 | 4.71 | 4.54 |
| Z | 16.07 | 15.89 | 15.98 | 15.88 | 16.02 | 16.03 | 16.03 | 16.09 | 16.00 |
| Ti | 0.00 | 0.00 | 0.00 | 0.01 | 0.01 | 0.01 | 0.01 | 0.00 | 0.00 |
| Fe | 0.02 | 0.02 | 0.10 | 0.07 | 0.02 | 0.02 | 0.02 | 0.02 | 0.04 |
| Cr | 0.00 | 0.00 | 0.00 | 0.00 | 0.00 | 0.00 | 0.00 | 0.00 | 0.00 |
| Mn | 0.00 | 0.01 | 0.01 | 0.00 | 0.00 | 0.02 | 0.00 | 0.00 | 0.01 |
| Mg | 0.03 | 0.03 | 0.03 | 0.06 | 0.03 | 0.02 | 0.01 | 0.01 | 0.03 |
| Ca | 0.33 | 0.28 | 0.25 | 0.29 | 0.32 | 0.27 | 0.31 | 0.30 | 0.29 |
| Na | 3.44 | 3.97 | 3.73 | 3.62 | 3.50 | 3.64 | 3.61 | 3.44 | 3.62 |
| K | 0.15 | 0.18 | 0.12 | 0.15 | 0.21 | 0.13 | 0.21 | 0.24 | 0.17 |
| X | 3.98 | 4.48 | 4.24 | 4.20 | 4.09 | 4.12 | 4.17 | 4.01 | 4.16 |
| **End-member composition** | | | | | | | | | |
| ab | 87.6 | 89.7 | 91.0 | 89.2 | 86.8 | 90.1 | 87.4 | 86.4 | 88.5 |
| an | 8.5 | 6.3 | 6.0 | 7.1 | 7.9 | 6.6 | 7.6 | 7.6 | 7.2 |
| or | 3.9 | 4.0 | 3.0 | 3.6 | 5.3 | 3.2 | 5.0 | 6.0 | 4.3 |

# The Thuathe meteorite fall of 21 July 2002

**A. Lombard[a*], H. de Bruiyn[a], N. Scholtz[a], H.E. Praekelt[a], A. Wilson[b] and A.E. Schoch[a]**

**The Thuathe meteorite fell on 21 July 2002 between 15:45 SAST (first sightings) and 15:49 (local sightings). The meteorite is classified as an H4/5 type ordinary chondrite, confirmed by whole rock and mineralogical analyses. The minerals found in the meteorite were kamacite, troilite, albitic plagioclase, forsteritic olivine, diopside, enstatite, and chromitic spinel. Temperatures were obtained from the orthopyroxene-clinopyroxene, orthopyroxene-olivine and clinopyroxene-olivine systems, that yielded values of 1200–1600°C. With respect to average chondrites, the Thuathe meteorite samples are depleted in Zr, and enriched in Rb, Th, Ta, Ba, La, Sr, Sc, Co and Ni.**

## Introduction

The Thuathe bolide entered the atmosphere above southern Africa on Sunday, 21 July 2002 at approximately 15:45 SAST. A possible position of impact was determined from reports of fireball sightings, sounds and shock waves. Eyewitness reports were requested from police stations, farmers, tour operators and many others in the southern and eastern Free State, South Africa. Positive responses were mapped in terms of direction of sighting. The locations of observers were determined with a global positioning system and compass bearings were taken of sighting directions. All led to approximately the same area within Lesotho (Fig. 1). The general appearance of a piece of the meteorite is shown in Fig. 2.

Witnesses were asked to complete a 'meteor reporting form' (Table 1), which included date and time of sighting, tremors and sounds. If possible, latitude and longitude were provided, together with direction of sighting. Other information included light intensity and colour of the meteorite trail, velocity, duration of light and sound, and fragmentation. The purpose of this communication is to report the sightings and to provide the first analytical results obtained from specimens.

The Thuathe fall was experienced as a meteorite shower. At least 500 meteorite stones of various sizes have been recovered.[1] The samples collected range in size from a few grams to 2.3 kg, and are irregular in shape. All of them contain chondrules and exhibit dark brown fusion crusts.

*Chemical composition.* The Thuathe meteorite proved to be an ordinary chondrite, intermediate between enstatite and carbonaceous chondrites. The chemical composition (Tables 2, 3) of chondrites facilitates classification. Major and trace-element analyses of whole rock samples were conducted by means of ICP-MS in the Geology Department on the Durban campus of the University of Natal. Entire samples were dissolved using an Anton Paar multiwave microwave sample preparation system, high temperature and high pressure to solution.

*Petrography and mineralogy.* Under the microscope, several

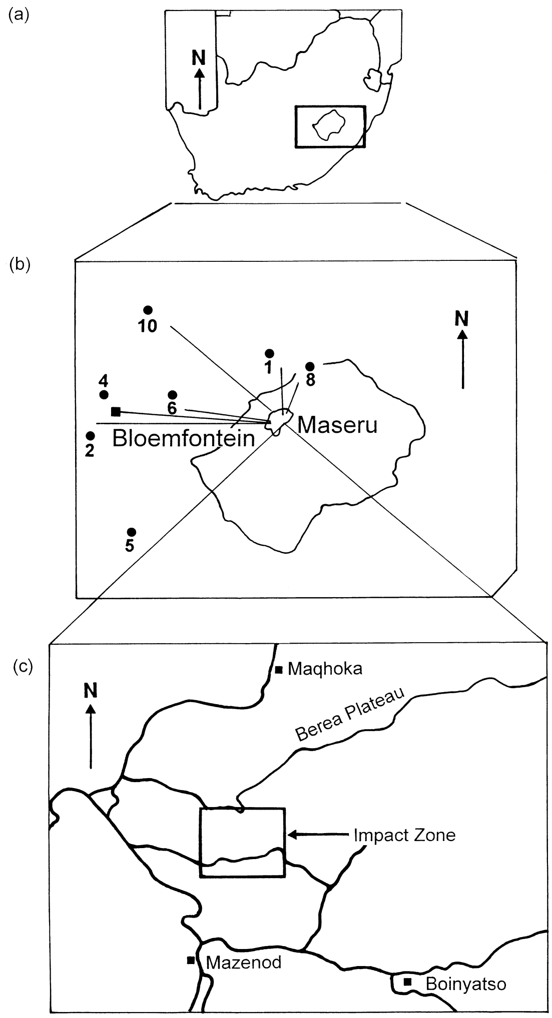


Fig. 1. (**a**) Locality map. (**b**) Position and direction of observations, numbers refer to Table 1. (**c**) The approximate 25-km$^2$ impact zone. Scale 1:250 000.

metal, sulphide, oxide and silicate phases could be distinguished. A Cameca Camebax electron microprobe was used with a 3-micron microbeam (15 kV and 30 nA) to identify the different minerals (PAP corrections and standards were used). The sulphide phase was troilite with subordinate chalcopyrite, and the oxide was chromite. The silicate phases included albitic plagioclase (an ~20%) and forsteritic olivine (fo ~85%). Pyroxene proved to be enstatitic (Fig. 3) and pigeonitic.

*Metamorphic temperatures.* In the absence of a succession of


**Fig. 2**. Photograph showing the general appearance of a sample of the Thuathe meteorite.

[a]Department of Geology, University of the Free State, P.O. Box 339, Bloemfontein 9301, South Africa.

[b]Department of Geology, University of Natal, Durban 4041, South Africa.

*Author for correspondence. E-mail: lombara@sci.uovs.ac.za

**Table 1**. Summaries of eye witness reports of the Thuathe meteorite observed on 21 July 2002.

| No. | Time SAST | Location of observer | Bearing from observer | Fireball duration | Fireball colour | Perceived velocity | Sounds, shock waves or or other general comments |
|---|---|---|---|---|---|---|---|
| 1 | 15:50 | Umpukane Farm on Clocolan/Marquard road 28°50′12″S, 27°30′25″E | 175° Moving vertically downwards | 4 s | White | Fast | No sounds or shock waves heard or felt. |
| 2 | 15:48 | Bloemfontein/Petrusburg road 29°35′15″S, 26°10′19″E | 098° Moving vertically downwards | 5s | White | Very fast | No sounds or shock waves heard or felt. |
| 3 | 15:50 | Alpha Estates Farm, Ladybrand district on Lesotho border | n/a | n/a | n/a | n/a | Shock waves felt. |
| 4 | 15:50 | Loch Logan, Bloemfontein 29°06′49″S, 26°12′34″E | 100° | 2 s | Whitewith orange tail | Fast | No sounds or shock waves heard or felt. |
| 5 | Approx. 16:00 | Rouxville Smithfield Road 30°15′48″S, 26°40′30″E | 022° | n/a | n/a | n/a | n/a |
| 6 | Approx. 16:00 | Botshabelo Mountain. 29°15′10″S, 26°45′30″E | 095° | 2 s | White | Fast heard or felt. | No sounds or shock waves |
| 8 | 15:50 | Pilot flying halfway between Ficksburg and Maseru | Moving vertically downwards | n/a | Light orange | Fast | Flew through meteor smoke trail at 40 000 ft at approx. 29°10′00″S, 27°45′00″E |
| 9 | Approx. 16:00 | Farm Goedehoop, Ladybrand district | n/a | n/a | n/a | n/a | Loud sound heard from Maseru. |
| 10 | Approx. 16:00 | Farm Leeufontein in Theunissen district | 150° | 4 s | White | Fast | No sounds or shock waves heard or felt. |

**Table 2**. Major element analysis of two samples of the Thuathe meteorite in mass percentage.

| Element | Maseru A | Maseru B |
|---|---|---|
| $SiO_2$ | 34.2900 | 34.8800 |
| $Al_2O_3$ | 1.9000 | 1.9700 |
| FeO | 33.4600 | 32.6600 |
| MnO | 0.2867 | 0.2997 |
| MgO | 21.9100 | 22.3800 |
| CaO | 1.5300 | 1.6100 |
| $Na_2O$ | 0.8200 | 0.6600 |
| $K_2O$ | 0.0900 | 0.0900 |
| $TiO_2$ | 0.0940 | 0.0966 |
| $P_2O_5$ | 0.2400 | 0.2500 |
| $Cr_2O_3$ | 0.4801 | 0.4949 |
| NiO | 1.9445 | 1.7719 |
| S | 2.8000 | 2.9000 |
| | 99.8400 | 100.0600 |

well-defined and experimentally calibrated mineral assemblages, mineral compositions are customarily used to infer metamorphic temperatures and pressures experienced by ordinary chondrites.[2] The systems orthopyroxene–clinopyroxene, orthopyroxene–olivine and clinopyroxene–olivine[3] were used for reference, from which temperatures of 1200–1600°C were deduced.

The metamorphic grade of the ordinary chondrite is difficult

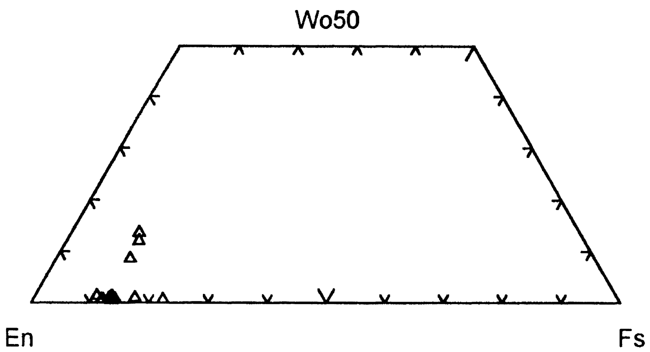


**Fig. 3**. Compositional distribution of pyroxene from the Thuathe meteorite as depicted on the pyroxene quadrilateral trapezium.

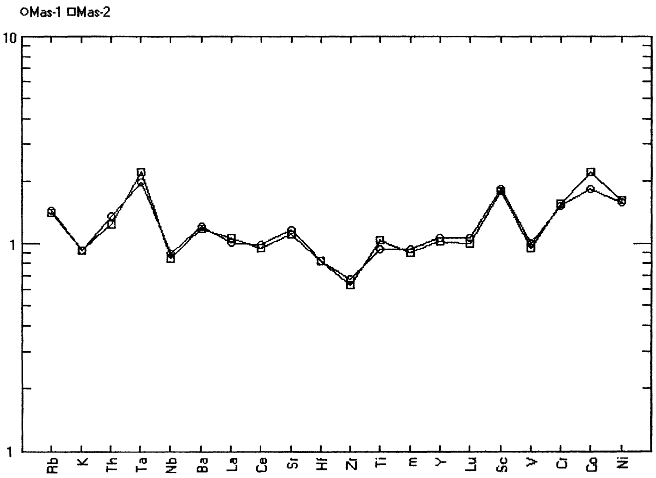


**Fig. 4**. Chondrite normalized chemical variation of two stones from the Thuathe meteorite plotted on a spidergram to determine its relative enrichment/depletion with respect to chondrite (after Wood[5]).

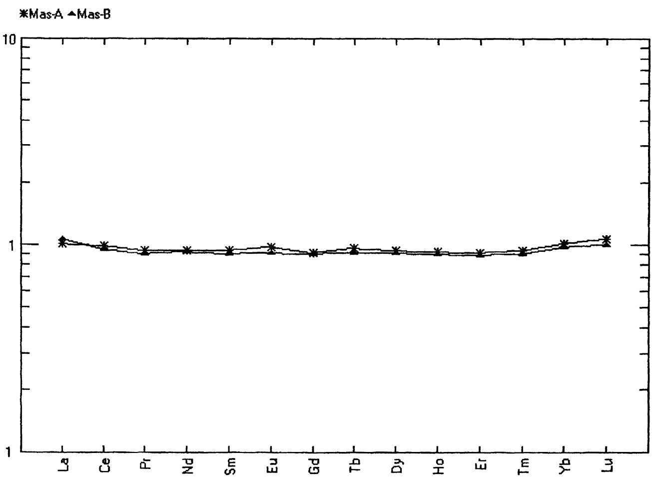


**Fig. 5**. Chondrite normalized REE (rare-earth element) distribution pattern from the Thuathe meteorite (after Sun[6]).

**Table 3**. Trace element analysis of two samples of the Thuathe meteorite in mass percentage.

| Element | Maseru A | Maseru B |
|---|---|---|
| P | 1 145.835 | 1 130.428 |
| Sc | 9.215 | 8.815 |
| V | 45.990 | 44.362 |
| Co | 814.078 | 989.599 |
| Ni | 14 055.402 | 15 459.993 |
| Cu | 89.866 | 83.806 |
| Zn | 60.880 | 59.333 |
| As | 1.662 | 2.624 |
| Rb | 2.566 | 2.486 |
| Sr | 11.505 | 11.033 |
| Y | 2.021 | 1.947 |
| Zr | 5.746 | 5.422 |
| Nb | 0.471 | 0.452 |
| Ba | 4.127 | 3.824 |
| La | 0.314 | 0.330 |
| Ce | 0.807 | 0.777 |
| Pr | 0.115 | 0.111 |
| Nd | 0.561 | 0.551 |
| Sm | 0.181 | 0.73 |
| Eu | 0.071 | 0.067 |
| Gd | 0.239 | 0.236 |
| Tb | 0.045 | 0.043 |
| Dy | 0.305 | 0.296 |
| Ho | 0.067 | 0.066 |
| Er | 0.195 | 0.189 |
| Tm | 0.031 | 0.030 |
| Yb | 0.210 | 0.204 |
| Lu | 0.034 | 0.032 |
| Hf | 0.149 | 0.148 |
| Ta | 0.041 | 0.046 |
| W | 0.208 | 0.237 |
| Pb | 0.453 | 0.385 |
| Th | 0.051 | 0.047 |
| U | 0.016 | 0.016 |

to estimate owing to the loss of volatiles that are less abundant in ordinary than in carbonaceous chondrites. The loss of volatiles can be as much as 75% of the original mass of a meteorite and even more for noble gases.[2] Low abundances of volatile elements are characteristic of ordinary chondrites.

*Classification.* The Thuathe meteorite proved to be an H-type ordinary chondrite, the classification of which was based on the atomic ratios Mg/Si, Fe/Si and Al/Si.[2] The petrological type of the meteorite was determined with the aid of the criteria of Wasson[4] and Dodd,[2] according to which the Thuathe meteorite belongs to the H4/5 type. Local shock melting was observed by means of optical microscopy, and the degree of shock was classified as S2–S3.[7]

*Chemical analysis.* The chemical composition of two stones indicated marked depletion of Zr, and enrichment in Rb, Th, Ta, Ba, La, Sr, Sc, Cr, Co and Ni, with respect to average chondrites (Fig. 4). The rare earth element spectrum is absolutely flat with no sign of LREE/HREE variation (Fig. 5). No Eu anomaly was detected.

We thank the Department of Geology, University of the Free State, for the use of facilities and for making funds available for field investigations. The use of analytical facilities at the Department of Geology, University of Natal, is gratefully acknowledged.

Received 3 December 2002. Accepted 14 April 2003.

1. Ambrose D. (2003). *Catalogue of Stones from the Strewn Field of the Thuathe Meteorite of 21 July 2002.* House 9 Publications, Lesotho.
2. Dodd R.T. (1981). In *Meteorites, a Petrologic-chemical Synthesis,* pp. 1–27, 77–132. Cambridge University Press, Cambridge.
3. More T. and Green D.H. (1978). Laboratory duplication of phase equilibria observed in natural garnet lherzolites. *J. Geol.* **86**, 83–97.
4. Wasson J.T. (1974). In *Meteorites, Classification and Properties,* pp. 11–60. Springer-Verlag, Heidelberg.
5. Wood D.A., Tarney J., Varet J., Saunders A.D., Bougault H., Joron J.L., Treuil M. and Cann J.R. (1979). Geochemistry of basalts drilled in the North Atlantic by IPOD Leg 49: implications for mantle heterogeneity. *Earth Planet. Sci. Lett.* **42**, 77–97.
6. Sun S.S. (1982). Chemical composition and origin of the earth's primitive mantle. *Geochim. Cosmochim. Acta* **46**, 179–192.
7. Ambrose D.P., Reimold W.U. and Buchanan P.C. (2003). The Thuathe meteorite of 21 July 2002, Lesotho: mapping the strewn field and initial mineralogical classification. *S. Afr. J. Sci.* **99**, 00–00.

N. Jb. Miner. Mh. Jg. **2004** (8) 357–360 Stuttgart, August 2004

# Antimony sulphides in the Thuathe meteorite of Lesotho

**Hendrik de Bruiyn, Annegret Lombard,** and **Aylva E. Schoch**

With 1 figure and 1 table

BRUIYN, H. DE, LOMBARD, A. & SCHOCH, A. E. (2004): Antimony sulphides in the Thuathe meteorite of Lesotho. – N. Jb. Miner. Mh. **2004** (8): 357–360; Stuttgart.

**Abstract:** The Thauthe meteorite that fell in July 2002 contains small grains (< 3 µm) of berthierite and stibnite. These antimony-bearing phases were identified by aid of energy dispersive and wavelength dispersive X-ray spectrometry. This is the first reported occurrence of antimony sulphides in a meteorite.

Key words: antimony, berthierite, stibnite, Thuathe meteorite

## Introduction

The Thuathe meteorite fell approximately 9 km east of Maseru, the capital of Lesotho, on 21 July 2002 (AMBROSE et al. 2003, LOMBARD et al. 2003). The meteorite was classified as an H4/5 type ordinary chondrite, chemically intermediate between enstatite chondrite and carbonaceous chondrite, with a shock degree of S2–S3. The meteoritic material were analysed by means of ICP-MS techniques and geochemically compared to the chondrite data of WOOD et al. (1979) that indicated depletion in Zr and enrichment in Rb, Th, Ta, Ba, La, Sr, Sc, Co and Ni (LOMBARD et al. 2003).

Mineralogically the meteorite consists of kamacite, troilite, albitic plagioclase, olivine ($fo_{85}$), diopside, enstatite and chromitic spinel. The purpose of this note is to report on antimony sulphidic particles that were detected during the mineralogical investigation of the constituent phases.

## Sample preparation

In order to ensure that the material did not undergo any alteration during the preparation of thin or polished sections, all cutting and polishing were done

DOI: 10.1127/0028-3649/2004/2004-0357 0028-3649/04/2004-0357 $ 1.00

using ethanol as lubricant. This also helped ensure that the material did not expand during the preparation of thin sections and thus fracture the glass slides.

## Results

Back-scatter electron images of the sample displayed some sections showing very high atomic mass (Fig. 1). These zones were analysed using an Oxford energy dispersive X-ray spectrometer on a Quanta 200 scanning electron microscope with a beam diameter of 1 µm. The grains containing antimony are very small (2–3 µm diameter) and are hard to find using conventional optical methods. The analytical data (Table 1, analyses 1 and 2) identifies the small grains as berthierite ($FeSb_2S_4$).

Wavelength techniques were also employed using a Cameca Camebax electron microprobe with 15 kV accelerating potential, 30 nA beam current and 2 µm beam diameter. The material was analysed using PAP intensity reduction techniques and mineral and pure element standards. The data depicted in Table 1 (analyses 3, 4 and 5), indicates that stibnite is also present, although it is a variety that contains a small amount of iron. According to Ramdohr (1980), terrestrial berthierite commonly decomposes to stibnite or marcasite.

**Table 1.** Chemical analyses (in weight per cent) and structural formulae of berthierite and stibnite from the Thuathe meteorite.

| | Berthierite | | | Stibnite | | | |
|---|---|---|---|---|---|---|---|
| | 1 | 2 | Mean | 3 | 4 | 5 | Mean |
| Fe | 13.13 | 12.75 | 12.94 | 1.37 | 1.30 | 1.25 | 1.30 |
| Sb | 56.98 | 57.37 | 57.18 | 69.58 | 69.63 | 69.95 | 69.72 |
| Ni | 0.00 | 0.44 | 0.22 | 0.00 | 0.08 | 0.05 | 0.05 |
| S | 29.98 | 30.23 | 30.11 | 29.15 | 29.07 | 28.65 | 28.96 |
| Total | 100.09 | 100.79 | 100.44 | 100.09 | 100.08 | 99.90 | 100.03 |
| | Structural Formulae | | | | | | |
| Fe | 1.00 | 0.97 | 0.98 | 0.08 | 0.08 | 0.07 | 0.08 |
| Sb | 1.99 | 2.00 | 1.99 | 1.92 | 1.92 | 1.92 | 1.92 |
| Ni | 0.00 | 0.03 | 0.02 | 0.00 | 0.00 | 0.00 | 0.00 |
| S | 3.98 | 4.00 | 3.99 | 3.05 | 3.04 | 2.99 | 3.03 |



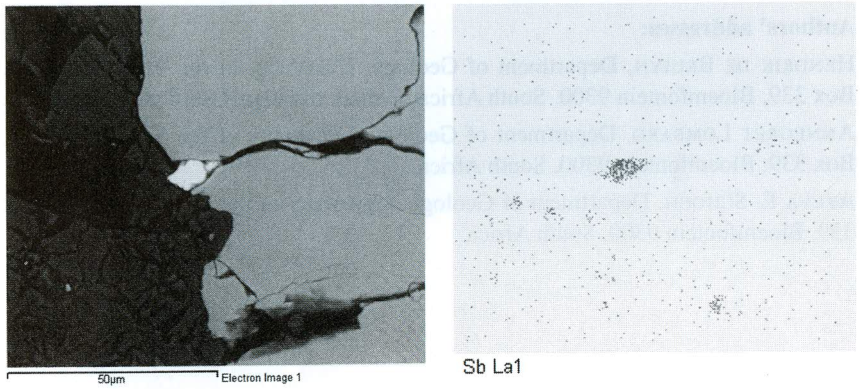


**Fig. 1** Back-scatter electron image (left) showing the distribution of the highly reflective antimony-bearing phases in the sample of the Thuathe meteorite and an antimony dot map (right) of the same area.

## Conclusions

The antimony in the Thuathe meteorite represents the first reported occurrence of antimony sulphides in meteoritic material (personal communication A. E. Rubin, September 2003). The presence of two different sulphides indicates that this is not a spurious occurrence and that antimony could well be present in other meteorites.

## References

Ambrose, D. P., Reimold, W. U. & Buchanan, P. C. (2003): The Thuathe meteorite of 21 July 2002, Lesotho: mapping the strewn field and initial mineralogical classification. – S. Afr. J. Sci. **99:** 153–159.

Lombard, A., de Bruiyn, H., Scholtz, N., Praekelt, H. E., Wilson, A. H. & Schoch, A. E. (2003): The Thuathe meteorite fall of 21 July 2002. – S. Afr. J. Sci. **99:** 160–162.

Ramdohr, P. (1980): The ore minerals and their intergrowths, Volume 2. – 2nd Ed., Oxford, Pergamon Press.

Wood, D. A, Tarney, J., Varet, J., Saunders, A. D., Bougault, H., Joron, J. L., Treuil, M. & Cann, J. R. (1979): Geochemistry of basalts drilled in the North Atlantic by IPOD leg 49: implications for mantle heterogeneity. – Earth Planet Sci. Lett. **42:** 77–97.

Received: September 30, 2003.

**Authors' addresses:**

HENDRIK DE BRUIYN, Department of Geology, University of the Free State, P. O. Box 339, Bloemfontein 9300, South Africa. E-mail: dBruiynH.Sci@mail.uovs.ac.za

ANNEGRET LOMBARD, Department of Geology, University of the Free State, P. O. Box 339, Bloemfontein 9300, South Africa.

AYLVA E. SCHOCH, Department of Geology, University of the Free State, P. O. Box 339, Bloemfontein 9300, South Africa.

# *32nd IGC - Florence, 2004*

## Abstract title

ANTIMONY MINERALS IN A METEORITE: A FIRST REPORT


## Authors

DE BRUIYN HENDRIK [1], LOMBARD ANNEGRET [1], SCHOCH AYLVA E. [2]

presenter's e-mail: dbruiynh.sci@mail.uovs.ac.za

1 - University of the Free State, South Africa
2 - University of the Free State



## Keywords

Thuathe meteorite

stibnite

berthierite

Lesotho


## Abstract


On the 21st July 2002 a fair-sized fireball was observed over the southern Free State, South Africa. At 13:47 GMT an explosion with a sound duration of approximately 10 seconds was heard over a distance of 16km from an area north of Maseru, Lesotho to the east. Nearly 500 stones constituting about 30 kg of meteorite were recovered from the strwen field on the Thuathe (Berea) Plateau. The Thuathe meteorite is classified as an H4/5 ordinary chondrite showing S2 to S3 shock features. Major and trace element analyses are in agreement with the textural classification. Microscopic blebs of antimony-containing material were identified by means of back-scatter electron microscopy and energy dispersive X-ray spectrometry. The presence of antimony was verified by wavelength X-ray spectrometry and different grains were analysed. The analyses confirm the presence of two phases namely berthierite (Sb2FeS4) and stibnite (Sb2S3).



***ACCEPTED as Poster Presentation***
***in session: "G18.01 - Comparing planetary systems"***

Oriental, il s'agit pratiquement d'une séquence sédimentaire à faciès Kellwasser s'étendant stratigraphiquement de la sous-zone inférieure à *rhenana* jusqu'à la sous-zone supérieure à *crepida*.

L'évenement kellwasser se manifeste par l'extinction de toutes les espèces de Conodontes exceptées quelques espèces d'*Icriodus*. Le renouvellement des faunes à la base du Famennien est marqué par des variations de forme et de réduction considérable de taille chez les espèces de *Palmatolepis* (LAZREQ, N. 1999).

L'analyse des biofaciès à Conodontes dont la distribution est liée à la bathymétrie (LAZREQ,N. 1999 ), a permis aussi une résolution fine. Elle met en évidence l'événement Kellwasser et des fluctuations eustatiques du niveau marin qui sont considérées comme l'une des causes de l'événement Kellwasser (SANDBERG & al., 1988). De même, des variations des valeurs de susceptibilité magnétique observées dans les coupes du Maroc Central ont été observées au niveau de la limite Frasnien-Famennien (RIQUIER, L. & al. 2004).

Une régression juste après la limite Frasnien-Famennien, ainsi que l'atteste la lacune de la sous-zone inférieure à *triangularis* de la base du Famennien se manifeste, par les nombreux hard-grounds, et des microstromatolithes ferrugineux particulièrement abondants au niveau de cette limite. Un remaniement synsédimentaire a été observé dans les coupes de l'Anti-Atlas (EL ALBANI A. & al. 2004)

**Références bibliographiques**

**El Albani, A.; Riquier, L.; Averbuch, O. ; Tribovillard, N.; Lazreq,N. ; Baidder, L.; Chakiri, S. 2004:** Concretions levels and hard-grounds in the Upper devonian series of Anti-Atlas: their significance for palaenvironmental analysis.- Devonian neritic-pelagic correlation and events, International Meeting on Stratigraphy, p. 58-59,Rabat, Morocco.

**Lazreq, N. (1999):** Biostratigraphie des conodontes du Givétien au Famennien du Maroc Central- Biofaciès et événement Kellwasser : Cour. Forsch.- Senckenberg/ 214/ 1-111/ 33 Figs., 3 Tab., 14 Pls./ Frankfurt a.M.

**Riquier, L.; El Albani, A.; Averbuch, O. ; Tribovillard, N.; Lazreq,N. ; Chakiri, S. 2004:** Paleoenvironmental changes at the Frasnian/Famennian boundary in Central Morocco.- Devonian neritic-pelagic correlation and events, International Meeting on Stratigraphy, p. 83-85,Rabat, Morocco.

**Sandberg, C.A.; Ziegler, W.; Dreesen, R.; Butler, J.L. 1988:** Late Frasnian Mass Extinction: Conodont Event Stratigraphy, Global Changes and possible causes. In: ZIEGLER, W. (ed.): 1st International senckenberg Conference and 5th European Conodont Symposium (ECOS V), Contributions I.- Cour. Forsch.- Inst. Senckenberg, 102: 263-307; Frankfurt a.M.

**Tucker, R.D., Bradley, D.C., Ver Straeten, C.A., Harris, A.G. & Mc Cutcheon, S.R., 1988:** New U-Pb zircon ages and the duration and division of Devonian time. Earth Planetary Science Letters, 158, 175-186.

## The Machinga meteorite – neither cosmic fish nor flesh?

**Lombard A*.; et Tredoux, M.**
*University of the Free State, South Africa*
**Corresponding author: Tel +27 51 4012414 Fax: +27 51 401381, E-mail : lombarda.sci@mail.uovs.ac.za*

The Machinga meteorite fell on 22 January 1981, at 10h00 local time, near the Mlelemba village in the southern Machinga province of Malawi (Graham et al., 1984). It had a total weight of 93.2 kg and was classified as a L6 ordinary chondrite (Graham et al., 1984; 1985). Though the study of meteorites may seem irrelevant in an African context, it is relevant to note that meteorite research is very important as it gives insight to the formation of our solar system and the universe. It is therefore an important field of study that should be developed especially in Africa where we are loosing too many specimens to the private meteorite trade, thus sterillizing very valuable scientific information.

A sample of this meteorite was obtained from a study on the mineralogy and geochemistry of various southern African meteorites. As part of the study the Machinga meteorite samples were analysed by mineralogical and geochemical methods and the data used to test its classification.

The chemistry of individual mineral grains were determined by using electron microprobe techniques at the University of the

Free State, South Africa. A Cameca Camebax electron microprobe was employed using a 2μm beam diameter, 15 kV acceleration potential and a 30 mA beam current. Mineral and pure metal standards were used in conjunction with PAP correction techniques (Pouchou and Picoir, 1984). Whole rock analyses were performed by means of inductively coupled plasma emission mass spectrometry (ICP-MS), at the University of Kwazulu-Natal, South Africa. Samples were ground with an agate mortar and pestle, digested and analyzed with and ELAN 6100 ICP-MS.

The mineralogy of the Machinga meteorite is ambiguous. Orthopyroxene, plagioclase and Fe-Ni phases point to a E6 chondrite composition, while the very rare occurence of olivine and chromite point to a L6 ordinary chondrite composition, as can be seen in Table 1.

| Minerals | E6 chondrite | L6 ordinary chondrite | Machinga |
|---|---|---|---|
| Orthopyroxene | Enstatitic (low Ca)[1] | Composition varies[2] | $En_{98}$ Low Ca |
| Olivine | No reported olivine[1] | Most abundant mineral in ordinary chondrites; Composition varies[2] | $Fo_{95}$ but occurs rarely |
| Plagioclase | $Ab_{93}$[1] | $An_{86}$[1] | $Ab_{85}$ |
| Troilite | Present[1] | Present[1] | Present |
| Fe-Ni phases (kamacite – taenite) | Kamacite only[2] | Kamacite-taenite[2] | Kamacite only |
| Apatite | Rare[3] | Rare[3] | Not encountered in this study, but reported by Koeberl et al. (1991) |
| Pentlandite | Rare accessory phase[3] | Rare accessory phase[3] | Not encountered in this study, but reported by Koeberl et al. (1991) |
| Chromite | Not encountered in literature study | Most abundant accessory mineral in ordinary chondrites[2] | Not encountered in this study, but reported by Koeberl et al. (1991) |

**Table 1: Mineralogy comparison of E6 chondrites, L6 ordinary chondrites and the Machinga meteorite. Literature references (1) Brearley and Jones, 1998; (2) Dodd, 1981; (3) Koeberl et al, 1991.**

During this investigation the previous classification (L6) of the Machinga meteorite (Graham et al., 1984; 1985) was challenged. According to the Dodd (1981), von Michaelis (1969) and Mason (1971) classification schemes based on Al/Si, Mg/Si and Fe/Si, Mg/Si ratios, the Machinga meteorite plots outside the L6 field, and showed an inclination to the E6 chondrite field (Fig 1), though not plotting within the E6 field.

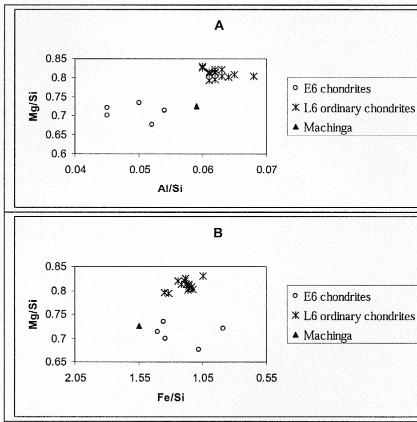


Figure 1: Classification of Machinga meteorite A = Al/Si versus Mg/Si and B = Fe/Si versus Mg/Si (Dodd, 1981; von Michaelis, 1969; Mason, 1971).

The data available in this study did not reveal the true classification of the Machinga meteorite. A more detailed study involving more trace elements, as well as isotopes, will be performed in future.

In conclusion we can see that the classification systems used to identify meteorites are not as accurate as we may think. The Machinga meteorite was previously classified as a L6 ordinary chondrite, but using new data its seems to be intermediate between the L6 ordinary chondrite group and the E6 chondrite group. Mineralogy, more extensive trace element data and especially isotopes can help refine this identification process, but a unification and streamlining of the various systems are also badly needed.

**References:**

**Brearley, A.J.; Jones, R.H. 1998.** Chondritic meteorites. *Reviews in Mineralogy* **36**, 398pp.

**Dodd, R.T. 1980.** *Meteorites – A petrologic-chemical synthesis.* Cambridge University Press., 368 pp.

**Graham, A.L., Crow, M.J., Chatupa, J.C and Mndala ,A.T. 1984.** The Machinga, Malawi, Meteorite: A recent L6 fall. *Meteoritics* **19**, 85-88.

**Graham A.L., Bevan A.W.R. and Hutchison R. 1985.** *Catalogue of meteorites.* University of Arizona Press, 460 pp.

**Koeberl, C., Reimold, W.U., Horsch, H.E. and Merkle, R.K.W. 1990**. New mineralogical and chemical data on the Machinga (L6) chondrite, Malawi. *Meteoritics* **25**, 23-26.

**Mason, B. 1971.** *Handbook for Elemental Abundances in Meteorites.* Gordon and Breach Publ., 555 pp.

**Mason, B. 1962.** *Meteorites.* John Wiley and Sons, Inc., 274 pp.

**Pouchou, J.L.; Picoir, F. 1984.** A new model for quantitative X-ray microanalysis. Part I: Application to analysis of homogenous samples. *Rech. Aérosp.,* **3,** 13-38.

**Von Michaelis, H., Ahrens, L.H.; Willis, J.P. 1969.** The Composition of Stony Meteorites II: The Analytical Data and an Assessment of their Quality. *Earth and Planetary Science Letters* **5**, 387-394.

## Prospects for exploitation of uganda geothermalwaters and environmental protection measures.

**Lubembe Nassuna, G.**
*Principal Documentation Officer, Department of Geological Survey and Mines, P.O.Box 9, Entebbe, UGANDA,.Email: nassuna02119@alumni.itc.nl or nassunagl@hotmail.com, Mobile: +256-77-515851*

Since colonial times Uganda has mostly relied on Nalubaale Dam for generation of electricity. Uganda has a population of

## Appendix F

## Published accredited articles and

## international conference poster presentation abstracts